Correspondence to:
G. Booth Rea,
gbooth@go.ugr.es

Two Cenozoic Extensional Phases in Mallorca and Their Bearing on the Geodynamic Evolution of the Western Mediterranean

Lluís Moragues[1], Patricia Ruano[1,2], José Miguel Azañón[1,2] [ID], Carlos J. Garrido[2], Karoly Hidas[3], and Guillermo Booth Rea[1,2] [ID]

[1]Departamento de Geodinámica, Facultad de Ciencias, Universidad de Granada, Granada, Spain, [2]Instituto Andaluz de Ciencias de la Tierra, CSIC-UGR, Granada, Spain, [3]Departamento de Investigación y Prospectiva Geocientífica, Instituto Geológico y Minero de España, Madrid, Spain

Abstract We study the structure of the Llevant ranges in Mallorca with special emphasis on the Cenozoic extensional evolution of the island, which we integrate in a new geodynamic model for the Westernmost Mediterranean. Mallorca underwent two Cenozoic rifting phases in the Oligocene and Serravallian, before and after the development of its Foreland Thrust Belt (FTB). The first extensional event produced Oligocene semigrabens (≈29–23 Ma) that were inverted during the Early-Middle Miocene (19–14 Ma) WNW-directed FTB development. The second rifting event produced the extensional collapse of the Mallorca FTB during the Serravallian (≈14–11 Ma). This later rifting was polyphasic, with two orthogonal extensional systems, producing first NE-SW, and then NW-SE extension. The Oligocene extension affected a major part of the Western Mediterranean, opening the Liguro-Provençal and other basins after the collapse of the Palaeogene AlKaPeCa orogen, and Mallorca, its former hinterland. Continued plate convergence nucleated a new subduction system in the Early Miocene that initiated along the Ibiza transform, producing the Mallorca WNW-directed FTB and subduction of the South-East Iberian passive margin. This process individualized the Betic-Rif slab and initiated its westward retreat. Serravallian extension occurred at the northern edge of the subduction system coeval to the Algero-Balearic basin opening. Extension initiated toward the SW direction of slab tearing and later rotated to a NW-SE direction, probably in response to flexural and isostatic rebound. Through these processes the Alboran domain archipelago was driven toward the southwest until the Late Miocene, contributing to the present isolation of Mallorca from its Betic hinterland.

Plain Language Summary We integrate the geological evolution of Mallorca Island into the larger framework of the Western Mediterranean. To this end we study the geological structure of Mallorca, finding that it underwent two thinning phases that occurred before and after a period of crustal thickening and shortening in the region between 19 and 14 Ma. The thinning phases coincided with the development of the western Mediterranean basins. The later crustal thinning occurred at the northern edge of the Betic-Rif subduction system, in relation to the tearing and retreat of a portion of lithospheric root that detached under Mallorca at around 14 Ma. This slab tearing mechanism occurring at the southern (along the present western Algerian margin) and northern edges of the subduction system favored westward retreat of the subducting mantle body presently imaged by seismic tomography under the westernmost Mediterranean. The geology of Mallorca Island supports its formation as part of the Betic orogen that was later isolated from its Betic hinterland by the opening of the Algero-Balearic basin. The Betic hinterland drifted westward, hundreds of kilometers away from Mallorca, as an archipelago, until its final docking between Northern Africa and Southeastern Iberia ~9 Ma ago.

1. Introduction

The Balearic Promontory (BP) is set at the core of the Western Mediterranean orogenic system, forming part of the Betic Foreland Thrust Belt (Betic FTB), developed by NW- to WNW-directed thrust tectonics during the Late Oligocene to Early Miocene (Alvaro, 1987; Gelabert et al., 1992; Sabat et al., 1988, 2011; Figure 1). However, the BP is missing a corresponding thick-skinned internal domain, and is surrounded by deep basins developed mostly during Tertiary back-arc rifting (e.g., Aïdi et al., 2018; Burrus, 1984; Cherchi &

Methodology: Lluís Moragues, Patricia Ruano, Karoly Hidas, Guillermo Booth Rea
Project Administration: Patricia Ruano, Guillermo Booth Rea
Resources: Lluís Moragues
Software: Patricia Ruano
Supervision: Patricia Ruano, Carlos J. Garrido, Guillermo Booth Rea
Visualization: Lluís Moragues, Patricia Ruano, Karoly Hidas, Guillermo Booth Rea
Writing – original draft: Lluís Moragues, Patricia Ruano, Guillermo Booth Rea
Writing – review & editing: Lluís Moragues, José Miguel Azañón, Carlos J. Garrido, Karoly Hidas, Guillermo Booth Rea

Montadert, 1982; Etheve et al., 2016; Ferrandini et al., 2003; Gelabert et al., 2002; Jolivet et al., 2006; Schettino & Turco, 2006; Figure 1). The relative timing between crustal thickening and extension in the region has been a subject of great debate, with most work suggesting that extension during the Oligocene to Early Miocene (26–19 Ma; Etheve et al., 2016; Schettino & Turco, 2006) was actually prior to crustal shortening that lasted until the Langhian (≈14–16 Ma; e.g., Sabat et al., 2011). While there is some consensus on the age of crustal shortening—with deformation in Mallorca migrating from SE to NW between the late Oligocene and the Langhian (e.g., Sabat et al., 2011)—the age and significance of crustal extension in Mallorca and adjacent marine basins are not well constrained.

Most work suggests that rifting in the region occurred between 30 and 16 Ma in the three basins surrounding the BP: the Valencia Trough to the Northwest, the Liguro-Provençal basin to the Northeast, and the Algero-Balearic basin to the South (Figure 1, e.g., Arab et al., 2016; Etheve et al., 2016; Leprêtre et al., 2013; Maillard & Mauffret, 1999; Schettino & Turco, 2006; Speranza et al., 2002; Watts & Torné, 1992). Some authors propose the rifting phase lasted longer, between 34 and 13 Ma, encompassing the development of the Mallorca FTB (Gelabert et al., 2002; Roca, 2001; Roca & Guimerà, 1992). Other work, however, has demonstrated the importance of Mesozoic rifting in the Valencia Trough, where a several kilometer thick sequence of Jurassic sediments is found above a thin continental crust (Ayala et al., 2015; Etheve et al., 2018). Mesozoic extension is also well documented onshore, along the Iberian Chain and Catalan Coastal Ranges (e.g., Guimerà et al., 2004; Marín et al., 2021; Roca et al., 1994). This domain of Mesozoic rifting was further extended during the Cenozoic in its transition toward the Liguro-Provencal Basin and along the Catalan Coastal Ranges, forming the differentiated Menorca basin in between (e.g., Marín et al., 2021; Parcerisa Duocastela et al., 2007; Pellen et al., 2016; Roca et al., 1999). Differential amounts of Tertiary extension between these domains were accommodated along NW-SE directed transfer fault zones such as the North Balearic and Central fracture zones, among others, in a process accompanied by important Early to Middle Miocene magmatism (Maillard et al., 2020; Pellen et al., 2016; Figure 1). The role of Oligocene to Early Miocene extension in the formation of the present Algero-Balearic basin to the South has also been questioned; for this region several authors have highlighted the importance of oceanic crust development during the Middle to Late Miocene (Booth-Rea et al., 2007; Booth-Rea, Ranero, & Grevemeyer, 2018; de la Peña, Grevemeyer, et al., 2020; de la Peña, Ranero, et al., 2020; Haidar et al., 2021; Jolivet et al., 2006; Mauffret et al., 2004). This process followed the westward retreat of the Gibraltar arc subduction system (Lonergan & White, 1997) and concomitant slab detachment or tearing along its Betic and Rif-Tell orogenic limbs, respectively (e.g., Duggen et al., 2003; García-Castellanos & Villaseñor, 2011; Hidas et al., 2016, 2019; Mancilla et al., 2015). Middle to Late Miocene extension has also been described onshore along its continental margins, in Northern Tunisia, the BP, and the South Eastern Betics (Booth-Rea et al., 2004, Booth-Rea, Gaidi, et al., 2018; Giaconia et al., 2014; Moragues et al., 2018). A two-phase opening model for the Algero-Balearic basin has likewise been proposed, with an initial Oligocene-Early Miocene NW-SE phase and a subsequent Middle to Late Miocene E-W phase (Aïdi et al., 2018; Driussi, Briais, & Maillard, 2015).

Cenozoic extension onshore Mallorca has not been extensively studied, and its relationships with the development of Western Mediterranean sedimentary basins and the collapse of surrounding fold and thrust belts are poorly understood. Most work describes SW-NE trending high-angle normal faults that extended the southeastern margin of the Tramuntana ranges, developing Middle to Late Neogene depocentres that include the Inca, Palma and Sa Pobla basins (Benedicto et al., 1993; Gelabert, 1998; Ramos-Guerrero et al., 2000; Sabat et al., 2011; Figure 1b). In addition, a couple of NW-SE trending normal faults were differentiated in the Central Ranges of Mallorca (Anglada-Guajardo & Serra-Kiel, 1986; Sabat et al., 2011). Paleostress analysis from small-scale faults suggests the existence of radial extension during the late Neogene (Céspedes et al., 2001). Preliminary field work and structural analysis moreover show that many of the supposed thrust contacts between nappes in the Tramuntana and Levant ranges could actually have been reworked by two sets of orthogonal low- and high-angle normal faults producing NW-SE and NE-SW trending extension during the Middle Miocene (Booth-Rea et al., 2016; Moragues et al., 2018). Against this background, we mainly aspire to elucidate the relationships between Cenozoic extension in Mallorca and its meaning for the general Cenozoic tectonic evolution of the Western Mediterranean, including some explanation for the nature and fate of the missing hinterland of the Mallorca FTB and the apparent simultaneity between crustal thickening and extension in the BP and the surrounding basins.
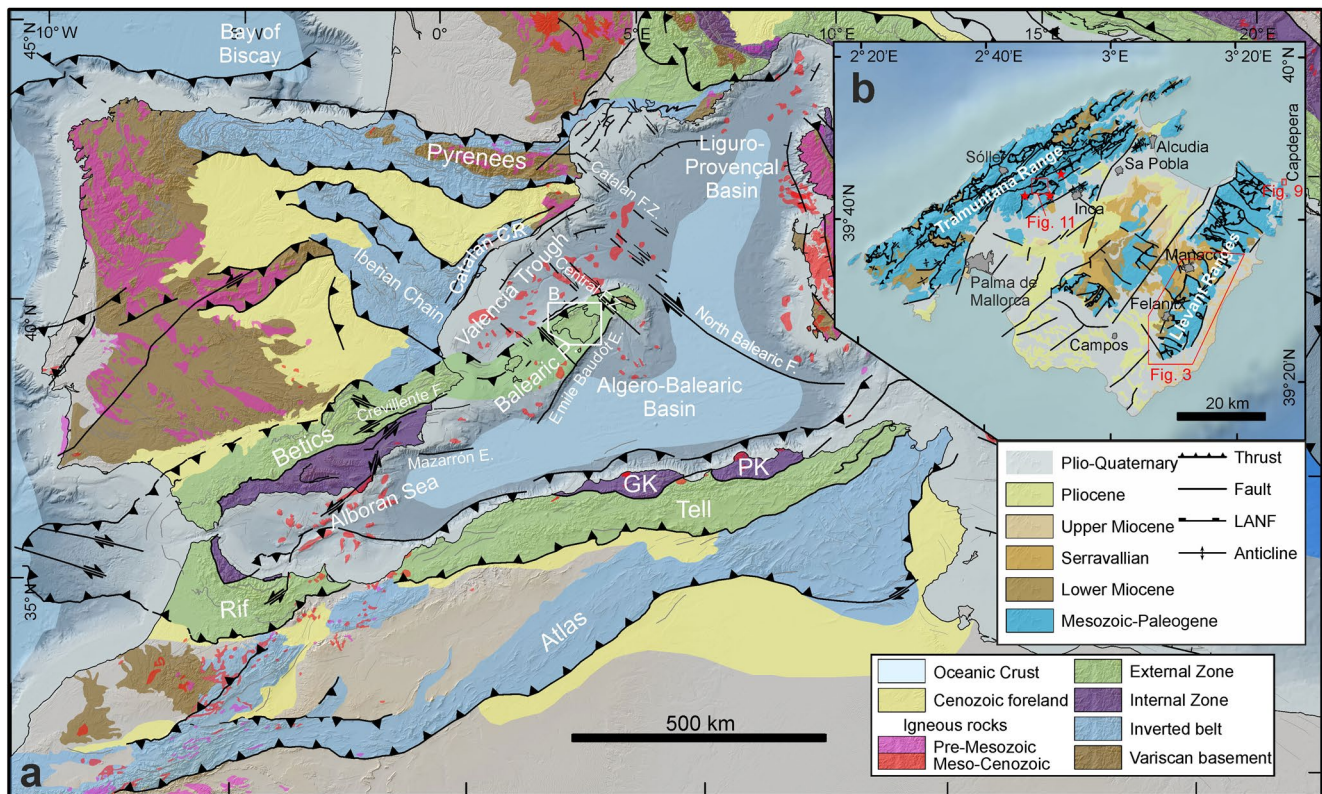
Figure 1. Tectonic map of the Western Mediterranean including main orogenic domains and basins (a). Inset shows the Geology of the Mallorca Island and location of the study areas (b). Red stars indicate localities where Oligocene sediments are detached over a low-angle normal fault.

In resolving the above questions we look into the Cenozoic extensional events in Mallorca, analyzing relationships between extensional faults and their related synrift deposits, and identifying the main grabens with the help of a residual gravity map of the island. We map the southern and central Llevant ranges, emphasizing the structural geology to shed light on the geometry, kinematics, and paleostress fields related to brittle faults as well as their relations with the overlying Tertiary sedimentary sequence. Extensional and shortening structures are distinguished to analyze their relative timing. Furthermore, the age of extensional deformation is determined in the context of syn-sedimentary features of the alluvial sequences related to normal faulting. We describe two rifting events in Mallorca that respectively occurred before and after the main shortening period that formed the Mallorca FTB in the Early Miocene. The role of these extensional events in the present isolation and structure of Mallorca is discussed. Finally, we integrate the tectonics of Mallorca with a wide range of previously published results from different orogenic belts and basins of the Western Mediterranean, combining structural and metamorphic data, radiometric dating, sedimentary provenance data, and vertebrate fossils to build a new geodynamic model for the evolution of the Western Mediterranean during the Cenozoic.

2. Geodynamic and Geological Settings

2.1. Geodynamic Setting

Mallorca is the largest island of the BP, representing an emerged archipelago over a relatively thin 22–26 km continental crust (e.g., Díaz & Gallart, 2009) (Figure 1). This crustal domain has a thin lithosphere, less than 70 km (Jiménez-Munt et al., 2003), and it overlies an anomalously slow upper mantle with a strongly NE-SW oriented Pn anisotropy, similar to the rest of the Betics (Díaz et al., 2013). Toward the Northwest it transitions to the extremely thin continental crust of the Valencia Trough (Etheve et al., 2018; Maillard & Mauffret, 1999; Torné et al., 1992). To the Northeast, the BP is bounded by the Late Oligocene to Middle Miocene Liguro-provencal oceanic basin, across the dextral North-Balearic Fracture Zone (NBFZ, e.g., Maillard

et al., 2020; Figure 1). Oceanic crust is also found to the Southeast of the BP, forming the Algero-Balearic basin (Aïdi et al., 2018; Booth-Rea et al., 2007, Booth-Rea, Ranero, & Grevemeyer, 2018; Grevemeyer et al., 2011; Leprêtre et al., 2013; Mauffret et al., 2004). The transition between the BP and Algero-Balearic basin domains occurs both across narrow transform domains like the Emile Baudot and Mazarron escarpments, and through wider extended continental crust domains, for example, South of Menorca (Driussi, Briais, & Maillard, 2015; Figure 1).

The Liguro-Provençal and Algero-Balearic basins are separated from each other by the NBFZ (Figure 1). Both are interpreted as back arc basins formed in the context of slab roll-back in relation to retreating Tethyan lithospheric mantle bodies, presently underlying the Calabrian, Gibraltar, and Algero-Tunisian orogenic arcs (e.g., Booth-Rea, Gaidi, et al., 2018; El-Sharkawy et al., 2020; Faccenna et al., 2004; Fichtner & Villaseñor, 2015; Jolivet et al., 2008; Lonergan & White, 1997; Piromallo & Morelli, 2003; Rosenbaum & Lister, 2004; Wortel & Spakman, 2000). The Liguro-Provencal basin formed behind the Oligocene to Early Miocene volcanic arc, built mostly along western Sardinia in relation to earlier stages of Calabrian slab subduction (e.g., Faccenna et al., 2001). The Algero-Balearic basin shows a more complex evolution, presenting segments of different ages, as made manifest by the heat flow and magnetic anomaly distribution, suggesting younger oceanic crust located at the western and eastern ends of the basin (Haidar et al., 2021; Poort et al., 2020). Moreover, the Algero-Balearic basin is underlain by at least two different Tethyan slab segments, underneath the Betics-Rif and Algerian-Tunisian orogenic arcs (e.g., Faccenna et al., 2014; Fichtner & Villaseñor, 2015; Kumar et al., 2020; van Hinsbergen et al., 2014). The westernmost segment of the Algero-Balearic basin formed behind the Alboran volcanic arc in the Eastern Alboran basin during the Middle to Late Miocene (Booth-Rea et al., 2007, Booth-Rea, Ranero, & Grevemeyer, 2018; de la Peña, Ranero, et al., 2020; Duggen et al., 2004, 2008). The present slab segmentation of the Western Mediterranean was probably determined by the location of transform faults inherited from the Mesozoic Tethys rifting stage (e.g., Angrand et al., 2020; Vergés & Fernàndez, 2012).

Slab retreat that gave rise to the western Mediterranean back-arc basins was facilitated by slab tearing or detachment at the edges of the western Mediterranean subduction arcs, along Subduction Transfer Edge Propagators (STEP; Badji et al., 2015; Booth-Rea, Gaidi, et al., 2018; Gallais et al., 2013; Govers & Wortel, 2005; Hidas et al., 2019; Jolivet et al., 2021; Mancilla et al., 2015; van Hinsbergen et al., 2014). Mantle flow driven by the above slab tectonic mechanisms produced dynamic topography around the western Mediterranean, some areas having subdued topography above the subducting slabs, others undergoing uplift in backarc regions with mantle upwelling (Faccenna et al., 2014). Such is the case of the BP, located over a largely positive dynamic topography (Faccenna & Becker et al., 2020).

2.2. Geological Setting of the BP

The BP rifted away from the East Iberian margin during the Jurassic, when the Valencia Trough basin initially developed (Etheve et al., 2018). The Balearic region showed a evolution similar to that of the SE Iberian margin during the Mesozoic, with Germanic type facies during the Triassic that evolved toward shallow platform facies in the Early Jurassic, represented by shallow marine carbonates, including dolostone and limestones (Alvaro et al., 1989; Bourrouilh, 1983; Colom, 1973; Figure 2). Ongoing extensional tectonics are marked by rupture of the platform and the deposition of lower Pleisbachian outer platform marls and marly limestones, followed by quartz-rich sandstones and microconglomerates (e.g., Alvaro et al., 1989; Sevillano et al., 2018). Since the Toarcian it has formed a deep marine environment featuring typical turbiditic talus facies with resedimented olistholiths (Kettle, 2016). This pelagic environment continued with Maiolica white nannofossil limestone during the Early Cretaceous and was later followed by the deposition of Barremian to Aptian gray-greenish marls with planktonic microfauna (Bourrouilh, 1983; Martin-Chivelet et al., 2019). Mesozoic rifting was segmented by NW-SE-oriented transform faults that determined the individualization of diverse blocks in the Tethys and Iberian realms, for example, the Ebro block (Angrand et al., 2020).

The Early Cretaceous deep basinal setting was interrupted by a hiatus from the Late Cretaceous to the Early Eocene—an event probably related to crustal thickening during the development of the Pyrenees (Verges et al., 2002), the Iberian Chain and Catalan Coastal Ranges (Guimerà et al., 2004; Liesa & Simón, 2009; Marín et al., 2021), and the AlKaPeCa orogenic domain in the Western Mediterranean (Azañón et al., 1997;
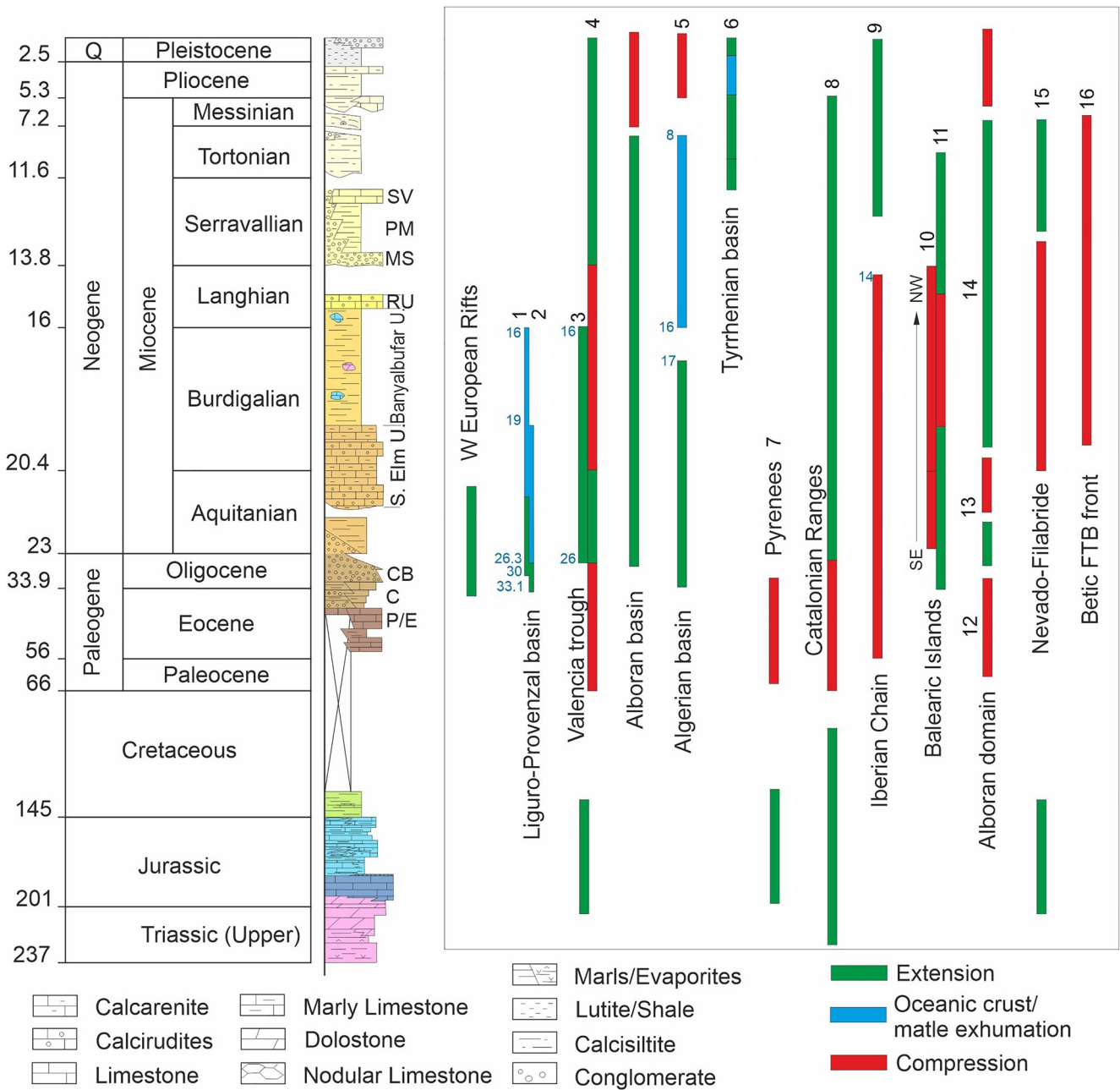
Figure 2. Stratigraphic sequence of the Mallorca Island (Mesozoic from Sabat et al., 2011; Palaeogene-Early Miocene (Colom, 1980; Martín-Closas & Ramos-Guerrero, 2005); Early Miocene to Tortonian (Ramos-Guerrero et al., 1989, 2000; Rodríguez-Perea, 1984); Tortonian to Quaternary, Ramos-Gerrero et al., 2000). Abbreviations of sedimentary unit names: C, Calvari Unit; CB, Cala Blanca Unit; MS, Manacor shales Unit; P/E, Peguera limestones and S'Envestida grainstones; PM, Pina marls Unit; RU, Randa calcarenites Unit; SV, Sa verdera Unit. Tectonic events over time (blue numbers) of Western Mediterranean domains based on: 1, Faccenna et al. (2004) and Burrus (1984); 2, Schettino and Turco (2006); 3, Vergés and Sàbat (1999); 4, Fontboté et al. (1990); 5, Aïdi et al. (2018); 6, Faccenna et al. (2004); 7, Vergés and Fernàndez (2012); 8, Marín et al. (2021); 9, Liesa and Simón (2009) and Simón et al. (2012, 2021); 10, Sabat et al. (2011); 11, present work; 12, Platt et al. (2005); 13, Hidas et al. (2013) and Balanyá et al. (1997); 14, García-Dueñas et al. (1992) and Lonergan and Platt (1995); 15, Platt et al. (2006); 16, Balanyá et al. (2007) and Iribarren et al. (2007).

Balanyá et al., 1997; Bouillin et al., 1986; Ramos-Guerrero et al., 1989; van Hinsbergen et al., 2014; Figure 2). Shortening directions in the Iberian Chain show a rotation from ESE-WNW in the Eocene to NE-SW in the Late Eocene to Oligocene, thus suggesting changes in the western Mediterranean stress field during the Palaeogene (Liesa & Simón, 2009). A related continental thickening event has been dated as Eocene to Early Oligocene in HP/LT rocks of the Alpujarride-Sebtide complex in the Internal Betics and

Rif (Bessière et al., 2021; Marrone et al., 2020, 2021; Platt et al., 2005), the Calabrian-Peloritani ranges (Heymes et al., 2010; Rossetti et al., 2001, 2004), the Kabylies (Bruguier et al., 2017), and Corsica (Di Vincenzo et al., 2016; Martin et al., 2011; Rossetti et al., 2015; Vitale Brovarone & Herwartz, 2013). Eocene Ar-Ar in phengite and U-Th-Pb in monazite radiometric ages are likewise obtained from the Nevado-Filabride complex at the core of the Betics (Augier, Agard, et al., 2005; Li & Massonne, 2018). However, these later ages contrast with Early to Middle Miocene ages obtained for the HP-LT metamorphic event and later peak metamorphism, based on Lu-Hf in garnet, U-Pb in zircon, Rb-Sr multimineral isochron geochronology, and U-Th-Pb in monazite (de Jong, 2003; Kirchner et al., 2016; López Sánchez-Vizcaino et al., 2001; Platt et al., 2006; Santamaría-López et al., 2019). Moreover, Ar-Ar ages from the Nevado-Filabride are interpreted to be influenced by excess Ar intake, related to submicroscopic illitization and fluid ingress during Miocene extension (de Jong et al., 2001). Thus, not all rocks in the Betic internal zones necessarily underwent the Eocene HP metamorphic event.

During this Paleogene continental thickening event, the BP probably formed part of the hinterland of the AlKaPeCa orogenic domain that was located along its southern margin, before the later opening of the Western Mediterranean basins (e.g., Booth-Rea et al., 2005, 2007; Bouillin et al., 1986; van Hinsbergen et al., 2014). The remains of this metamorphic terrane presently form part of the Alboran domain of the Internal Betics-Rif (Al), the Kabylies in the Tell (Ka), and the Calabria-Peloritani terrane in the Calabrian arc (PeCa). Most authors propose that the AlKaPeCa orogen had southward tectonic vergence, developed in relation to northwestward subduction of the Tethys lithosphere (e.g., Booth-Rea et al., 2005; Chertova et al., 2014; Jolivet et al., 2008; van Hinsbergen et al., 2014; Wortel & Spakman, 2000). Initial crustal thickening involved continental rocks of the European margin, producing a thick crustal stack with several superposed nappes of the Malaguide-Alpujarride complexes, presently preserved in the Eastern Betics (Booth-Rea et al., 2004; Lonergan, 1993). This nappe stack shows southwards vergence in the Betics, after undoing paleomagnetic rotations (Lonergan, 1993). Subduction of the oceanic Tethys lithosphere probably did not initiate until the Neogene, as evidenced by a Tethyan Flysch Sr-Nd-Pb isotopic signature in the Middle to Late Miocene Alboran volcanic arc that is not present in Paleogene volcanic rocks and dikes crosscutting the Alpujarride-Malaguide thrust stack (Varas-Reus et al., 2017). There is furthermore no evidence of a developed Palaeogene volcanic arc domain related to this thickening event in the Alboran and Kabylian domains (e.g., Lustrino et al., 2011).

The Late Cretaceous to Early Eocene hiatus in Mallorca was followed by Eocene continental paralic facies that evolve toward a shallow marine transgression in the Middle Eocene (late Lutetian-Bartonian, ≈45–37 Ma), respectively, represented by the Peguera limestones and S'Envestida grainstones (Martín-Closas & Ramos-Guerrero, 2005; Ramos-Guerrero et al., 1989; Figure 2). Continental deposition continued with some sedimentary gaps during the Late Eocene to Early Miocene with the deposition of conglomeratic wedges, sandstones and lacustrine carbonates of the Cala-Blanca formation that transition to shallow marine facies toward the SE, between the Priabonian and the Aquitanian (≈37–20.4 Ma, Martín-Closas & Ramos-Guerrero, 2005; Ramos-Guerrero et al., 1989). The Cala-Blanca formation has been dated as Oligocene on the basis of rodents (e.g., Adrover et al., 1977) and charophytes (Martín-Closas & Ramos-Guerrero, 2005). The top of this mostly continental sequence is probably signaled by Aquitanian marine marls (Colom, 1980; Colom & Sacares, 1968; Figure 2). Cala-Blanca conglomeratic wedges, dated as latemost Priabonian to Early Rupelian, have likewise been described as filling extensional semigrabens in Menorca (≈35–28 Ma, Bourrouilh, 1983; Martín-Closas & Guerrero, 2005; Sabat et al., 2018).

The Alboran orogenic domain, which was probably located South of the BP in the Oligocene, was extended in a back-arc setting coeval both to extension in Menorca and deposition of the Cala-Blanca conglomerates, exhuming the subcontinental mantle garnet lherzolite to plagioclase facies conditions (e.g., Balanyá et al., 1997; Booth-Rea et al., 2005, 2007; Garrido et al., 2011; Marchesi et al., 2012). Oligocene extensional depocenters are also described at the top of the Alboran domain, in the Malaguide complex (Geel & Roep, 1998). The Paleogene Malaguide-Alpujarride thrust stack was extended by low-angle normal faults and detachments at this time (Booth-Rea et al., 2004; Lonergan & Platt, 1995), concommitant to late Oligocene to Early Miocene tholeiitic dikes in the Malaguide domain (Duggen et al., 2004; Torres-Roldán et al., 1986), and calc-alkaline high-MgO andesite cumulates (Marchesi et al., 2012), arc-tholeiite gabbros (Hidas et al., 2015), and chromitites (González-Jiménez et al., 2017) in the Ronda peridotites. Thick layers

of Burdigalian rhyolitic ignimbrites dated at 19 Ma also occur in the Tramuntana Ranges of Mallorca (Marti et al., 1992; Mitjavila et al., 1990). This extension—which probably continued up to the Burdigalian—was coeval with the Liguro-Provencal basin's opening toward the NE (Cherchi & Montadert, 1982; Ferrandini et al., 2003; Schettino & Turco, 2006; Speranza et al., 2002; Figure 2).

Marine sedimentation began again in the Early Burdigalian, first with unconformable shallow calciruditic and calcarenitic platform facies of the Sant Elm formation in the Burdigalian (≈20.4–19 Ma, Donoso et al., 1982; Fornos et al., 1991; Rodríguez-Perea, 1984), and later followed by deeper marine flysch deposits of the Banyalbufar formation in the Burdigalian to Langhian (19–14 Ma, Alvaro et al., 1984; Ramos-Guerrero et al., 1989; Rodríguez-Perea, 1984) (Figure 2). The turbiditic marls of the Banyalbufar formation were deposited in an unstable foredeep context related to the development of the Mallorca FTB; they evolved into a piggy back type setting as the basin was incorporated into the Betic imbricated thrust stack up to the Langhian (≈16–14 Ma, Alvaro, 1987; Gelabert, 1998; Ramos-Guerrero et al., 1989; Sabat et al., 2011). At this stage, the Valencia Trough behaved as a foredeep basin, with the Betic deformation front lying along its southeastern margin (Fontboté et al., 1990; Watts & Torné, 1992). The Banyalbufar turbidites include abundant resedimented blocks and olistoliths of Palaeogene, Mesozoic, and Paleozoic rocks, provenant from the Mallorca FTB hinterland to the S (Donoso et al., 1982; Moragues et al., 2018; Pomar & Rodríguez-Perea, 1983). Thus, Mallorca went from being the hinterland of the Alboran and Kabilian orogenic domains in the Paleogene, to becoming part of the foreland of the Betic orogen after the Oligocene to Early Miocene extensional collapse of the region and its subsequent contractive inversion. Shallow platform calcirudites and grainstones in the *Randa* massif—attributed to the late Burdigalian to Langhian—locally show spaced stylolitic cleavage that attests to active shortening in the Llevant Ranges at the time (Gelabert, 1998; Sabat et al., 2011). Shortening, mostly SE-NW directed, also occurred at this time in the External Betics, the Iberian Chain and other intraplate regions of Iberia (Andeweg et al., 1999; Liesa & Simón, 2009; Simón, 1986).

The onset of postorogenic sedimentation is marked by continental deposits in the Serravallian (13.8–11.6 Ma), represented by alluvial and lacustrine environments where silts, gypsum, gravels, limestones, and marls prevail (Figure 2). Three members can be discerned: the Manacor silts and conglomerates, the Pina marls, and the Son Verdera limestones (Pomar et al., 1983; Ramos-Guerrero et al., 2000; Ramon & Simo, 1986). The sediments show large lateral thickness variations related to their deposition during the activity of SW-NE-striking normal faults along the SE border of the Tramuntana ranges (Benedicto et al., 1993). Middle-Miocene extensional structures strongly thinned the Early Miocene nappe stack, in two orthogonal directions, especially in the Llevant ranges (Moragues et al., 2018). During the Middle Miocene, the BP must have formed an archipelago with nearby islands in the Western Mediterranean featuring similar insular fauna. For instance, Serravallian continental sediments in the Central Betics have glirid fauna resembling that found in Mallorca (Bover et al., 2008; Suarez et al., 1993).

Marine flat lying limestones seal most of Mallorca's deformation, although they appear to be locally affected by SW-NE trending normal faults along the southeastern foothills of the Tramuntana and Llevant ranges (Gelabert, 1998; Sabat et al., 2011). Tortonian reefal and Messinian littoral carbonates occur along the coast and pass landwards to continental detrital deposits (Pomar et al., 1983). Offshore Mallorca, SW-NE trending normal faults cut the late Miocene sedimentary sequence, including the Messinian (Driussi, Maillard, et al., 2015).

3. Methods

We mapped the southern and central parts of the Llevant ranges in SE Mallorca with special attention to the effects of extensional overprinting upon the Early Miocene FTB structure of the island (Figure 3). Post-FTB extension has been largely neglected in the tectonic evolution of Mallorca, yet may prove key to understanding the structure of this orogenic region presently isolated among sedimentary basins. Its extension is evidenced by three geological cross-sections of the Llevant ranges (Figure 4). We contrasted previous maps and geological cross-sections of the region, mostly published in the IGME 1:50,000 geological maps (Alvaro-López et al., 1983; Barnolas et al., 1983), or by Casas and Sabat (1987), Freeman et al. (1989), Pares et al. (1986), and Sabat et al. (1988). The main faults and basins we observed were compared to residual gravimetric map for Mallorca (Ayala et al., 1994; IGME, 2003). The previously published residual
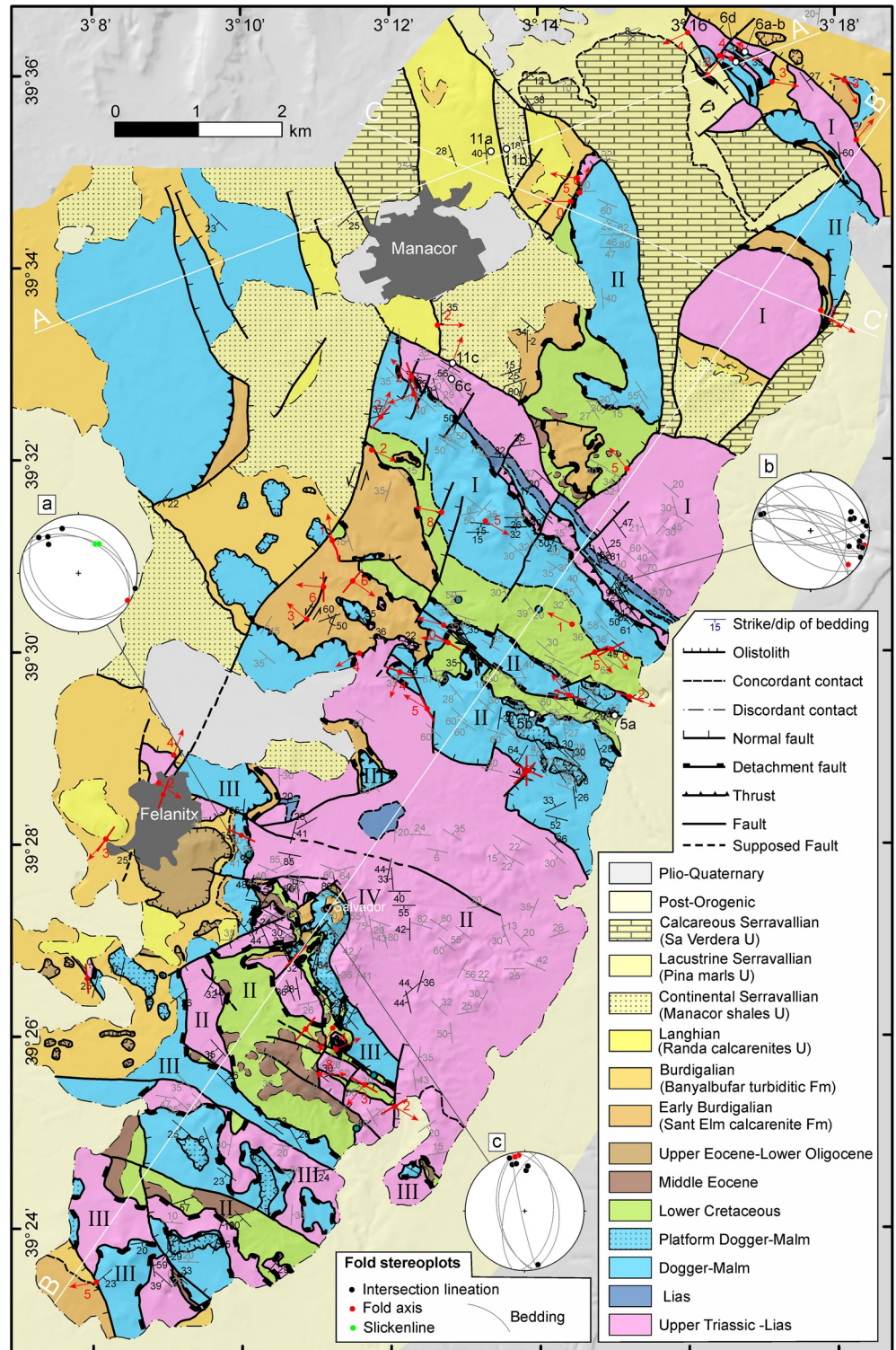
Figure 3. Geological map of the Llevant Ranges. Red lines and arrows, fault strike and kinematic vectors (red arrows). Red numbers, dip angles in tens of degrees. Bedding: our data in black, IGME data in gray (Alvaro-López et al., 1983). White dots, location of Figures 5, 6, and 12. White lines, location of cross-sections in Figure 4. Roman numbers indicate the tectonic units.
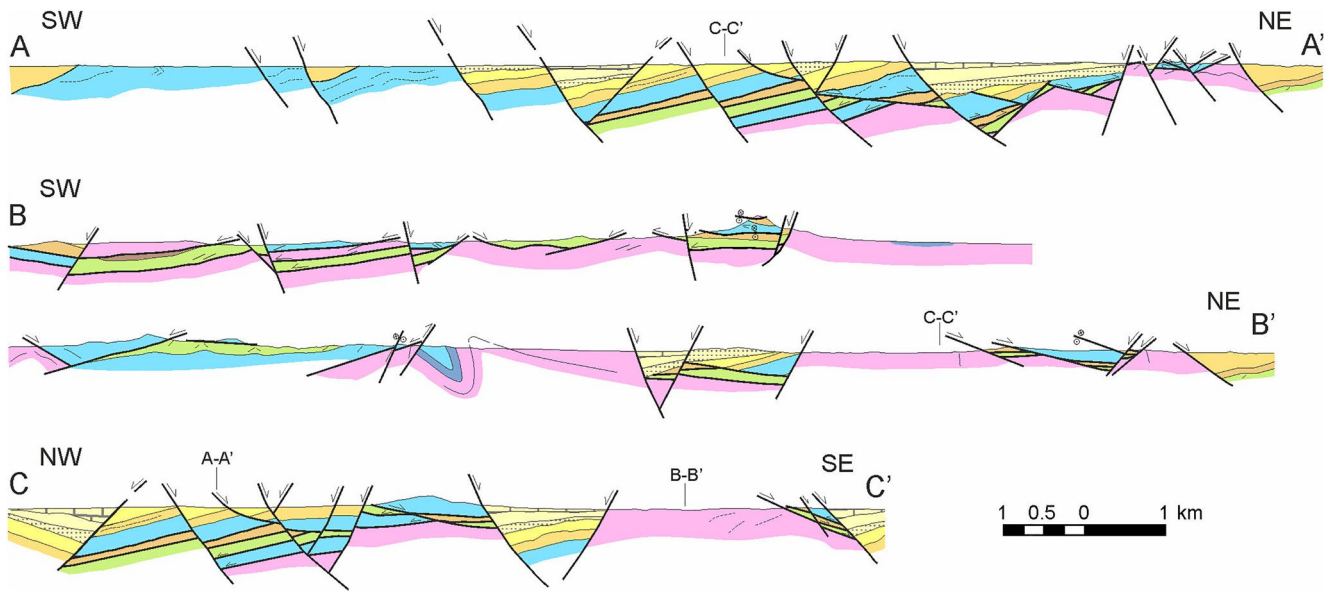
Figure 4. Cross-sections throughout the Llevant Ranges. Legend and location in Figure 3.

gravimetric map was obtained from 3,843 gravimetric data (Ayala et al., 1994). A density of 2.6 g/cm³ was used for the Bouguer reduction (IGME, 2003). The regional anomaly was calculated using a third-order polynomic adjustment. Finally, the residual anomaly we illustrate was obtained through subtraction of the regional anomaly from the Bouguer anomaly (Ayala et al., 1994; IGME, 2003).

Fault orientation and kinematics were measured at 90 sites, giving a total of 704 fault measurements (Figure 7). In sites offering sufficient fault-slip data, a stress inversion analysis was carried out to derive the paleo-stress state using a Search Grid method (Etchecopar et al., 1981; Galindo-Zaldívar & González-Lodeiro, 1988) and a Gauss paleostress method (T-Tecto 3.0 software; Žalohar & Vrabec, 2007). The first two methods, following Bott's equation (Bott, 1959) call for finding the best-fitting tensor, with the minimum sum of angular misfits between the predicted theoretical striae and the real striae. Any remaining (non-fitting) faults are automatically used in the Search Grid method by the algorithm to locate other possible tensors. In the case of multi-phase stress field determination, the phase number is related to the amount of assigned faults in each phase having no chronological meaning. The stress state is given by the orientation of the main axis of the stress tensors: maximum (σ_1), intermediate (σ_2), and minimum (σ_3) stress, plus their axial ratio (R, $(\sigma_2 - \sigma_3)/(\sigma_1 - \sigma_3)$). In the Gauss paleostress method, the results agree with Amonton's Law in that they detect the globally highest local maxima for the sum of compatibility functions (angular misfit and shear-normal stress ratio) in view of all fault-slip data. Yet only four faults are needed to mathematically determine a stress tensor, meaning this solution may not be statistically significant. The minimum number of faults required to reliably establish the significance of a given stress tensor solution has been widely discussed (e.g., Angelier, 1979; Casas et al., 1990; Etchecopar, 1984; Simón, 2019), and tends to range between 15 and 10 faults, but more in extreme cases (Arlegui & Simón, 1998).

The results obtained with the Search Grid and Etchecopar methods are similar, and consistent with the Gauss method results. This fact guarantees the reliability of the obtained results. At any rate, Orife and Lisle (2006) describe a method useful to discriminate between significant and non-significant stress tensors taking into account the number of faults (n) that define the stress tensor solution and the average misfit angle (α, in Table 1). Such a quality criterion cannot be achieved, as these authors affirm, in solutions obtained with fewer than 10 faults. For the above reasons, out of the 56 stress tensor solutions obtained at 33 stations, we present just 26 significant stress tensors, determined with at least 10 faults in this study. Still, although paleostress fields comparable to contemporary stresses may be obtained using the above methods (Lacombe, 2012), our results should be interpreted with caution; pitfalls are known to plague the process of fault measurement, analysis and interpretation (Hippolyte, et al., 2012; Sperner & Zweigel, 2010).

Table 1
Stress Tensors and Stress Orientation Obtained From Fault Population Analysis by Grid Search Method (Galindo-Zaldívar & González-Lodeiro, 1988)

Site	Longitude	Latitude	N	Phase	n	σ_1	σ_2	σ_3	R	α
SL1	3.210418	39.417993	18	1	12	125/80	343/8	252/6	0.36	7.4
SL2	3.1580792	39.4410548	13	1	10	71/52	170/7	266/37	0.75	11.4
SL3	3.2275809	39.4469889	19	1	13	42/68	140/3	231/22	0.61	12.6
SL7	3.172338	39.396186	17	1	12	73/37	256/53	164/1	0.75	12.7
SL9	3.164206	39.464175	14	1	11	14/74	276/2	186/16	0.49	9.4
SL13	3.186562	39.43308	22	1	16	236/68	144/1	54/22	0.16	11
SL14	3.182084	39.446015	14	1	10	280/55	148/25	46/23	0.73	7.8
SL15	3.191788	39.419328	19	1	13	39/70	200/19	292/6	0.19	14.4
SL16	3.231101	39.447547	19	1	15	338/74	188/14	96/8	0.13	13.5
SL17	3.188088	39.414076	20	1	14	242/57	101/27	2/18	0.19	13.13
SL20	3.2290541	39.5438878	25	1	15	219/68	95/12	9/22	0.29	14.5
SL21	3.242382	39.5401823	29	1	23	351/78	178/11	87/1	0.14	7.8
SL23	3.2109706	39.5236949	13	1	11	63/83	212/6	303/3	0.06	8.3
SL24	3.2443092	39.5817774	33	1	19	289/77	47/6	139/11	0.55	16.1
SL24	3.2443092	39.5817774	33	2	10	260/48	117/36	13/19	0.79	10.3
SL25	3.154895	39.5832976	24	1	16	242/66	101/19	6/14	0.5	12
SL27	3.2497111	39.4799626	25	1	17	226/72	29/17	121/5	0.24	13.8
SL28	3.2524711	39.4932762	21	1	18	48/74	245/15	154/4	0.53	9.3
SL31	3.281447	39.6025116	25	1	15	291/86	172/0	82/4	0.62	15.4
SL33	3.2765473	39.6027547	34	1	25	92/83	342/3	251/7	0.2	15.9
SL34	3.1868972	39.4348498	25	1	13	120/81	311/9	221/2	0.5	8.9
SL34	3.1868972	39.4348498	25	2	10	201/48	57/37	313/18	0.78	9.8
CP_Normal	3.476	39.712	15	1	12	11/80	234/7	143/7	0.2	13.8
CP_Strike-S	3.476	39.712	14	1	10	270/23	144/54	11/26	0.74	11.8
CP_Reverse	3.476	39.712	17	1	14	132/10	42/4	291/79	0.05	13.7
T-1	2.827	39.726	22	1	16	161/71	40/10	307/16	0.77	9.7

Note. Successive columns indicate: Site, station name, and geographical coordinates (longitude and latitude); *N*, number of faults measured in each site; Phase, different stress state of each site. The number of the phase is related to the number of assigned faults in each phase without any chronological meaning; *n*, number of faults used for defining each phase; σ_1, σ_2, and σ_3, orientation of principal stress axes; *R*, stress ratio = $(\sigma2 - \sigma3)/(\sigma1 - \sigma3)$; α, average misfit between theoretical and real striation.

Our geodynamic reconstruction was carried out by integrating novel field observations and previously published Eocene-Middle Miocene geodynamic evolution models of the Western Mediterranean, after Booth-Rea et al. (2007), Etheve et al. (2016), Haidar et al. (2021), Leprêtre et al. (2018), Romagny et al. (2020), van Hinsbergen et al. (2020), and references therein. The framework of our model is constrained by the paleogeographic positions and motions of Africa, Iberia and Adria relative to the Eurasian plate, based on Handy et al. (2010) and Rosenbaum et al. (2002). The Atlantic and Tethys ocean floor structure is reconstructed after Sallarès et al. (2011), and the Cenozoic seafloor evolution after Poort et al. (2020). Ages of volcanism are compiled from Lustrino et al. (2011), Marti et al. (1992), and Maury et al. (2000). When there is magmatic evidence of oceanic subduction—for example, a volcanic arc with tholeiitic or calcoalkaline rocks in the orogenic belts—we locate the deformation front at ~200 km from the volcanics. The position of coastlines refers to Jolivet et al. (2006), including stratigraphic data and continental vertebrate distribution from Azzaroli (1990), Bover et al. (2008), Boukhalfa et al. (2020), Costamagna and Schäfer (2013), de la Peña, Ranero, et al. (2020), Martín-Closas and Ramos-Guerrero (2005), Mennecart et al. (2017), and Suarez et al. (1993).
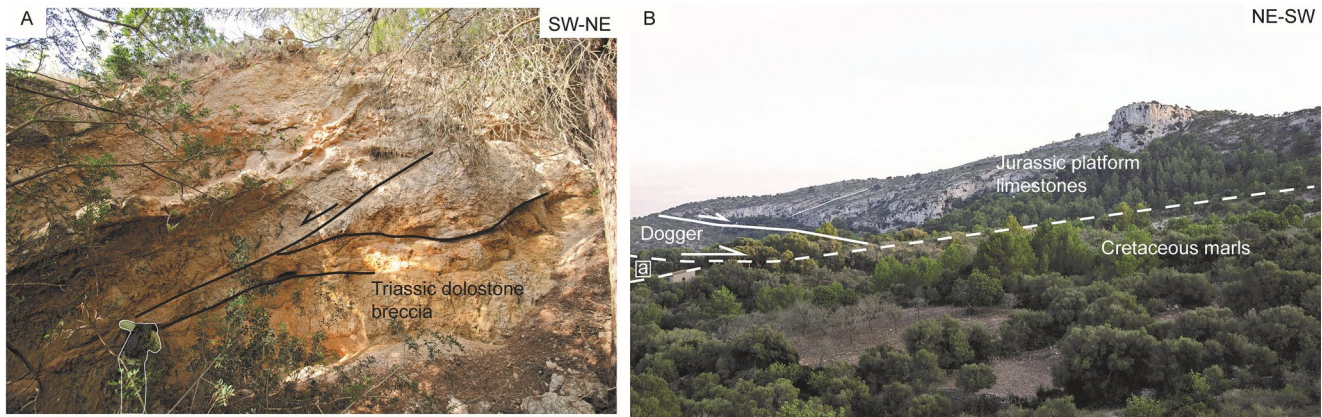
Figure 5. Extensional structures reworking the contacts between Nappe I and II in the Llevant ranges. (a) Outcrop of Triassic dolostones of Nappe II strongly brecciated by SW-directed LANFs. This small outcrop is located between Middle Jurassic limestones above and Cretaceous marls of Nappe I below, in a position like a, in Figure 5b. (b) Panoramic view of a low-angle normal fault cutting through Jurassic limestones of Nappe II that detaches over Cretaceous marls of the underlying Nappe I. The inset indicated as (a) represents the approximate structural position of the cataclastic breccias shown in (a).

4. Results

4.1. Structure of the Llevant Ranges

We produced a new geological and structural map for the southern and central parts of the Llevant ranges (Figure 3). The region features smooth relief determined by the Llevant ranges, surrounded by mostly flat domains where Early to Late Miocene sediments occur. The boundaries between the uplifted ranges and the sedimentary depocenters are mostly high-angle normal faults, except at the southeastern side of the Llevant ranges, where they are overlain unconformably by Tortonian marine calcirudites and grainstones (post-orogenic sediments in Figure 3). Two orthogonal systems of high-angle normal faults, trending NW-SE and NE-SW, cut the Llevant range sedimentary sequence, up to the Serravallian sediments (Figure 3 and cross-sections in Figure 4). Thus, geological cross-sections trending both NE-SW and NW-SE across the Llevant ranges (see sections a–a′, b–b′, and c–c′in Figure 4) indicate the presence of horsts and grabens related to the two orthogonal extensional systems. Such is the case of the Manacor graben, bounded by a high-angle NW-SE striking fault with NE transport along its southern boundary—namely, the Manacor fault—as well as by NE-SW trending faults along its eastern boundary. In both cases, the faults separate Triassic dolostones in their footwalls from Serravallian alluvial sediments in the respective hangingwalls. In some places the high-angle faults also show strike-slip kinematics; for example, the NE-SW trending Felanitx fault, which runs parallel to the road between Felanitx and Manacor villages (Figure 3), would have sinistral displacement according to the intersection between the main fault plane and small-scale Riedel faults.

The main horsts in the region are cored by the remains of at least four nappes of the Early Miocene thrust stack, numbered I–IV, from bottom to top (Figure 3). Each nappe is represented from top to bottom by an incomplete lithological sequence of Triassic dolostones to Early Miocene calcarenites of the Sant Elm formation. Meanwhile, Nappe III includes Burdigalian turbidites of the Banyalbufar formation together with Late Burdigalian to Langhian platform grainstones and calcirudites. The Early Miocene sediments of Nappe III are also locally overthrusted by Triassic dolostones (Figures 3 and 4). The deepest nappe (I) crops out to the S-SE of Manacor. It shows several moderately inclined SW-vergent folds with WNW-ESE oriented axes and intersection lineations, the anticline at the core of the nappe being cut by a retro-NE-transport reverse fault (stereoplot b in Figure 3, cross-section in Figures 4b and 4b′). This nappe, which includes a continuous stratigraphic section from Triassic dolostones to Cretaceous marls, is bounded to the W and above by a LANF with SW-directed transport. Small Triassic dolomitic extensional horses occur along the LANF surface, between Cretaceous marls (below) and Middle Jurassic marls and limestones (above), resulting from the thinning of a previous overlying nappe (Figure 5a). The Triassic dolostones are strongly comminuted and cut by low-angle faults with SW-directed transport (Figures 4b, 4b′, and 5a). To the W of Felanitx, the hangingwall of the above LANF forms the largest Triassic outcrops of Nappe II, showing a ramp geometry including Triassic dolostones and overlying Jurassic limestones tilted over the Cretaceous marls

of the underlying nappe I (Figure 5b). Listric normal faults cut through the Jurassic and root in the LANF (Figures 3, 4b, 4b′, and 5b). To the Northeast, Nappe I is bounded by the Manacor NE-transport high-angle normal fault that shows Serravallian alluvial sediments and Cretaceous marls in its hangingwall.

Nappe II is cut by a SW-transport high-angle normal fault to the South of Felanitx, and toward the SW it appears again in several tectonic windows, at the footwall of SW-transport LANFs. One of these LANFs cuts through Nappe II, erasing its Jurassic sequence; Triassic dolostones can be found in its footwall, and Cretaceous to Eocene sediments in the hangingwall. Nappe III is formed by Triassic dolostones, Jurassic marly limestones, and unconformably overlying Early Miocene calcirudites and grainstones of the Sant Elm unit. It crops out extensively toward the SW of the region mapped in Figure 3. Gently plunging, moderately inclined folds in Nappe III show mostly N-S to NW-SE oriented axes, and westward to southwestward vergence near Salvador mountain and Felanitx, respectively (stereoplots a and c, Figure 3). Finally, nappe IV is represented by a small outcrop of Triassic dolostones overthrusting Early Miocene calcirudites of the Sant Elm formation at the top of the nappe pile, in Salvador Mountain by Felanitx (see cross-section b, Figure 4). Both Nappes III and IV locally preserve their original thrust surface, with westward directed transport in Salvador Mountain to the SE of Felanitx.

4.2. Fault Kinematics and Paleostress Analysis

The thrust planes related to Mallorca FTB development and the nappes they bound are pervasively overprinted by extensional brittle shear planes, especially in the most pelitic lithologies, that is, the Cretaceous and late Jurassic pelagic marl (Figures 6a–6c). More competent lithologies, such as Triassic dolostone, are strongly faulted and brecciated (Figures 6c and 6d). Slicken lines along normal fault planes mark variable directions of transport, though mostly NE-SW and NW-SE directed (Figures 3, 4, and 7). Geometric and kinematic analysis of fault contacts between lithological units in the Llevant Ranges suggest that the Mallorca FTB was strongly thinned and extended in two orthogonal directions after the Early Miocene thrusting phase, yet preserving the previously established nappe superposition (Moragues et al., 2018; and in a wider region in Figure 7). These faults produce stratigraphic omissions along their contacts toward the direction of transport. In many cases, the different rock bodies in the Llevant ranges are bounded entirely by LANFs, forming extensional horses at different scales. A careful analysis of the low-angle brittle fault surfaces shows that they cut down into the structural pile in the direction of transport, which attests to their extensional nature (Figures 4 and 6d). Several contacts previously interpreted as stratigraphical are moreover reworked by LANFs (Figures 3 and 4).

Most of the fault measurement stations clearly evidence NE-SW directed extension, marked in the paleostress results by a subvertical σ_1 and subhorizontal NE-SW oriented σ_3, according to the Search Grid, Etchecopar, and Gauss paleostress determinations. This extension is especially prominent in the stations measured to the SW of the mapped region (fault stations 3, 5, 7, 9, 17, and 34 in Figure 7). The shape of the stress ellipsoid for the NE-SW extension varies, but can often be defined by intermediate to high axial ratio values ($R \geq 0.3$)—for example in stations 3, 7, 14, and 34, indicating equalaxial ($R = 0.3$–0.6) to oblate ($R \geq 0.6$) shapes. Two of these fault measurement stations reveal a second paleostress field when using the Search Grid method, mostly indicating NW-SE-directed extension, transverse to the previous one (stations 24 and 34). At station 7 we harvest different results from the Gauss and Search Grid methods, respectively giving NE-SW and NW-SE main horizontal extension. However, this apparent incongruency is due to the fact that the Grid Search method defined two different stress fields with NW-SE and NE-SW extension, but one comprised only seven faults, hence not shown. Several stations giving a well-determined NE-SW extensional stress field also yielded a second NW-SE extensional stress field defined by fewer than 10 faults. Station 23 has radial extension with a very low R value: 0.06 with a subvertical σ_1. A similar pattern of extension can be observed in the region of Manacor, to the N of the mapped region, where stations 20–22, 24, and 31–33 show a phase of NE-SW extension that likewise reflects mostly equalaxial to oblate paleostress fields, whereas stations 21 and 33 show a prolate shape. NE-SW extension is further made manifest by normal faults measured in tilted Serravallian sediments of the Manacor basin at station 29, and along individual faults bounding these sediments. Faults measured in tilted Langhian sediments (station 30) can be interpreted as belonging to two orthogonal NW-SE and SW-NE fault sets, although the striae are not well preserved in these faults, impeding their paleostress analysis. Some of the fault measurement stations
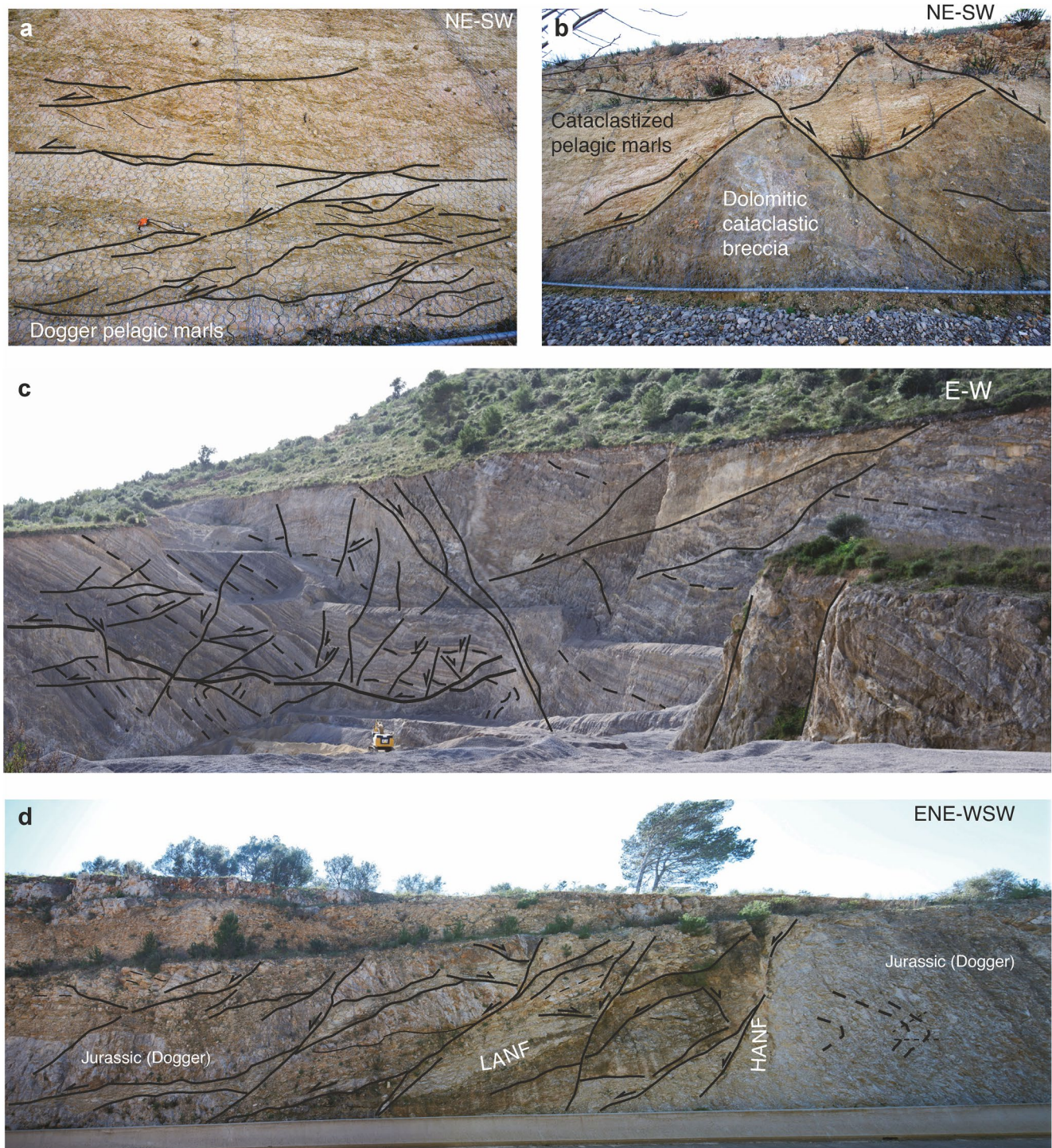
Figure 6. Extensional structures affecting the Mallorca FTB stack in the Llevant ranges. (a) Brittle extensional shear zone with NE-directed transport developed in Jurassic marls. (b) Extensional shear zone between Jurassic marls and Triassic dolostone cut by later SW-directed normal faults. (c) Extensional structures cutting through Triassic dolostone in a quarry nearby Manacor. (d) Low-angle normal fault system cutting through folded Middle Jurassic limestones and marls, later cut by high-angle normal faults with ENE-directed transport. Photo locations in Figure 3.
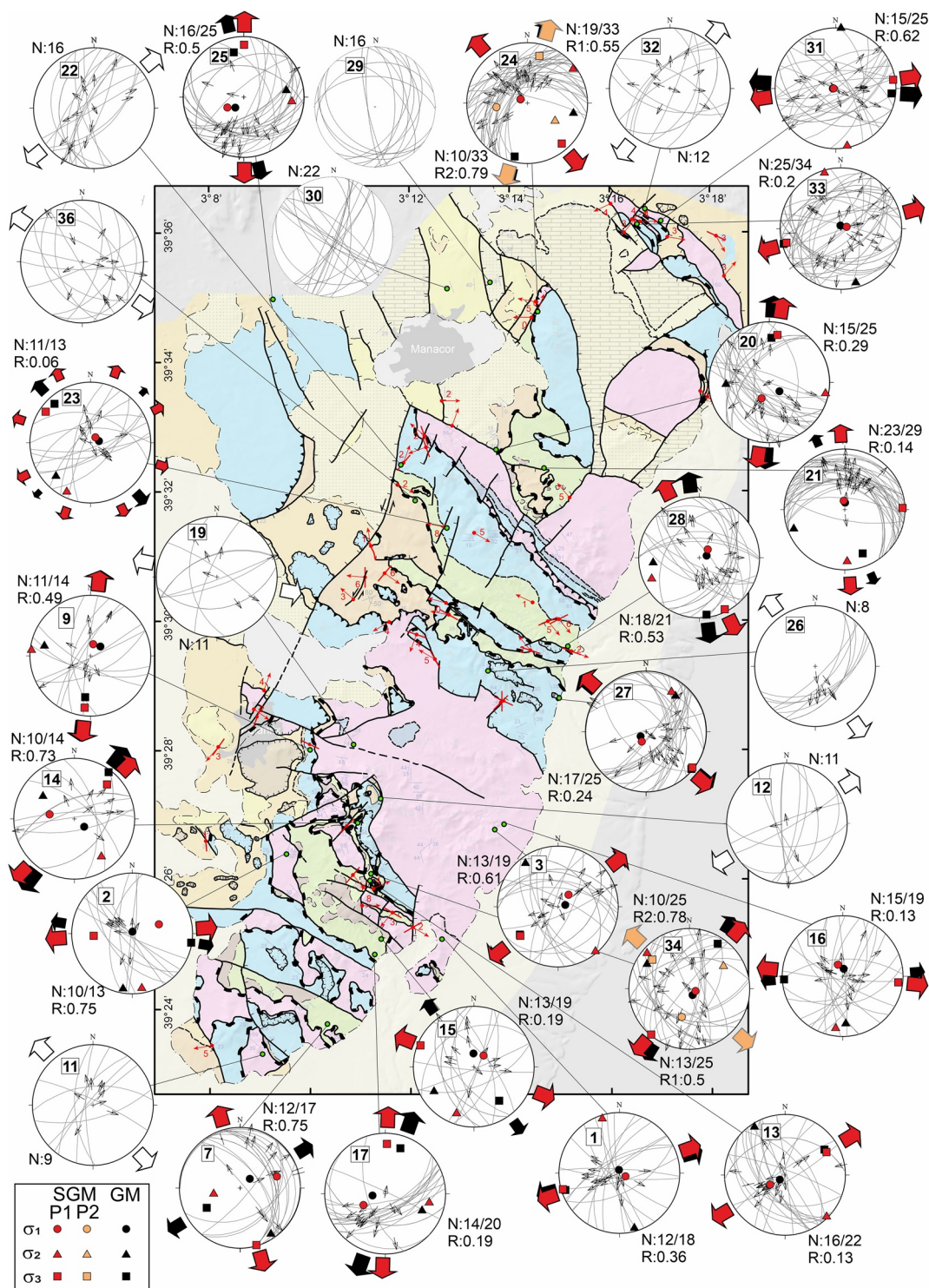
Figure 7. Fault measurement stations with paleostress results obtained through the Search Grid (SGM; Galindo-Zaldívar & González-Lodeiro, 1988) and Gauss paleostress methods (GM; Žalohar & Vrabec, 2007). Stereoplots being of equal area, lower hemisphere projections show faults with arrows indicating slip vectors and stress tensor results, main axes (square) and axial ratios (R, $(\sigma_2 - \sigma_3)/(\sigma_1 - \sigma_3)$) for different stress phases (P1–P2). Also, the main sigma three orientations are shown with black (GM), red (SGM), and white arrows (probable extension assumed from field measured kinematic criteria). The location of paleostress analysis stations and numerical results are presented in Table 1. N represents the number of faults, the first number, those used to determine the stress field; the second, for the number of faults measured in the field. If only one number is given, it represents measured faults in stations without sufficient data to determine a significant paleostress tensor.
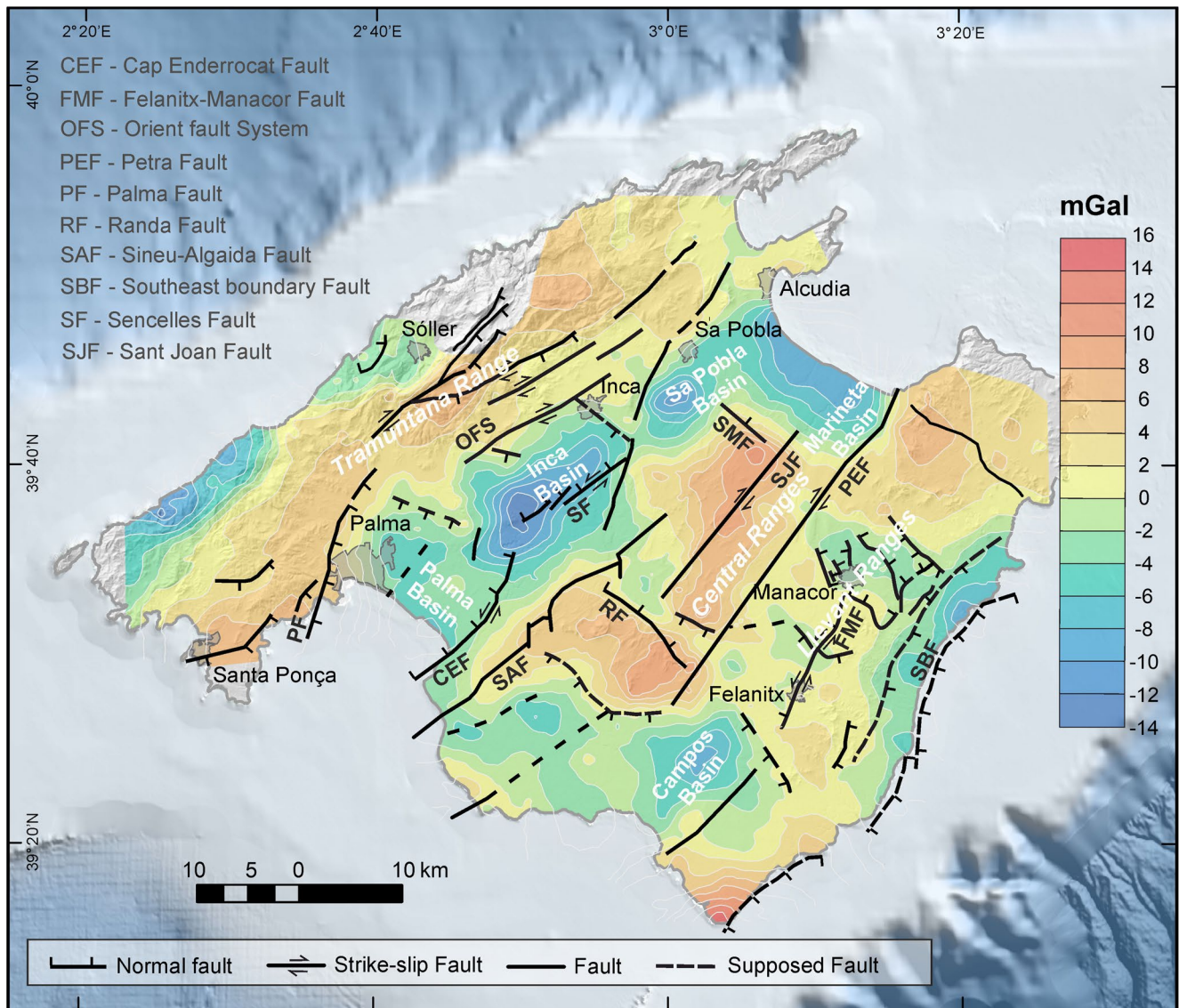
Figure 8. Residual gravity anomaly map of Mallorca (modified from Ayala et al., 1994; IGME, 2003) with main faults and Middle Miocene basins coincident with negative gravity anomalies.

indicate NE-SW extension (stations 20, 22, 24, 32, and 33). NW-SE extension is the dominant paleostress result obtained along the eastern side of the mapped region, for instance, at stations 16 and 26–28, and at stations 15 and 36 elsewhere. In a few fault stations the main extensional phase tended to be more N-S, as in paleostress stereoplots 9 and 25 (Figure 7).

4.3. Gravity Anomalies and the Extensional Structure of Mallorca

At the scale of Mallorca Island, larger grabens are evident in the regional gravity anomaly map. They produce negative anomalies that coincide with Serravallian sedimentary outcrops in the Inca, Sa Pobla, Marineta, Manacor, Campos, and Palma basins (Figure 8). The larger grabens show either NW-SE or NE-SW elongation and are offset laterally by NE-SW-oriented lineaments that coincide in most cases with NE-SW strike-slip faults, for example, the dextral Orient and Sant Joan faults (Booth-Rea et al., 2016) and the sinistral Sencelles (Mas et al., 2014) or Felanitx-Manacor faults (Figure 8). These strike-slip faults offset NW-SE oriented normal faults bounding the main sedimentary depocenters, as the Santa Margalida fault in the Marineta basin (Ramos-Guerrero et al., 2000), the Randa fault in the Central Ranges (Anglada-Guajardo

& Serra-Kiel, 1986), and the Manacor fault in the Llevant Ranges. We infer other possible NW-SE faults bounding the Inca, Campos and Palma basins, marked by segmented lines in Figure 8. In other cases, the lineaments may correspond to NE-SW oriented normal faults along the SE margin of the Llevant Ranges (Sabat et al., 2011), which could partially affect the Tortonian sediments, even though they seal extensional structures overall (Figure 3).

The grabens that coincided with topographic lows in the region show both NW-SE and SW-NE orientation, bounded by normal faults with these orientations. Following a general pattern, the normal faults bounding the grabens produce extension in two orthogonal directions (Figures 3 and 8). A large NE-SW elongated negative gravity anomaly occurs parallel to the Southeastern coast of Mallorca (Figure 8), which probably marks an important sedimentary depocenter determined by NE-SW trending faults such as the Southeast boundary Fault, probably active up to the Late Miocene, as observed offshore (Driussi, Maillard, et al., 2015).

4.4. Cenozoic Extensional Structures Deformed by Early Miocene Thrusting

Stratigraphic studies in Mallorca suggest that Oligocene to Aquitanian (≈29–23 Ma) continental deposits of the Cala Blanca Formation were coeval to extensional faulting (Martín-Closas & Ramos-Guerrero, 2005; Ramos-Guerrero et al., 1989, 2000). Notwithstanding, Paleogene extensional structures that formed before nappe tectonics in Mallorca have not been identified up to date. Here, we describe two well-preserved outcrops from the Northeastern Llevant Ranges and Tramuntana Range that serve to demonstrate the syn-extensional nature of these deposits.

The Capdepera semigraben is preserved Northeast of Mallorca (Figures 1b and 9). The semigraben structure is filled by a continental carbonate breccia body with a wedge geometry that shows an internal fan-shape progressive unconformity, where the breccias dip between 55° and 15° toward the SE (N150°E; Figures 9, 10a, and 10b).

The breccia is formed by angular fragments of mostly Jurassic limestone and Triassic dolostone (Bourrouilh, 1983). It is affected by high-angle normal faults with meter-scale spacing. In some cases, these faults are defined by clastic dikes, formed by soft-sediment deformation during faulting (Figure 10c), frequently permeated by a tar matrix. At the base of the wedge, the breccia is separated from underlying Jurassic limestones by a low-angle normal fault with NW-directed transport (the Capedera LANF; Figure 10d). This LANF presently dips ∼10° toward the SE in its northern outcrops, where it occurs in the hangingwall of a normal fault that eventually cuts it. In turn, it dips gently toward the SW on the footwall, to the Southeast (Figures 9 and 10e). The transport sense is defined by several kinematic criteria including the offset of sedimentary bedding, rotation of older bedding layers, and orientation of Riedel faults (see stereoplot a in Figure 9). Some of the normal faults cutting the breccia detach along this low-angle fault surface (Figure 10d). The Capdepera LANF is cut and displaced by other high-angle normal faults that cut through the breccia wedge, so that the breccia shows changes in facies and thickness, with finer grained clastics and thicker deposits over the hangingwall (Figures 9 and 10e). These faults are also permeated by black hydrocarbons. All the above extensional structures show NW-directed tectonic transport (Figures 9a and 10b–10e).

The southern boundary of the breccia wedge is a subvertical fault zone that separates Triassic dolostones to the south from Jurassic limestones and the overlying Oligocene breccia to the north (Figure 10f). This fault zone shows complex kinematics with two different sets of striae. The older set shows down-dip normal displacement marked by striations and grooves. Meanwhile, the footwall of the fault is affected by pervasive steeply SE-dipping faults with NW-directed reverse kinematics marked by stepped calcite fibers. In the proximity of the main bounding fault, the breccia shows a subvertical, SE-dipping spaced and anastomosed stylolithic cleavage (Figure 11a). The stress field determined using calcite stepped fibers from the thrust planes indicates a prolate NW-SE compressional ellipsoid in Capdepera (steroplot b in Figure 9). Finally, the fault surface has late horizontal slickenlines indicating dextral strike-slip kinematics (stereoplot c in Figure 9). This small outcrop is preserved between, and cut by, three strike-slip faults: a sinistral NW-SE striking one, plus two younger dextral NE-SW ones that also offset the sinistral fault (Figures 9 and 11b). The stress field determined from the latter strike-slip faults that crosscut the Capdepera graben gives an oblate transcurrent stress field having a main WSW-ENE-directed horizontal shortening axis (stereoplot c in Figure 9).
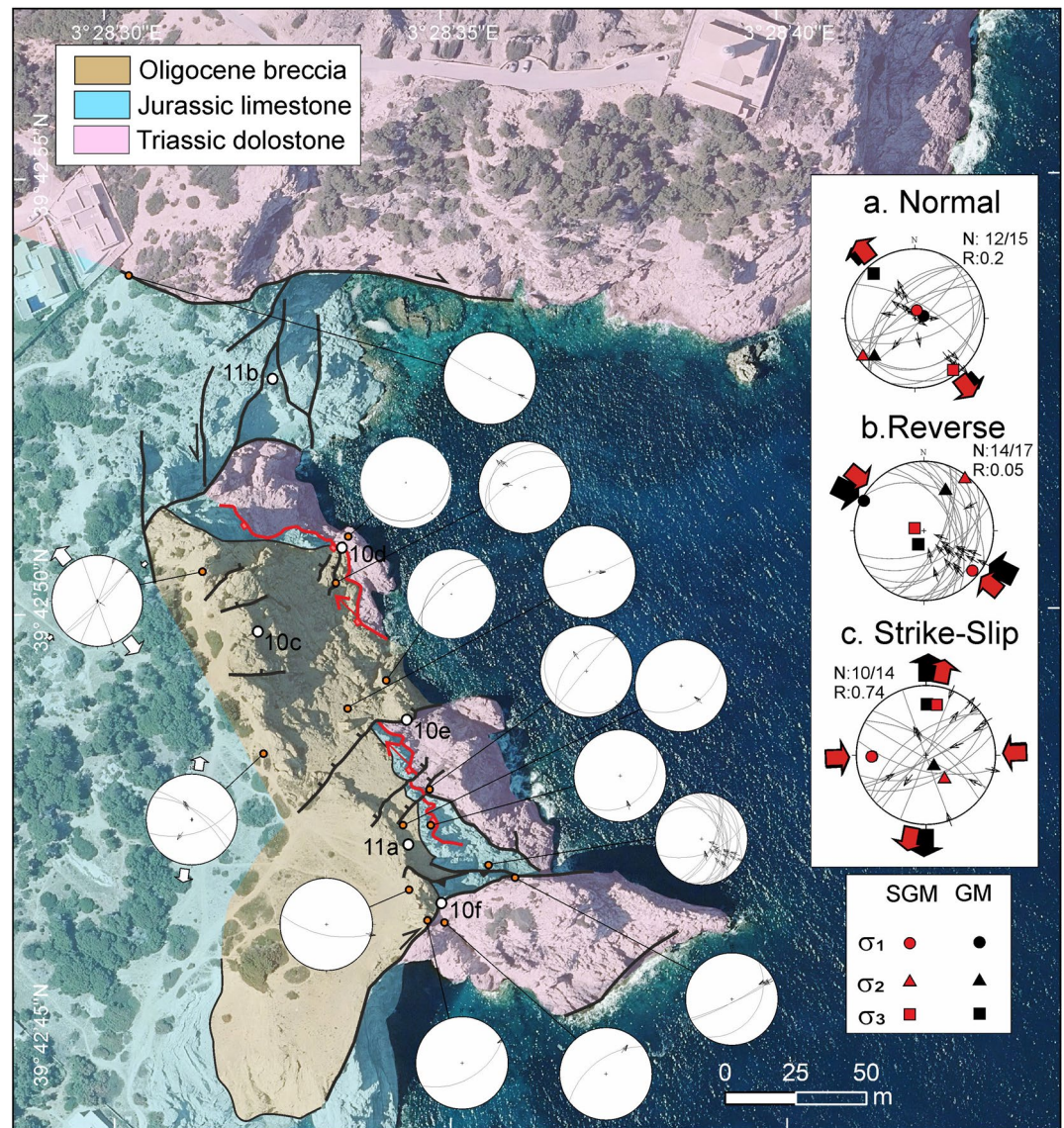
Figure 9. Structural map of the Capdepera Oligocene semigraben. Stereoplots of equal area; lower hemisphere projections show faults with arrows indicating slip vectors. Streoplot of paleostress results sorted by fault kinematics, axis (square), and axial ratio of each phase (R, $(\sigma_2 - \sigma_3)/(\sigma_1 - \sigma_3)$) of stress tensors. σ_1 and σ_2 axes are shown with black (GM), red (SGM), and white (kinematic criteria) arrows. White dots, location of photos in Figures 10 and 11. The Capdepera LANF with NW transport is depicted in red.

The Oligocene Cala-Blanca conglomerates mapped in the 1:50,000 MAGNA maps of Soller and Inca (Olmo-Zamora et al., 1981, 1982) in the Tramuntana ranges show further strong evidence of being deposited during activity of NW-directed listric low-angle normal faults. In several cases—for example, in Penya de sa Bastida in Alaro, in Biniarroi and to the W of Lloseta (red stars in Figure 1b)—the Cala-Blanca conglomerates appear detached over Cretaceous marls across a low-angle fault with NW-directed transport. The Cretaceous marls show penetrative deformation by C′-type shear bands, thus indicating NW to WNW hangingwall transport. The Cala-Blanca conglomerates are also strongly faulted by high-angle normal faults, mostly antithetic to the underlying LANF. Furthermore, some of the faults are defined by clastic dikes indicating soft sediment deformation.

Oligocene extension is likewise evident in Solleric, to the East of Orient (location in Figure 1b). Here, the Cala-Blanca conglomerates outcrop forms a 2 km long NE-SW oriented ridge that is imbricated between
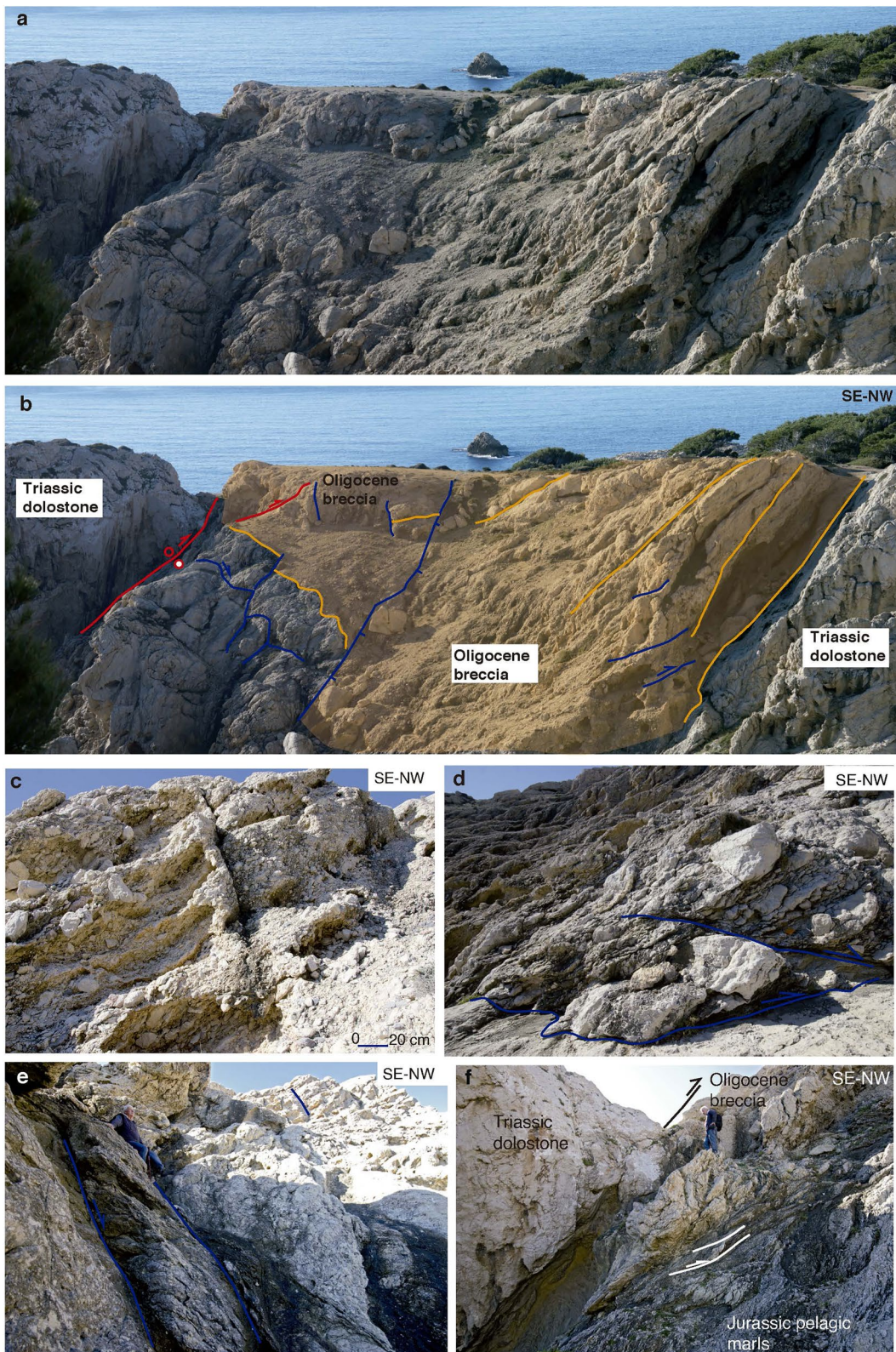
Figure 10.

two WNW-directed reverse faults. The underlying one overthrusting the Oligocene conglomerates and their underlying Jurassic basement, upon Cretaceous marls. Meanwhile, the Oligocene Solleric ridge is overthrusted by Triassic dolostones and overlying Liassic limestones (Figure 11c).

The Cala-Blanca conglomerates dip mostly 50°–60° toward the SE (stereoplot in Figure 11d), although the dip-angle decreases at the top of the section, marking an internal angular unconformity. The basal contact is a LANF separating Oligocene conglomerates in the hangingwall from underlying Cretaceous and Jurassic marls and marly-limestones. The LANF dips gently toward the NE; slicken-lines indicate transport toward N310°E (see fault kinematic data after rotating to undo bedding tilt, Figure 11e). Toward the NW the fault steps down into Early Jurassic platform limestones (Figure 11c). Lenses of Cretaceous marls bounded by low-angle faults occur between the Oligocene conclomerates and the underlying Jurassic sequence. The Cala-Blanca conglomerates are intensly faulted by normal faults that root into the underlying LANF (Figures 11b and 11f); within the conglomeratic sequence they display a complex deformation history, with tilted conjugate sets of faults where the normal fault synthetic to the main underlying LANF dips 20° to the NW, whereas the antithetic fault tilts 80° toward the SE (Figures 11d and 11g). These tilted conjugate faults are moreover cut by posterior sets of untilted faults. Pre-diagenetic extensional deformation in these conglomerates is also evident, with the presence of clastic dikes indicating WNW-ESE directed extension. The paleostress field determined from small-scale faults that cut the Oligocene breccias in the Solleric ridge shows an oblate shape ellipsoid ($R = 0.77$) giving NW-SE extension, though the normal faults measured in Capdepera give a prolate ($R = 0.20$) NW-SE extensional stress field (Figures 11e and 9a, respectively).

The Solleric ridge is cored by Liassic limestones that define an open NE-SW trending anticline which, in turn, folds the overlying LANF and Middle Jurassic to Oligocene sedimentary sequence. In the southeastern limb of the anticline, the normal faults cutting the Oligocene conglomerates are further rotated, so that both conjugate fault sets appear as reverse faults dipping gently toward the SE and NW, while the bedding of the Cala-Blanca conglomerates and underlying middle Jurasic marls dips 70° toward the SE.

4.5. Age of Post-Nappe Extension

Deformation related to the development of the Mallorca FTB reaches up to the Late Burdigalian-Langhian calcirudites of the Randa formation (Donoso et al., 1982; Pomar & Rodríguez-Perea, 1983) marked by a spaced stylolithic cleavage in the Mallorca Central Ranges, imbricated in the thrust stack in the Tramuntana Range (Gelabert, 1998). Concerning extension, both systems of normal faults producing NE-SW and NW-SE-directed extension affect Serravallian sediments in the mapped region of the Llevant Ranges (Figures 3 and 7). See for example fault kinematic stations 29 and 30, respectively, measured on Serravallian and Langhian sediments, and photos of the sediments tilted by these normal faults in Figures 12a and 12b. Furthermore, the main boundaries of the basins hosting these sediments are defined by normal faults of the two orthogonal extensional systems that cut Serravallian sediments (see kinematic arrows on faults bounding the sediments in Figure 3, cross-sections in Figure 4, and photos of the Manacor quarry in Figure 12c). A number of Serravallian outcrops moreover show progressive unconformities where the alluvial sediments have decreasing dip up-sequence from 40° to 0°. Thus, the infilling of the Manacor basin can be characterized by wedge-shaped Serravallian sedimentary syn-rift bodies (cross-sections in Figure 4). This feature is also evidenced by the strong thickness changes manifested by Serravallian sediments in the Mallorca basins, observed as lows in the gravity anomaly map of Figure 5 and pointed out by previous authors in the Margalida and Inca basins, where this sequence reaches a thickness of 1,000 m in the later (Benedicto et al., 1993; Ramos-Guerrero et al., 2000).

Most of the LANFs mapped in the Llevant Ranges—and in the main extensional fabrics general—that thin the region show NE-SW kinematics (Figure 7). These LANFs are frequently cut by later listric higher-angle

Figure 10. Oligocene extensional structures in the inverted Capdepera semigraben. (a) Panoramic view of the Capdepera Oligocene semigraben. Notice progressive unconformity developed in the Oligocene breccia wedge (b). Interpretation of the structure of the Capdepera semigraben. (c) Small-scale normal fault cutting through the Capdepera Oligocene breccia, marked by the development of a clastic dike. (d) Detachment at the base of the Capdepera graben, between Oligocene breccia in the hangingwall and Triassic dolostone in the footwall. Notice small Riedel faults rooting into the detachment. (e) High-angle normal fault that cuts through the Capdepera detachment, permeated by a black tar matrix. (f) Main high-angle fault bounding the Capdepera semigraben, inverted as a reverse and later dextral strike-slip fault. Note strongly sheared Jurassic pelagic marls with abundant shear criteria and calcite veins.
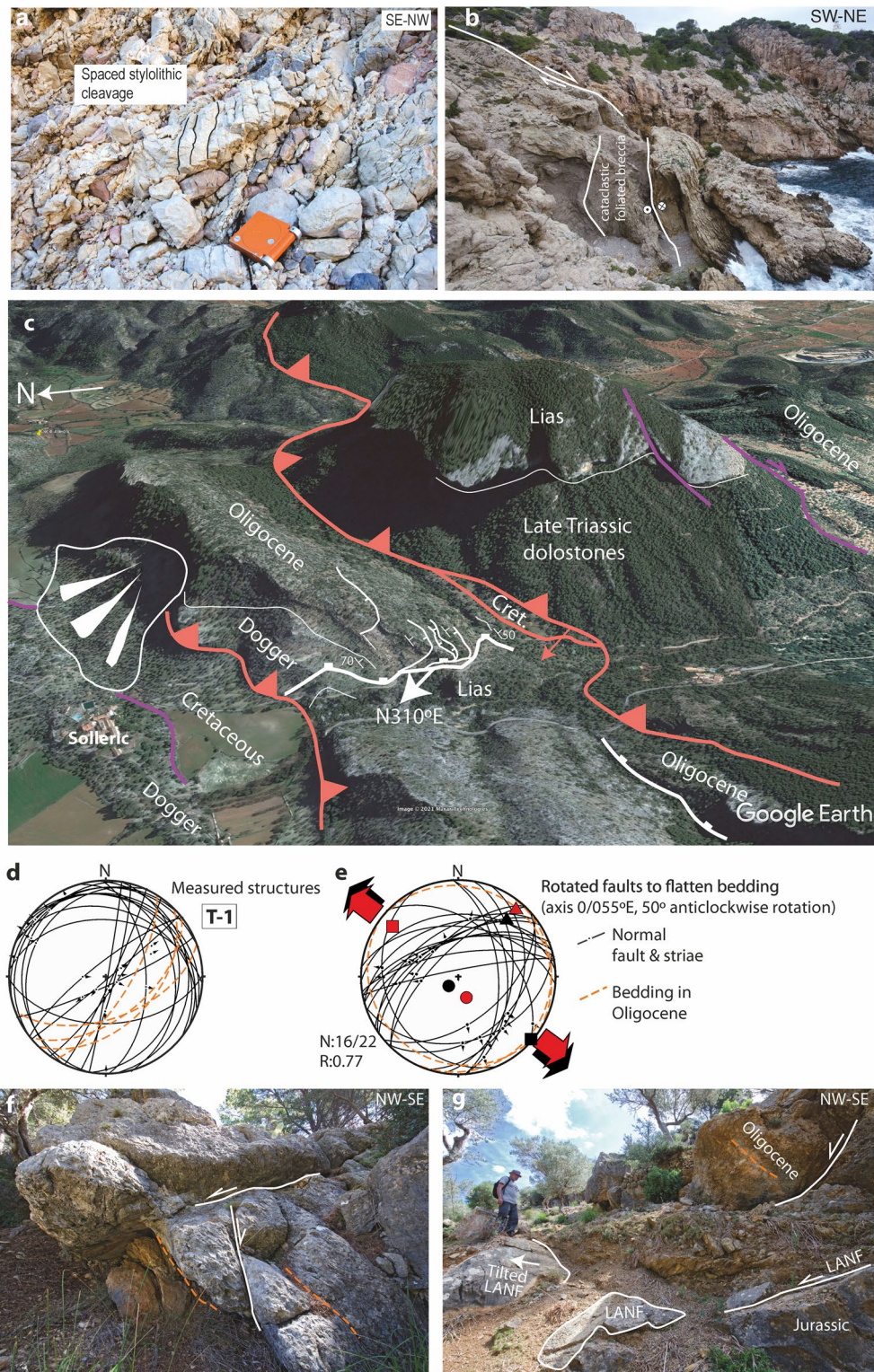
Figure 11.

Figure 12. Early and Middle Miocene sediments from the Manacor basin cut by post-FTB extensional faults. (a) Late Burdigalian to Langhian calcirudites cut and tilted by the activity of Serravallian normal faults with NE-directed transport from the locality were fault station 30 in Figure 7 was measured. (b) Serravallian syn-rift sediments in the same road cut as c, also tilted and cut by normal faults (where fault measurement station 29 was obtained). (c) NE-directed normal fault between Triassic dolostone and Serravallian conglomerates and silts at the southern border of the Manacor depocenter. The photograph locations are shown in Figure 3.

faults with the same kinematics as bounding the Serravallian basins. In turn, normal faults producing NW-SE extension are generally high-angle structures that cut the previous extensional system. Hence we infer a clearly crosscutting relationship, indicating that NW-SE extension occurred after NE-SW extension. Both systems of normal faults appear to be sealed by late Miocene limestones along the SE border of the Llevant Ranges (Figure 3).

Figure 11. Foto-panel showing Miocene structures in Capdepera, and Oligocene ones at Solleric in Tramuntana. (a) Spaced stylolithic cleavage affecting the Capdepera Oligocene breccia. (b) NE-SW dextral and NW-SE sinistral strike-slip faults cutting the Capdepera semigraben. Notice subvertical fold affecting Jurassic marls within the sinistral fault zone. (c) Google Earth 3D view of the Oligocene Solleric ridge in the Tramuntana ranges. Notice the LANF (white) cut by later thrusts in orange. The Oligocene beds are strongly tilted and cut by normal faults that root in the LANF, which cuts down toward the NW into Early Jurassic limestones. (d) Stereographic projection of faults and striae affecting Oligocene conglomerates. (e) Same data as in (d), rotated to flatten bedding in Oligocene conglomerates. Note two conjugate sets of normal faults producing NW-SE extension. Paleostress legend in Figure 7 (f) Oligocene Cala Blanca breccias cut by a conjugate set of normal faults that are tilted toward the SE. (g) Basal contact of the Solleric Oligocene conglomerate tilted over a LANF that cuts an older fault surface. Both with NW-directed transport.

5. Discussion

Most authors have interpreted that the structure of the Llevant ranges was chiefly controlled by the Early Miocene thrusting and growth of the Mallorca FTB, where all tectonic contacts are interpreted as thrusts or lateral ramps of the thrust system. This resulted in the imbrication of up to seven nappes formed by Triassic to Early Miocene sediments (Casas & Sabat, 1987; Parés et al., 1986; Sabat et al., 1988). Related to this shortening, the rocks in the Llevant and Tramuntana ranges folded, locally showing a spaced anastomosed stylolitic cleavage. The folds and related kinematic structures, for example, calcite fibers growing on the folded bedding, show variable orientation among different localities, indicating reverse WNW- to W-directed displacement (Casas & Sabat, 1987; Gelabert et al., 1992). Our data also indicate variable directions of shortening, with SW-directed vergence in the deeper Nappe I south of Manacor (stereoplot b with NW-SE oriented fold axes and intersection lineation in Figure 3) and westward to southwestward vergence in Nappe III, in localities near Felanitx (stereoplots a and c in Figure 3).

Nonetheless, our main finding is that Mallorca underwent two Tertiary extensional phases before and after the development of its FTB during the Early Miocene. The first phase of extension occurred in the Oligocene (29–23 Ma) during the deposition of the Cala Blanca alluvial conglomerates; the second during the Middle Miocene (14–11 Ma). The latter extensional phase preserved the lithological repetitions established during the Mallorca FTB development, but only very rarely are the original thrust surfaces preserved, having been cut or reworked by the subsequent extensional fault system (Figure 3 and cross-sections in Figure 4). LANF with flat and ramp geometry developed in the wake of heterogeneous stratigraphic rheology owing to the crustal stack of the Mallorca FTB, where weak pelagic marls alternate with stronger dolostone and limestone lithologies (Figure 6d). Extensional tectonics were polyphasic, with main faults cutting older LANF, partly sealed by Serravallian syn-tectonic sediments. It is noteworthy that the LANF cut down into the structural pile, producing omission in the direction of transport (Figure 4b and 4b′). Here we integrate the newly observed extensional phases into the previously established Early Miocene FTB framework of development in Mallorca; they are furthermore included in a revised geodynamic evolution for the Western Mediterranean covering the period from the Eocene to the Middle Miocene (Figures 13–16).

5.1. Eocene Tectonic Setting for the BP

Our analysis of the geodynamic evolution of the BP and the Western Mediterranean stems from the Eocene (Figure 13). Eocene continental and shallow marine sediments seal a period of topographic development and erosion in Mallorca reportedly related to Palaeogene shortening that affected diverse mountain belts of the western Mediterranean, including the Pyrenees, the Iberian Chain, the Catalan Coastal Ranges, the Atlas, and the AlKaPeKa orogen (e.g., Azañón et al., 1997; Balanyá et al., 1997; Bouillin et al., 1986; Guimerà et al., 2004; Ramos-Guerrero et al., 1989; van Hinsbergen et al., 2014; Verges et al., 2002; Figure 2). Based on published data—mostly from the Alboran domain in the Betics—we propose that the BP formed the hinterland of the Alboran and Kabilyan (AlKa) domains of the Paleogene AlKaPeKa orogen (Figure 13). Remains of the AlKa orogen segment are now represented by the Alpujarride-Malaguide and Sebtide-Ghomaride thrust stacks in the Betics and Rif, formed by continental rocks compatible with a North Iberian Massif origin, according to detrital zircon age populations; thus they would correspond to the nearby Paleozoic sequence of Menorca and the Catalan Coastal Ranges (Azdimousa, Jabaloy-Sánchez, Talavera, et al., 2019; Jabaloy-Sánchez et al., 2021; Martínez et al., 2016). The lower plate of this continental subduction system was represented by the Alpujarride-Sebtide complex, which underwent HP/LT metamorphism (e.g., Azañón et al., 1997; Booth-Rea et al., 2002; Goffé et al., 1989) dated as Paleocene-Eocene based on Ar/Ar in phengite (Bessière et al., 2021; Marrone et al., 2020, 2021; Platt et al., 2005). The Ronda peridotite represents the subcontinental lithospheric section of the Alpujarride, and probably reached its primary conditions recorded in garnet lherzolite facies under 2.4–2.7 GPa and 1020°C–1100°C at this time (Garrido et al., 2011; Figure 13). Subduction of the East Ligurian Tethys would not yet have initiated in the AlKa domain, considering the absence of Eocene arc volcanics in the Betics-Rif and Tell orogenic belts, although they do occur in Sardinia, corresponding to the PeCa orogenic segment of AlKaPeKa (e.g., Lustrino et al., 2011; Figure 13).
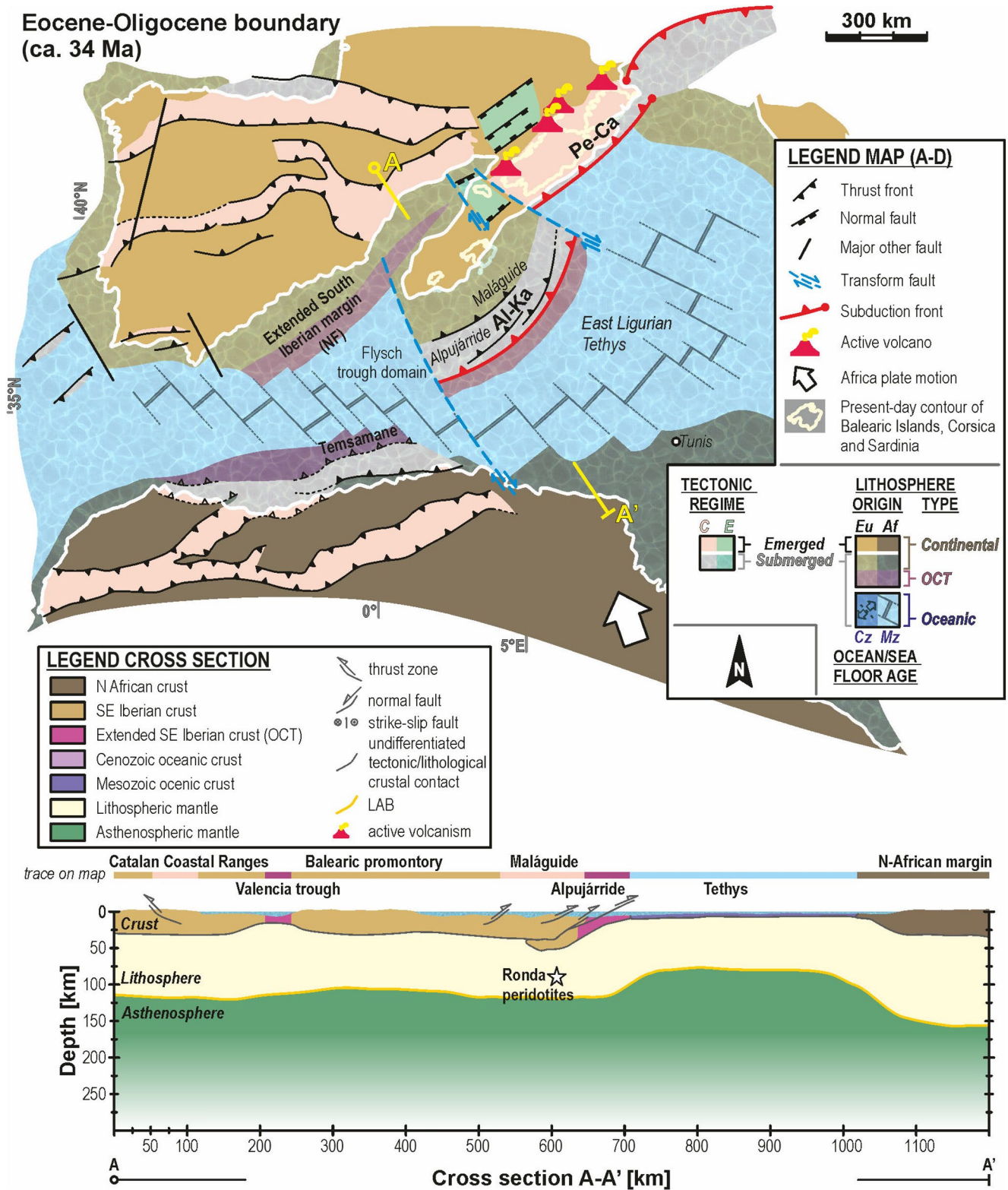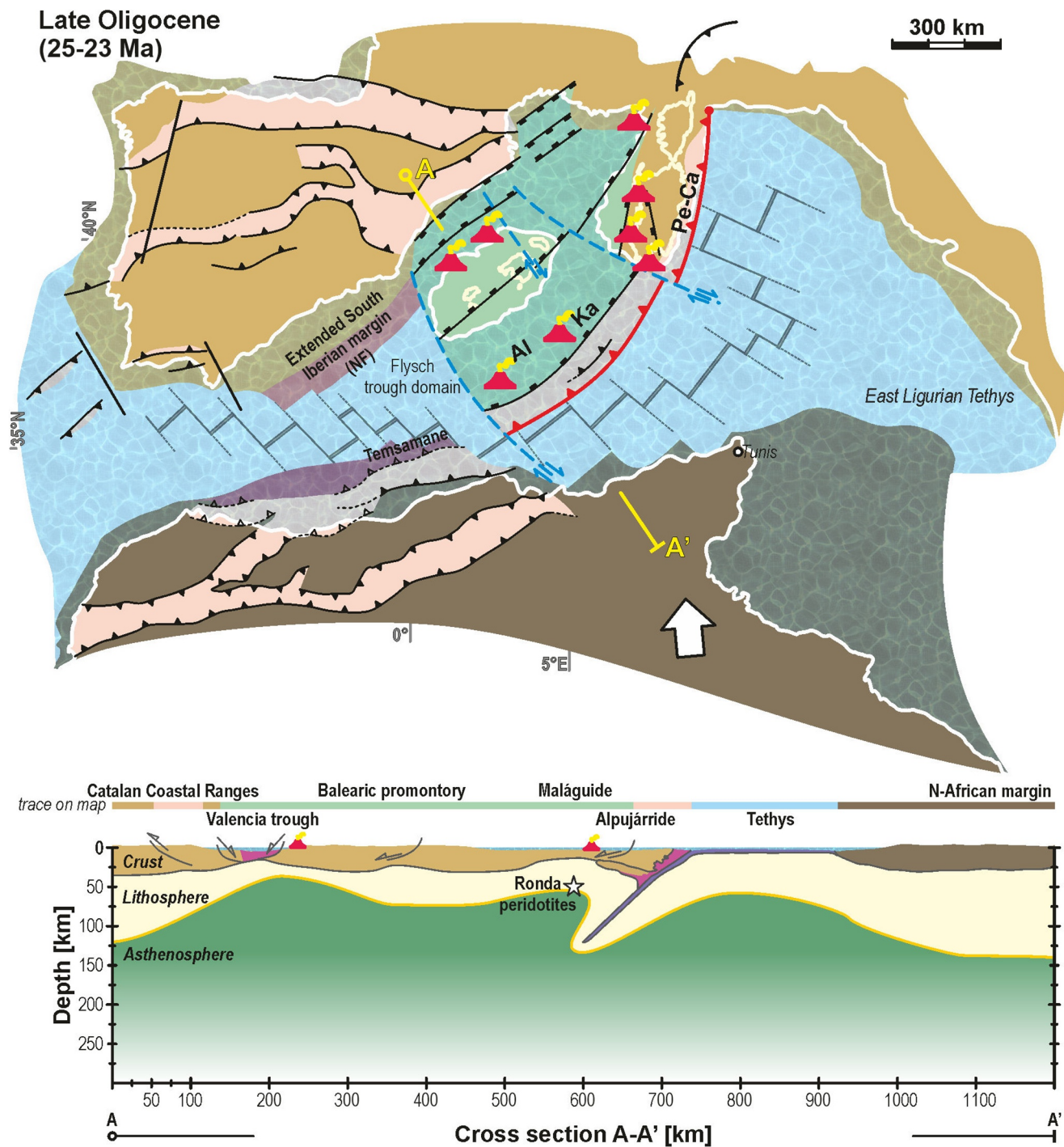
Figure 13.

Figure 14. Geodynamic reconstruction for the Western Mediterranean in the Late Oligocene to Early Miocene (25–23 Ma). Ronda peridotite location from Booth-Rea et al. (2005) and Garrido et al. (2011). Legend in Figure 13.

Figure 13. Geodynamic reconstruction of the Western Mediterranean for the late Eocene (34 Ma) and lithospheric-scale cross-section across the Balearic promontory and the continental AlKa orogen. Abbreviations in the map: Al, Alborán domain; Ka, Kabylia; Pe, Peloritan domain; Ca, Calabria; NF, Nevado-Filábrides; GK, Grande Kabylie; PK, Petite Kabylie. Abbreviations in the legend: OCT, ocean-continent transition; C/E, compressive/extensional active tectonics; Eu/Af, European/African origin of the lithosphere; Cz/Mz, Cenozoic/Mesozoic age of the seafloor and ocean floor, respectively. The Africa plate motion and the paleo-position of the city of Tunis are shown after Handy et al. (2010) in each stage. Ronda peridotite location from Booth-Rea et al. (2005) and Garrido et al. (2011). See Section 3 for further details on the reconstruction.
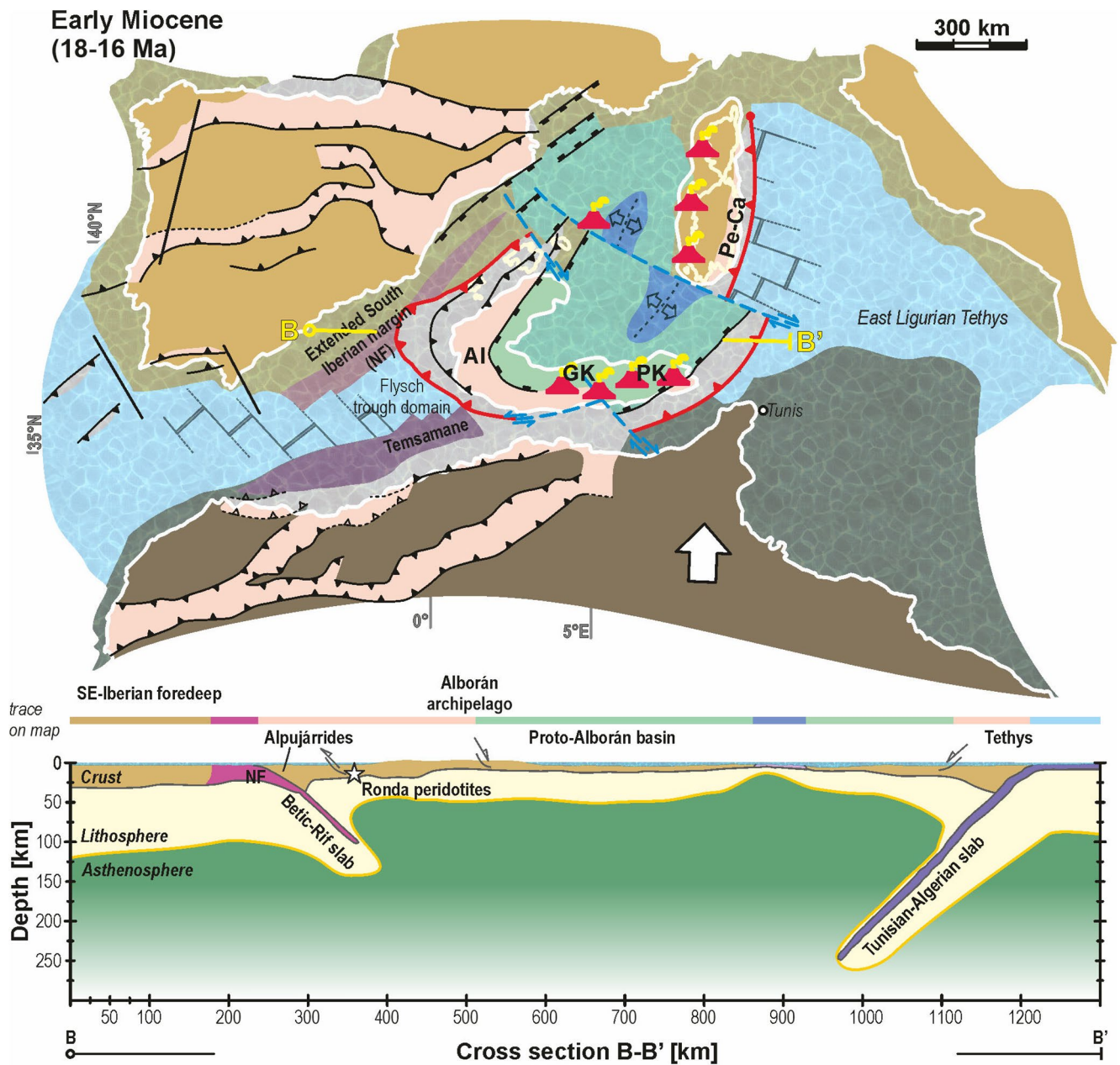
Figure 15. Geodynamic reconstruction for the Western Mediterranean in the Early Miocene (18–16 Ma). Ronda peridotite location from Booth-Rea et al. (2005) and Garrido et al. (2011). Legend in Figure 13.

5.2. Oligocene Extensional Detachments and Grabens

The Oligocene is represented in Mallorca by the Cala Blanca conglomerates. They are stratigraphically dated, using charophytes and rodents, as Chattian to Aquitanian (e.g., Adrover et al., 1977; Martín-Closas & Ramos-Guerrero, 2005). The breccias in Capdepera have not been dated directly. However, because these breccias share the same facies of the Cala Blanca formation, and are affected by spaced stylolitic cleavage as well as cut by meter-scale reverse faults related to the Early Miocene thrusting, they are necessarily older than the Mallorca FTB. The extensional system observed in Capdepera indicates a process of sequential extension, the development of LANF systems with NW-directed hangingwall transport being cut by posterior high-angle normal faults (Figures 9 and 10b). Such extensional geometry is typical of highly extended terrains (Booth-Rea et al., 2004; Martínez-Martínez et al., 2002; Serck et al., 2020). Moreover, the Solleric
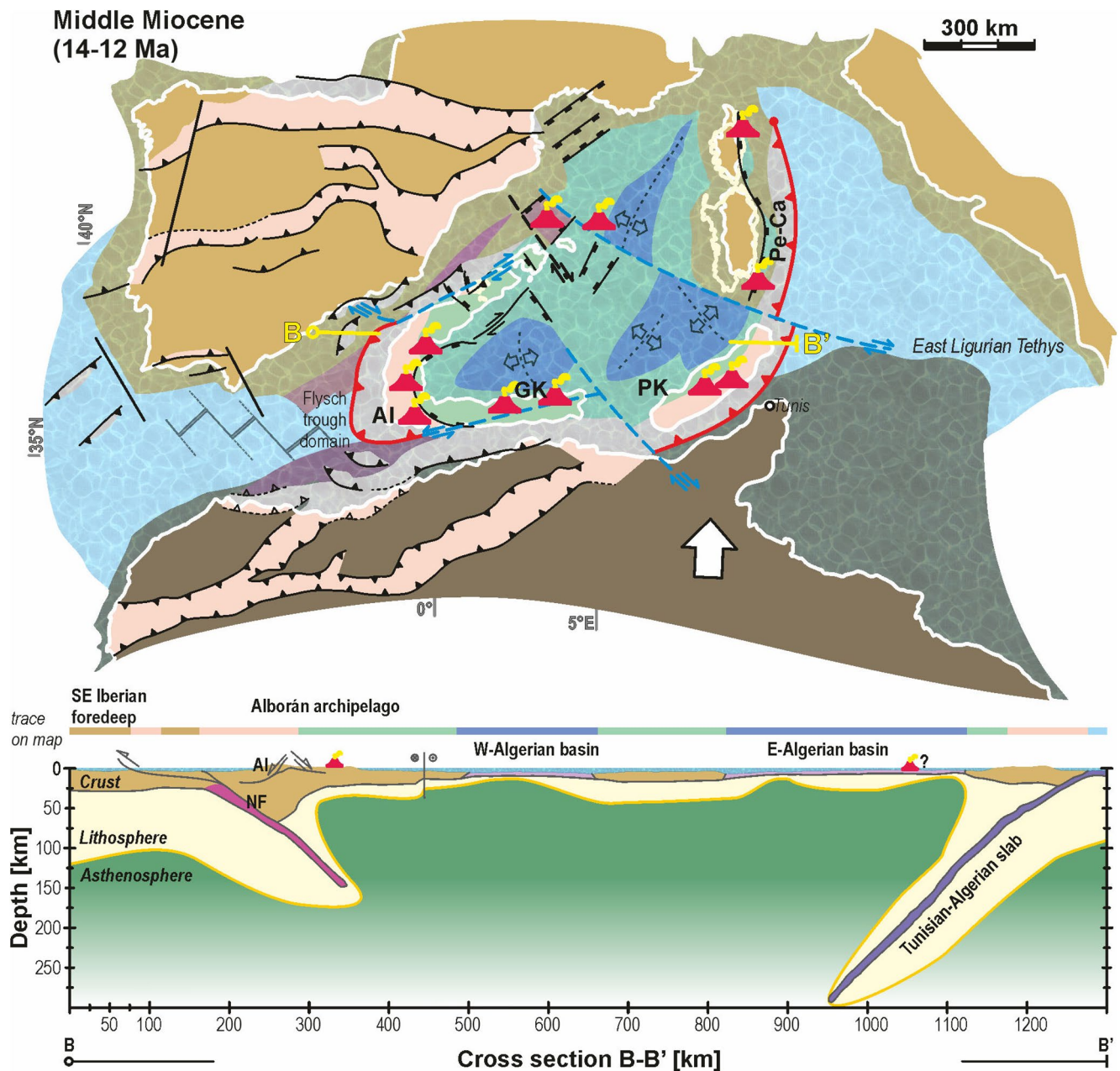
Figure 16. Geodynamic reconstruction of the Western Mediterranean region for the Middle Miocene time period. Legend in Figure 13.

Ridge in the Tramuntana Ranges forms a large Oligocene extensional block tilted ~50° and detached over a LANF that cuts down into the Early Jurassic sequence, with its NW-directed hangingwall transport.

The internal unconformity within the Oligocene conglomerates and evidence of pre-diagenetic deformation in the rocks suggests they were deposited coeval to the extensional deformation, which clearly pre-dated the Mallorca FTB. Sequential extension tilting older faults and later folding made older LANFs appear to be thrusts, with upward hangingwall displacement (e.g., the Capdepera and Solleric LANFs, Figures 10d and 11g). Further outcrops in the Tramuntana ranges involve low-angle normal faults with northwestward transport, affecting the Oligocene and underlying Mesozoic sequence, then cut by later thrusts (red stars in Figure 2b). Hence, kinematic data and paleostress fields derived from these fault systems in Capdepera and Solleric (Figures 9a and 11e) support a phase of NW-SE directed extension in Mallorca during the Oligocene. The Oligocene northwards extension probably pre-dates half-grabens and low-angle detachments

in Menorca, dated around 35–28 Ma (Martín-Closas & Ramos-Guerrero, 2005; Sabat et al., 2018), and Ibiza (Etheve et al., 2016), overlapping the opening of the Liguro-Provencal basin (Cherchi & Montadert, 1982; Ferrandini et al., 2003; Rehault et al., 1984; Schettino & Turco, 2006; Speranza et al., 2002). We did not analyze the potential role of older Mesozoic extension identified in the Valencia Trough and Catalan Coastal Ranges (Etheve et al., 2018; Marín et al., 2021), most likely taking place in Mallorca under similar kinematics as in the Oligocene.

Oligocene to Early Miocene extension has been described at different lithospheric depths in the part of the Alboran domain that now crops out in the Internal Betics, for example in the Ronda subcontinental peridotite sequence (Bessière et al., 2021; Booth-Rea et al., 2005; Garrido et al., 2011; Precigout et al., 2013); or at shallower crustal depths, with low-angle normal faults and detachments denudating the Paleogene Alpujarride-Sebtide-Malaguide thrust stack (Booth-Rea et al., 2004, 2005; Lonergan & Platt, 1995; Marrone et al., 2021). This extension affected the AlKa segment of the AlKaPeKa orogenic domain, formed during the Late Cretaceous to Palaeogene, whose hinterland is expressed as the BP (Figure 13). Late Oligocene extension, around 25 Ma, is likewise described in the Kabylies (Saadallah & Caby, 1996). Furthermore, Eocene to Aquitanian (40–23 Ma) depleted gabbros are described in the Kabylies, having formed either backarc or forearc oceanic crust of a proto-Algerian basin (Abbassene et al., 2016; Chazot et al., 2017; Fernandez et al., 2020). Such Oligocene extension in a back-arc type setting is described for the entire Mediterranean realm, and attributed to a decrease in absolute northward motion of Africa triggered by the Africa/Arabia-Eurasia collision that slowed down Africa (Jolivet & Faccenna, 2000).

In sum, our work supports a generalized extensional suprasubduction setting for the late Oligocene in the Western Mediterranean (Figure 14), a panorama that could explain contradictory hypotheses for the development, for example, of the Valencia trough, where both Mesozoic and Tertiary extensional phases have been proposed (Etheve et al., 2018; Roca & Guimerà, 1992).

5.3. Early Miocene FTB Development

Shortening and tectonic inversion followed in the Early Miocene. For instance, the main high-angle normal faults bounding the Capdepera graben were inverted, as attested by a second family of slicken lines defined by calcite fibers, thus indicating NW-directed reverse kinematics, a related spaced cleavage, and small-scale reverse faults (stereoplot 9b and Figures 10f and 11a). Furthermore, the Oligocene extensional structures are cut by thrusts and folded in the Tramuntana range and Capdepera (Figures 9, 10f, 11a, and 11c).

Shortening structures measured in this work show variable orientations with fold vergence and thrust transport toward the NW to SW (stereoplots in Figures 3 and 9b). However, the significance of this variability in the orientation of kinematic data is not clear. Paleomagnetic rotations in the Llevant and Tramuntana Range affecting folded structures with orthogonal strikes, respectively, NW-SE and SW-NE, give similar values of 40° clockwise rotation, suggesting that these structures formed originally at 90° (Freeman et al., 1989). Other paleomagnetic results from Mallorca indicate variable amounts of both clockwise and anticlockwise rotations affecting Early Miocene sediments and volcanics, interpreted to have occurred in the Early Miocene thrusting phase and during later extension (Parés & Roca, 1996). Therefore, new paleomagnetic data—for example, from the application of fold tests and sampling the whole Cenozoic sedimentary sequence—are probably necessary before we can secure a clear idea of the original orientation of the Mallorca FTB and earlier structures. At any rate, the existence of folds trending orthogonally between the Tramuntana and Llevant ranges could reflect the original curvature of the Betic-Rif arc during the Early Miocene.

The Mallorca FTB is interpreted to have formed between the Late Oligocene and the Langhian (e.g., Gelabert, 1998; Sabat et al., 2011), though we find that most nappes in the Llevant ranges have the Sant Elm formation at the top, dated as Burdigalian (Rodríguez-Perea, 1984). Early Miocene rhyolites of the Puig de l'Ofre, dated by K-Ar on sanidine phenocrysts at 19 Ma, along with Langhian sediments, are imbricated in the thrust stack at the Tramuntana Range (Marti et al., 1992; Mitjavila et al., 1990). Accordingly, the main FTB building phase would have been shorter in duration, between the Burdigalian and the Langhian (19–14 Ma; Figures 2 and 15). This timing and its WNW- to NW-directed kinematics coincide with the main deformation phase in the External Betics and the Flysch Trough accretionary wedge, including Burdigalian

sediments in the nappe stack (e.g., de Capoa et al., 2007; Guerrera et al., 2005; Luján et al., 2006). FTB development in the Betics and the Gulf of Cadiz continued at least until the Late Miocene (Iribarren et al., 2007; Jiménez-Bonilla et al., 2016; Martín-Martín, Guerrera, et al., 2018), accompanied by important strike-slip faulting (e.g., de Galdeano & Vera, 1992; Geel & Roep, 1998; Jiménez-Bonilla et al., 2020; Martín-Martín, Estévez, et al., 2018; Pérez-Valera et al., 2013).

The Mallorca FTB development was coeval to the ESE-directed continental subduction of the South Iberian passive margin that underwent HP/LT metamorphism during the Early to Middle Miocene to the Southwest of Mallorca (e.g., Booth-Rea et al., 2015; Kirchner et al., 2016; López Sánchez-Vizcaino et al., 2001; Platt et al., 2006; Figure 15). As mentioned in the geological setting, older Palaeogene ages have been published for the South Iberian Nevado-Filabride units (Augier, Agard, et al., 2005; Augier, Jolivet, & Robin, 2005; Li & Massonne, 2018) and questioned in light of the Early Miocene age obtained from older mineral phases such as garnet (Platt et al., 2006), or the possible excess of meteoric Ar incorporation suggested by de Jong et al. (2001).

At an early stage of this renewed contractive reorganization, the Alpujarride complex underwent its final northward-directed thrusting phase, involving the previously thinned Alpujarride section (Azañón et al., 1997; Balanyá et al., 1997, 1998; Booth-Rea et al., 2005; Simancas, 2018). Between the Early and Middle Miocene, the final exhumation of the Alboran Domain—formed by the Malaguide-Ghomaride and Alpujarride-Sebtide complexes—occurred atop the orogenic wedge (e.g., Booth-Rea et al., 2004; García-Dueñas et al., 1992; Lonergan & Johnson, 1998; Lonergan & Platt, 1995; Platt et al., 2003, 2005; Marrone et al., 2021; Figure 15). Extension coeval to FTB development at the front of the orogenic wedge is a common feature of the Western Mediterranean orogens (e.g., Jolivet et al., 1994; Martínez-Martínez & Azañón, 1997; Platt & Vissers, 1989; Rossetti et al., 1999) that has been related to roll-back of subducted Tethys lithosphere segments (Faccenna et al., 2004; Lonergan & White, 1997) presently imaged as mantle lithospheric slabs under the Western Mediterranean (Bezada et al., 2013; Fichtner & Villaseñor, 2015; Piromallo & Morelli, 2003; Wortel & Spakman, 2000).

This Early Miocene shortening phase also affected the Oligocene proto-Algerian basin, inverted and incorporated into the newly developed orogenic wedge, its vestiges now present as amphibolites in the Kabylies or as extremely thinned sub-continental mantle emplaced in the crust as in the Ronda peridotite of the Western Betics (Booth-Rea et al., 2005; Fernandez et al., 2020; Garrido et al., 2011; Hidas et al., 2013; Marchesi et al., 2012) and the Collo peridotites in the Kabylies (Bouillin & Kornprobst, 1974; Laouar et al., 2017; Leblanc & Temagoult, 1989). Part of the proto-Algerian basin presently occupies the Western Alboran basin, since it drifted westwards hundreds of km in a forearc position behind the retreating Betic-Rif slab (Booth-Rea et al., 2007, Figure 15).

The Early Miocene contractive reorganization of the region and the initial individualization of the Betic-Rif Tethys slab, according to our proposal, was probably triggered by forced convergence across a former transform that separated the AlKaPeCa orogenic domain from the rest of the western Tethys during the Palaeogene (Figures 13 and 14). Equivalent subduction initiation along a collapsing transform has been proposed by Hall et al. (2003) and successfully reproduced using 3D thermomechanical modeling (Zhou et al., 2018). This transform fault, and the North Balearic one, were probably inherited from the Mesozoic rifting stage and must have determined the present slab segmentation pattern of the Western Mediterranean. A similar transform was proposed by Cohen (1980) and Vergés and Fernàndez (2012) in their model of flipped vergence between the Betic-Rif and Algerian Tell orogens. However, we assign this structure a different role during the Western Mediterranean evolution. During the Palaeogene it may have transferred shortening from the AlKaPeCa orogenic domain toward the Atlas to the SW, permitting the preservation of an undeformed Tethys domain and the Nevado-Filabride Ocean Continent Transitional (OCT) Iberian domain to the W (Figure 13). Yet later it bounded the domain of Oligocene orogenic collapse and conditioned the development of the proto-Algerian basin (Figure 14). Finally, during the Early Miocene, around 20 Ma, it most likely played a key role through its collapse (e.g., Zhou et al., 2018), initiating a new westward migrating subduction system under the load of the still-developing Betic-Rif thrust stack (Figure 14).

The 3D configuration we propose in Figures 13–16 can explain the puzzling structure of the Betics, whose Oligocene back-arc lithosphere—represented by the Ronda subcontinental peridotite and the overlying

crustal sequence intruded by back-arc suprasubduction dikes (Hidas et al., 2015; Marchesi et al., 2012)—directly overlies the Flysch Trough sedimentary cover, scraped off the Tethys oceanic lithosphere in the forearc (e.g., Luján et al., 2006), with no volcanic arc in between. Thus, this domain went from occupying a back-arc position, related to NW-directed subduction in the Palaeogene, to a forearc position owing to newly induced Eastward-directed subduction from the Early to Late Miocene (Figure 16). Our proposal moreover reconciles certain data regarding the provenance of the Alboran domain, including Paleozoic rocks from the Malaguide, Ghomaride, and Alpujarride complexes, whose age patterns derived from detrital zircon populations coincide with those from the Variscan European margin. This is especially clear for the Malaguide and Ghomaride complexes, having detrital zircon population ages equivalent to those of the Paleozoic rocks presently cropping out in Menorca, the Northeastern Iberian massif, and the South of France (Azdimousa, Jabaloy-Sánchez, Talavera, et al., 2019; Jabaloy-Sánchez et al., 2021).

5.4. Middle Miocene Extension of the Mallorca FTB

This research study shows that Mallorca Island also underwent important extensional tectonics during the Middle Miocene coeval to the oceanic opening of the Algero-Balearic basin (Figure 16). Extension was polyphasic, first entailing the activity of multiple LANFs thinning the previous nappe stack in a NE-SW direction at different structural levels. The LANFs were later cut by high-angle normal listric faults bounding horst and grabens, thereby producing extension in two orthogonal NE-SW and NW-SE directions. The grabens are mostly filled by Serravallian (14–11 Ma) alluvial sediments that show syn-rift internal progressive unconformities. In turn, the pre-rift Late Burdigalian to Langhian Randa calcarenites were cut and strongly tilted by the extensional system, especially at the margins of the Manacor basin (Figure 12a). The fact that the Middle Miocene basins also contain Early Miocene sediments does not mean that extension began in the Early Miocene; rather, it would reflect differential preservation from erosion of the older sediments in the hangingwall of the faults.

The kinematics of extension were determined using slicken lines, Riedel faults, offset bedding and minor brittle shear zones with C′ shear bands (Figure 5a). The faults show variable directions of transport, with two main orthogonal sets indicating SW-NE and NW-SE trending extension that are evident in the geological map, the cross-sections and in fault measurement sites in Figures 3, 4 and 7, respectively. Paleostress inversion results confirm the existence of two well-differentiated stress fields producing NE-SW to N-S and NW-SE extension (Figure 7). Fault measurement sites 1–3, 9, 13, 14, 20, 21, 33, 31, and 34 offer significant paleostress fields indicating NE-SW to N-S extension (Figure 7). Site 24 by Manacor shows two well-constrained paleostress fields giving NE-SW and NW-SE extensional stress fields. Within the Llevant Ranges we also observe spatial variations in the importance of one or the other extensional system, the NW-SE directed extension being especially clear along their Southeastern margin (sites 15, 16, and 26–28 in Figure 7), coinciding with a marked NE-SW-trending negative gravimetric anomaly parallel to the shoreline (Figure 8). Even though, this variability in extensional directions during the Serravallian could reflect radial extension (Céspedes et al., 2001), we find that, in general, normal faults producing NE-SW trending extension are older and more penetrative than the ones producing NW-SE extension. Furthermore, the results from paleostress inversion indicate mostly stress ratios R above 0.3 (Figure 7), which are larger than the ones observed in well-documented radial extension stress fields, having R values below 0.1 (e.g., Simón-Gómez, 1989; Liesa et al., 2019). In our work only one station was found to be compatible with radial extension—site 23, with a stress ratio R of 0.06 (Figure 7). Still, we have clear evidence of NW-SE extension affecting Middle Miocene sediments in the Manacor basin, as described for other regions of Mallorca, such as the Inca basin (Benedicto et al., 1993). However, we must not forget the existence of an older Oligocene NW-SE trending extension in the island. There could also be Mesozoic extensional structures not identified to date that produce NW-SE extension, as described for the Valencia Trough (Etheve et al., 2018). In view of these considerations, we propose that Middle Miocene extension in Mallorca developed sequentially, first producing NE-SW extension, then orthogonal NW-SE extension, which, locally and along the Mallorca margins offshore, continued up to the latest Miocene (Driussi, Maillard, et al., 2015).

Recognizing the presence of Middle Miocene LANFs in the Llevant Ranges comes to strongly alter the previously established structure of the region, which was interpreted entirely as contractive (e.g., Sabat

et al., 1988). We identified LANFs cutting contacts that could have been interpreted as inverted stratigraphic features, for example between Jurassic limestones overlying Cretaceous marls. Yet we find that the interpreted stratigraphic contact supposedly forming the reversed limb of a large NE-vergent recumbent syncline is actually a westward transport LANF that locally has small extensional horses formed by Triassic dolostones in between, meaning no syncline exists (Figures 5a and 5b). The deepest nappe in the region we mapped is located SW of Manacor, though at present it forms a horst structure hosting a series of NW-SE oriented folds in its core, bounded toward the East by a high-angle normal fault that cuts through Serravallian sediments in its hangingwall (cross-section b and b′, Figure 4).

The Serravallian grabens are well imaged as regions with negative gravity anomalies in Figure 8. They are segmented and offset laterally by SW-NE oriented strike-slip faults that we interpret as transfer faults developed during the Middle Miocene rifting phase (Figure 8). These faults show both dextral and sinistral kinematics and also bound the main Middle Miocene sedimentary depocenters in the island: the Inca, Sa Pobla, Manacor, Felanitx and Santa Margalida basins (Figure 8). Dextral-oblique kinematics are observed in the Orient and Sant Joan faults (Booth-Rea et al., 2016), whereas sinistral kinematics are found in the Sencelles and Felanitx faults (Figure 8, Mas et al., 2014). Faulting runs parallel to the Emile Baudot scarpment, which roughly separates the Mallorca continental crust from the Algero-Balearic basin oceanic domain, and has been interpreted as a transform fault (Acosta et al., 2001; Etheve et al., 2016; Jolivet et al., 2021). In previous studies, the transfer faults described are mostly NW-SE directed—for example, the North Balearic, Central and Ibiza fault zones accommodate the NW-SE opening of the Ligurian and Minorca basins (Maillard et al., 2020; Pellen et al., 2016). Strike-slip faults with this orientation also occur on Mallorca Island, some of them interpreted as transfer faults related to the Early Miocene FTB development (Gelabert, 1998; Sabat et al., 1988). Furthermore, NW-SE trending faults with both sinistral and dextral strike-slip kinematics can be found in the Llevant ranges, yet they tend to be shorter than the NE-SW trending ones, which cut through most of the island. In some cases these faults show two sets of striae, indicating both normal and strike-slip displacements. The fact that parallel strike-slip faults with opposite kinematics are found in the same region is indicative of extensional transfer faults (e.g., Giaconia et al., 2014; Martínez-Martínez, 2006), here interpreted in association with the NE-SW directed extensional system. Some may be related to the older FTB development, however; for example, the thick sinistral fault zone cutting the Capdepera semigraben, itself cut by later dextral NE-SW trending faults (Figures 9 and 11b).

5.5. Implications for Refining the Geodynamics of the Western Mediterranean

Serravallian extension in Mallorca coincided with a period of deep paleogeographic changes on the island, which evolved from a mostly marine realm to a continental one (Ramon & Simo, 1986)—a process that altered its sediment provenance. During the Burdigalian and Langhian, the turbidite systems in Mallorca, fed from the South (Rodríguez-Perea, 1984), included clasts of "exotic" Paleozoic grauwackes resembling the Carboniferous sequence that crops out in Menorca and the Malaguide complex at the top of the Betic internal zones (Bourrouilh, 1983; Cohen, 1980; Hollister, 1942), for which a common NE Iberian Massif origin was recently proposed (Jabaloy-Sánchez et al., 2021). This implies the existence of a Paleozoic emerged hinterland of the Mallorca FTB located to the South during the Early Miocene, compatible with the Malaguide complex of the Alboran domain (Figure 15). During the Serravallian, small strongly subsident continental basins with internal drainage developed (Benedicto et al., 1993; Ramon & Simo, 1986; Ramos-Guerrero et al., 2000), probably fed by local horsts that formed during extension, mainly coincident with the present ranges. Thus, Middle Miocene extension actually coincided with a topographic build-up and continentalization in Mallorca.

We propose that this topographic uplift and coeval extension could be related to flexural and isostatic rebound after an "unloading" of Mallorca through extensional collapse of its orogenic hinterland and excision of its lithospheric mantle root, perhaps driven by tectonics (slab detachment or edge-delamination). The latter tectonic mechanism has been proposed by several authors under the Betics setting during the Late Miocene until the Pliocene or Present, driving concomitant topographic uplift and thinning of the South Iberian lithosphere (Capella et al., 2020; Chertova et al., 2014; Duggen et al., 2003; García-Castellanos & Villaseñor, 2011; Mancilla et al., 2015; Negredo Moreno et al., 2020; Sun & Bezada, 2020). Slab detachment may have initiated in the Serravallian further to the NE, below part of the BP, to later propagate toward the SW. This hypothe-

sis is supported by similar deformational behaviors followed by topographic rebound in the Eastern Betics and Mallorca, including a close association between extension and strike-slip transfer-fault development, as proposed for the southern margin of Mallorca (Acosta et al., 2001; Driussi, Briais, & Maillard, 2015) and the Eastern Betics (Giaconia et al., 2014; Mancilla et al., 2015; Pérez-Valera et al., 2013). In both regions, extensional tectonics propagated into the external FTB with two orthogonal directions of extension, both parallel and transverse to the orogen trend, which acted sequentially in time (Balanyá et al., 2012; Booth-Rea et al., 2004; Rodríguez-Fernández et al., 2011). Furthermore, extension and related strike-slip deformation were accompanied in the Betics and Mallorca by Neogene clockwise paleomagnetic rotation of the order of 35°–40° (e.g., Freeman et al., 1989; Lonergan & White, 1997; Mattei et al., 2006). In the Eastern Betics, the subducted South-Iberian domain (Nevado-Filabride complex) was exhumed by SW-directed brittle-ductile extensional detachments to a large extent during the Middle to Late Miocene (Augier, Agard, et al., 2005; Augier, Jolivet, & Robin, 2005; Martínez-Martínez & Azañón, 1997; Martínez-Martínez et al., 2002), followed by important thinning afterward, in the Late Tortonian (Auguier et al., 2013; de la Peña, Ranero, et al., 2020), thus producing SE-directed extension along the Almenara detachment (Booth-Rea et al., 2012). In general, this extension can be related to the opening of the western part of the Algerian basin between the Middle and Late Miocene in a back-arc setting (Booth-Rea et al., 2007, Booth-Rea, Gaidi, et al., 2018; Mauffret et al., 2004) or to the relaxation of body forces stored in the Betic internal zones.

The hypothesis of SW-directed tearing or detachment of the Betic-Rif slab initiating under the MP and later propagating toward the SW would explain the shared lithospheric characteristics of Mallorca and the Betics, like the SW-NE oriented Pn mantle anisotropy (Díaz et al., 2013) and the thin crustal and lithospheric thicknesses measured in Mallorca and the Eastern Betics (Díaz & Gallart, 2009; Jiménez-Munt et al., 2003; Mancilla et al., 2015), after having lost their orogenic root. At present, the lithospheric features of Mallorca hardly fit earlier tectonic models for the island, evoking Early Miocene NW-directed crustal thickening followed by only minor SE-directed extension in the Middle to Late Miocene (e.g., Gelabert, 1998; Sabat et al., 2011). Middle Miocene SW-directed extension in Mallorca is, however, compatible with some models proposed for the opening of the Algero-Balearic basin to the SE (e.g., Booth-Rea et al., 2007; de la Peña, Ranero, et al., 2020; Haidar et al., 2021; Mauffret et al., 2004).

The different periods of back-arc rifting in the Western Mediterranean basins correlate in a broad sense with contrasting heat flow values in the region, showing a clear increase from East to West within the Algero-Balearic basin, suggesting a Middle Miocene or younger age for its opening to the West, and an older Oligocene to Early Miocene age for the Ligurian and central basin areas (Poort et al., 2020). Yet heat flow values also increase toward the Southeastern end of the Algerian basin, south of Sardinia. Meanwhile, the Valencia Trough shows relatively low heat flow, compatible with an older rifting phase. As the Mallorca domain extended in the Middle Miocene, the Betics extension propagated from the Internal Zones northwestward—toward the Betic FTB—in the Late Miocene, producing sedimentary depocentres that seal the contact between the Internal and External domains, for example, the Fortuna, Lorca, Guadix-Baza and Granada basins (Booth-Rea et al., 2004; de la Peña, Ranero, et al., 2020; Rodríguez-Fernández et al., 2011). Meanwhile, the Easternmost Algerian basin followed an evolution parallel to its westernmost segment, but with an opposite eastward direction of extension (Figure 16). This extension propagated into Northern Tunisia in the Late Miocene, causing the collapse of the Tunisian Tell (Booth-Rea, Gaidi, et al., 2018). Extension of FTB domains as we describe for Mallorca likewise occurred in other western Mediterranean orogens, including the Appennines, Betics, Rif, Tunisian Tell and Sicily (e.g., Barreca et al., 2016; Booth-Rea et al., 2012; Booth-Rea, Gaidi, et al., 2018; Booth-Rea, Ranero, & Grevemeyer, 2018; Carmignani & Kligfield, 1990; de Ruig, 1995; Roca et al., 2006, 2013; Rodríguez-Fernández et al., 2011); in most cases it may be related to delamination or detachment of a segment of the subcontinental lithospheric mantle at the edge of the corresponding orogenic arcs (e.g., Azdimousa et al., 2019; Booth-Rea, Gaidi, et al., 2018; Chiarabba & Chiodini, 2013; Duggen et al., 2003; Keller et al., 1994; Levander et al., 2014; Mancilla et al., 2015; Roure et al., 2012).

Presently, the BP is bounded to the south by the oceanic Algero-Balearic basin along the steep Emile Baudot and Mazarron scarpments, interpreted as transform boundaries (Acosta et al., 2001; Driussi, Briais, & Maillard, 2015; Etheve et al., 2016). These faults would form part of a wide STEP zone, together with other parallel dextral ones that crop out onshore in the Southeastern Betics, such as the Crevillente, Alpujarras,

Torcal, and the Orient fault in Mallorca. This system of transform faults, together with a symmetrical STEP fault system along the North-Maghrebian margin, probably contributed to the west-south westward stretching and displacement of the Alboran Domain during the Middle to Late Miocene (e.g., Giaconia et al., 2014; Haidar et al., 2021; Hidas et al., 2019; Mancilla et al., 2015; Medaouri et al., 2014; Pérez-Valera et al., 2013).

During the Serravallian, the BP and the Betic internal zones shared very similar insular vertebrate glirid fauna (Bover et al., 2008; Suarez et al., 1993). Hence, either the Alboran Domain formed a large archipelago together with the BP at the time, or it traveled southwestwards over a long distance since the Middle Miocene, away from Mallorca, following the roll-back of the Betic-Rif slab (e.g., Booth-Rea et al., 2007; Chertova et al., 2014; Driussi, Briais, & Maillard, 2015; Faccenna et al., 2004; Lonergan & White, 1997; Figure 16). Considering that a Paleozoic hinterland existed to the south of Mallorca during the Early Miocene—as evidenced by the presence of exotic clasts of this age in the Banyalbufar turbidites (Bourrouilh, 1983; Hollister, 1942)—the second option or a combination of the two seems more realistic. To the SW, the Betic hinterland, represented by the Alboran Domain, was separated at that time from Iberia by a deep foredeep basin in the External Betics (de Galdeano & Vera, 1992; Geel et al., 1992; Martín-Martín, Guerrera, et al., 2018). The Valencia Trough was the NE continuation of the External Betic Serravallian foredeep, although the thrust front there had resumed its activity after the Langhian (Etheve et al., 2016; Leprêtre et al., 2018). This domain, along with the Great and Petit Kabilies domains, underwent separation from the African emerged land to the South through an Early to Middle Miocene foredeep along Northern Algeria and Tunisia (Guerrera et al., 2005; Jolivet et al., 2006; Roure et al., 2012, Figure 16). We therefore propose that the Alboran domain archipelago was driven southwestward in a forearc setting until the Late Miocene, producing the present isolation of the Mallorca FTB from its corresponding Betic hinterland. This model implies very large displacements, in the order of 600 km, between Mallorca and its corresponding Paleozoic hinterland since the Early Miocene, comparable to the length of the subducted Tethyan lithospheric mantle slab presently underlying the Betics (e.g., Bezada et al., 2013; Faccenna et al., 2004). This hypothesis contrasts with models suggesting very minor displacements—below 200, or even 100 km—for the Betic hinterland with respect to Iberia (e.g., Frasca et al., 2015; Pedrera et al., 2020; Vergés & Fernàndez, 2012). Still, we believe that the geodynamic evolution proposed here would explain the great diversity of available geological and geophysical data presented for the geological setting: sediment provenance (Bourrouilh, 1983; Cohen, 1980; Donoso et al., 1982; Hollister, 1942; Moragues et al., 2018; Pomar & Rodríguez-Perea, 1983), detrital zircon population ages (Jabaloy-Sánchez et al., 2021), subducted slab bodies (e.g., Bezada et al., 2013; Faccenna et al., 2014; Fichtner & Villaseñor, 2015), tectonic evolution (this work and references therein), Algero-Balearic basin development (e.g., Booth-Rea et al., 2007; de la Peña, Ranero, et al., 2020; Haidar et al., 2021; Mauffret et al., 2004), fossil faunal dispersal (e.g., Martín-Suarez et al., 2012; Suarez et al., 1993), and the extensional collapse of the Mallorca and Betic FTB as discussed in this work. We do hold that some of these data, for example, sediment provenance analysis in the Mallorca basins, calls for future work using updated heavy mineral dating and analysis methods.

Finally, our geodynamic reconstruction offers clues as to the distribution of emerged forearc and volcanic arc land masses in the Western Mediterranean (Figures 13–16), isolated by marine gateways from Africa and Iberia between the Early Miocene and the Tortonian, when terrestrial vertebrates from the Iberian mainland were found for the first time (≈9 Ma) in sediments overlying the Alboran domain (Martín-Suarez et al., 2012). Overall, we envisage a process that, together with the Messinian salinity crisis, most likely contributed to the presently biodiverse hotspot of the Southwestern Mediterranean (e.g., Hewitt, 2011 and references therein; Booth-Rea, Ranero, & Grevemeyer, 2018).

6. Conclusions

Two Cenozoic rifting phases predate and postdate, respectively, the main Early Miocene shortening and FTB development in Mallorca. The earlier extensional phase produced NW-directed extensional detachments and semigrabens filled by Oligocene breccias, coeval to the opening of the Liguro-Provencal basin and extensional collapse of AlKaPeCa. This extension produced the first Alpine structures observed in Mallorca after its hinterland position with respect to the AlKaPeCa orogenic domain during the Paleocene-Eocene.

The Mallorca promontory underwent Burdigalian to Langhian WNW-ESE shortening, and the development of its FTB structure was coeval to the subduction of the Southeast Iberian passive margin and the birth of the Betic-Rif eastward dipping subduction system. The second rifting phase produced the extensional collapse of the Mallorca FTB during the Middle Miocene, coinciding with the opening of central parts of the Algero-Balearic back-arc basin and the westward drift of the Alboran Domain and the proto-Algerian basin, presently represented by the western Alboran basin.

The Serravallian extension was of a polyphaser nature, initiated mostly with NE-SW-directed extension and then evolving toward NW-SE-directed transport. This rifting was accommodated along LANFs that cut through the previous FTB structure and were later cut by high-angle normal faults bounding the main Middle-Miocene sedimentary depocenters. The basins in Mallorca are strongly segmented by SW-NE oriented strike-slip faults, both sinistral and dextral; the Orient, Sencelles, Sant Joan, and Felanitx ones acted as transfer faults of the Serravallian extensional system, and run parallel to the present transform continent-ocean transition along the Emile-Baudot scarpment.

Middle Miocene extension coincided with topographic build-up in Mallorca, manifested by continentalization of the region, a development of internal drainage basins and changes in the sediment provenance, eventually sourced from nearby horst highs. We relate this topographic development and coeval extension to flexural and isostatic rebound after initial detachment or tearing of the Betic-Rif mantle slab to the South of the BP.

The Mallorca FTB developed coevally and with the same kinematics as the Betic FTB. However, shortening in the Betics continued throughout the Middle and Late Miocene, during the extensional collapse of Mallorca and the opening of the western domain of the Algero-Balearic basin, following the retreat of the Betic-Rif slab.

Our data therefore supports that the Mallorca FTB was part of the Betic orogen during the Early Miocene, and later became stranded and isolated from its hinterland domain owing to the development of the Central and Western segments of the Algero-Balearic basin in the Middle to Late Miocene. Altogether, this process entailed important W to SW-directed displacements of the Betic hinterland in a forearc domain, that is, an archipelago, across the Western Mediterranean until its docking by SE Iberia in the Tortonian.

Data Availability Statement

All the data is accessible and presented in the manuscript figures and Table 1. It is also available through https://digibug.ugr.es/handle/10481/68016 (doi: 10.30827/Digibug.68016) and the gravimetric map was obtained from 3843 gravimetric data through Ayala et al. (1994).

References

Abbassene, F., Chazot, G., Bellon, H., Bruguier, O., Ouabadi, A., Maury, R. C., et al. (2016). A 17Ma onset for the post-collisional K-rich calc-alkaline magmatism in the Maghrebides: Evidence from Bougaroun (northeastern Algeria) and geodynamic implications. *Tectonophysics*, *674*, 114–134. https://doi.org/10.1016/j.tecto.2016.02.013

Acosta, J., Muñoz, A., Herranz, P., Palomo, C., Ballesteros, M., Vaquero, M., & Uchupi, E. (2001). Geodynamics of the Emile Baudot Escarpment and the Balearic Promontory, western Mediterranean. *Marine and Petroleum Geology*, *18*, 349–369. https://doi.org/10.1016/S0264-8172(01)00003-4

Adrover, R., Hugueney, M., & Mein, P. (1977). *Fauna africana oligocena y nuevas formas endémicas entre los micromamíferos de Mallorca (Nota preliminar)* (pp. 137–149). Bolletí de la Societat d'Història Natural de les Balears.

Aïdi, C., Beslier, M.-O., Yelles-Chaouche, A. K., Klingelhoefer, F., Bracene, R., Galve, A., et al. (2018). Deep structure of the continental margin and basin off Greater Kabylia, Algeria – New insights from wide-angle seismic data modeling and multichannel seismic interpretation. *Tectonophysics*, *728–729*, 1–22. https://doi.org/10.1016/j.tecto.2018.01.007

Alvaro, A., Barnolas, A., Cabra, P., Comas Rengifo, M. J., Fernández López, S. R., Goy, A., et al. (1989). El Jurásico de Mallorca (Islas Baleares). *Cuadernos de Geologia Iberica*, *13*, 67–120.

Alvaro, M. (1987). La tectónica de cabalgamientos de la Sierra Norte de Mallorca, Islas Baleares. *Boletin Geologico y Minero*, *98*(5), 34–41.

Alvaro, M., Barnolas, A., del Olmo, P., Ramírez del Pozo, J., & Simo, A. (1984). El Neógeno de Mallorca: Caracterización sedimentológica y bioestratigráfica. *Boletin Geologico y Minero*, *XCV-I*, 3–25.

Alvaro-López, M., del Olmo, P., Ramírez del Pozo, J., Sabat, F., & Barnolas, A. (1983). *MAGNA, Hoja 700 Manacor. Mapa Geológico de España 1:50.000*. Instituto Geológico y Minero de España.

Andeweg, B., De Vicente, G., Cloetingh, S. A. P. L., Giner, J., & Martin, A. M. (1999). Local stress fields and intraplate deformation of Iberia: Variations in spatial and temporal interplay of regional stress sources. *Tectonophysics*, *305*(1–3), 153–164. https://doi.org/10.1016/s0040-1951(99)00004-9

Angelier, J. (1979). Determination of the mean principal directions of stresses for a given fault population. *Tectonophysics*, *56*, T17–T26. https://doi.org/10.1016/0040-1951(79)90081-7

Anglada-Guajardo, E., & Serra-Kiel, J. (1986). El Paleógeno y tránsito al Neógeno en el área del Macizo de Randa, Mallorca. *Boletin Geologico y Minero*, *97*(5), 40–49.

Angrand, P., Mouthereau, F., Masini, E., & Asti, R. (2020). A reconstruction of Iberia accounting for Western Tethys–North Atlantic kinematics since the late-Permian–Triassic. *Solid Earth*, *11*(4), 1313–1332. https://doi.org/10.5194/se-11-1313-2020

Arab, M., Rabineau, M., Deverchere, J., Bracene, R., Belhai, D., Roure, F., et al. (2016). Tectonostratigraphic evolution of the eastern Algerian margin and basin from seismic data and onshore-offshore correlation. *Marine and Petroleum Geology*, *77*, 1355–1375. https://doi.org/10.1016/j.marpetgeo.2016.08.021

Arlegui, L. E., & Simón, J. L. (1998). Reliability of palaeostress analysis from fault striations in near multidirectional extension stress fields. Example from the Ebro Basin, Spain. *Journal of Structural Geology*, *20*, 827–840. https://doi.org/10.1016/s0191-8141(98)00012-1

Augier, R., Agard, P., Monié, P., Jolivet, L., Robin, C., & Booth-Rea, G. (2005). Exhumation, doming and slab retreat in the Betic Cordillera (SE Spain): In situ40Ar/39Ar ages and P–T–d–t paths for the Nevado-Filabride complex. *Journal of Metamorphic Geology*, *23*(5), 357–381. https://doi.org/10.1111/j.1525-1314.2005.00581.x

Augier, R., Jolivet, L., couto, D. D., & Negro, F. (2013). From ductile to brittle, late-to post-orogenic evolution of the Betic Cordillera: Structural insights from the northeastern internal zones. *Bulletin de la Societe Geologique de France*, *184*(4–5), 405–425. https://doi.org/10.2113/gssgfbull.184.4-5.405

Augier, R., Jolivet, L., & Robin, C. (2005). Late Orogenic doming in the eastern Betic Cordilleras: Final exhumation of the Nevado-Filabride complex and its relation to basin genesis. *Tectonics*, *24*(4). https://doi.org/10.1029/2004tc001687

Ayala, C., Pous, J., Sàbat, F., Casas, A., Rivero, L., & Gelabert, B. (1994). Modelización gravimétrica de la isla de Mallorca. *Revista de la Sociedad Geologica de Espana*, *7*(3–4), 215–227.

Ayala, C., Torne, M., & Roca, R. (2015). A review of the current knowledge of the crustal and lithospheric structure of the Valencia Trough Basin. *Boletin Geologico y Minero*, *126*(2–3), 533–552.

Azañón, J. M., Crespo-Blanc, A., & García-Dueñas, V. (1997). Continental collision, crustal thinning and nappe forming during the pre-Miocene evolution of the Alpujarride Complex (Alboran Domain, Betics). *Journal of Structural Geology*, *19*, 1055–1071. https://doi.org/10.1016/S0191-8141(97)00031-X

Azdimousa, A., Jabaloy-Sánchez, A., Münch, P., Martínez-Martínez, J. M., Booth-Rea, G., Vázquez-Vílchez, M., et al. (2019). Structure and exhumation of the Cap des Trois Fourches basement rocks (Eastern Rif, Morocco). *Journal of African Earth Sciences*, *150*, 657–672. https://doi.org/10.1016/j.jafrearsci.2018.09.018

Azdimousa, A., Jabaloy-Sánchez, A., Talavera, C., Asebriy, L., González-Lodeiro, F., & Evans, N. J. (2019). Detrital zircon U-Pb ages in the Rif Belt (northern Morocco): Paleogeographic implications. *Gondwana Research*, *70*, 133–150. https://doi.org/10.1016/j.gr.2018.12.008

Azzaroli, A. (1990). Palaeogeography of terrestrial vertebrates in the perityrrhenian area. *Palaeogeography, Palaeoclimatology, Palaeoecology*, *77*(1), 83–90. https://doi.org/10.1016/0031-0182(90)90100-l

Badji, R., Charvis, P., Bracene, R., Galve, A., Badsi, M., Ribodetti, A., et al. (2015). Geophysical evidence for a transform margin offshore Western Algeria: A witness of a subduction-transform edge propagator? *Geophysical Journal International*, *200*(2), 1029–1045. https://doi.org/10.1093/gji/ggu454

Balanyá, J. C., Crespo-Blanc, A., Azpiroz, M. D., Exposito, I., & Luján, M. (2007). Structural trend line pattern and strain partitioning around the Gibraltar Arc accretionary wedge: Insights as to the mode of orogenic arc building. *Tectonics*, *26*. https://doi.org/10.1029/2005TC001932

Balanyá, J. C., Crespo-Blanc, A., Díaz-Azpiroz, M., Expósito, I., Torcal, F., Pérez-Peña, V., & Booth-Rea, G. (2012). Arc-parallel vs back-arc extension in the Western Gibraltar arc: Is the Gibraltar forearc still active? *Geológica Acta*, *10*, 249–263.

Balanyá, J. C., García-Dueñas, V., Azañón, J. M., & Sánchez-Gómez, M. (1997). Alternating contractional and extensional events in the Alpujarride nappes of the Alboran Domain (Betics, Gibraltar Arc). *Tectonics*, *16*, 226–238. https://doi.org/10.1029/96TC03871

Balanyá, J. C., Garcia-Duenas, V., Azanon, J. M., & Sanchez-Gomez, M. (1998). Comment on "Alternating contractional and extensional events in the Alpujarride nappes of the Alboran Domain (Betics, Gibraltar arc)" – Reply. *Tectonics*, *17*, 977–981.

Barnolas, A., Pares, J. M., Sabat, F., Álvaro, M., Ramírez del Pozo, J., Alvarado, M., et al. (1983). *MAGNA 725 Felanitx, Mapa Geológico de España 1:50.000*. IGME.

Barreca, G., Scarfi, L., Cannavo, F., Koulakov, I., & Monaco, C. (2016). New structural and seismological evidence and interpretation of a lithospheric-scale shear zone at the southern edge of the Ionian subduction system (central-eastern Sicily, Italy). *Tectonics*, *35*(6), 1489–1505. https://doi.org/10.1002/2015tc004057

Benedicto, A., Ramos-Guerrero, E., Casas, A., Sabat, F., & Baron, A. (1993). Evolución tectonosedimentaria de la cubeta neógena de Inca (Mallorca). *Revista de la Sociedad Geologica de Espana*, *6*, 167–176.

Bessière, E., Jolivet, L., Augier, R., Scaillet, S., Précigout, J., Azañón, J. M., et al. (2021). Lateral variations of pressure-temperature evolution in non-cylindrical orogens and 3-D subduction dynamics: The Betic-Rif Cordillera example. *BSGF-Earth Sciences Bulletin*, *192*(1), 8.

Bezada, M. J., Humphreys, E. D., Toomey, D. R., Harnafi, M., Dávila, J. M., & Gallart, J. (2013). Evidence for slab rollback in westernmost Mediterranean from improved upper mantle imaging. *Earth and Planetary Science Letters*, *368*, 51–60. https://doi.org/10.1016/j.epsl.2013.02.024

Booth-Rea, G., Azanon, J. M., & Garcia-Duenas, V. (2004). Extensional tectonics in the northeastern Betics (SE Spain): Case study of extension in a multilayered upper crust with contrasting rheologies. *Journal of Structural Geology*, *26*, 2039–2058. https://doi.org/10.1016/j.jsg.2004.04.005

Booth-Rea, G., Azañón, J. M., Goffe, B., Vidal, O., & Martínez-Martínez, J. M. (2002). High-pressure, low-temperature metamorphism in Alpujarride Units of southeastern Betics (Spain). *Comptes Rendus Geoscience*, *334*, 857–865. https://doi.org/10.1016/s1631-0713(02)01787-x

Booth-Rea, G., Azanón, J. M., Martínez-Martínez, J. M., Vidal, O., & García-Dueñas, V. (2005). Contrasting structural and P-T evolution of tectonic units in the southeastern Betics: Key for understanding the exhumation of the Alboran Domain HP/LT crustal rocks (western Mediterranean). *Tectonics*, *24*, 1. https://doi.org/10.1029/2004TC001640

Booth-Rea, G., Azañón, J. M., Roldán, F. J., Moragues, L., Pérez-Peña, V., & Mateos, R. M. (2016). WSW-ENE extension in Mallorca, key for integrating the Balearic Promontory in the Miocene evolution of the western Mediterranean. *Geotemas*, *16*, 81–84.

Booth-Rea, G., Gaidi, S., Melki, F., Marzougui, W., Azañón, J. M., Zargouni, F., et al. (2018). Late Miocene extensional collapse of Northern Tunisia. *Tectonics*, *37*, 1626–1647. https://doi.org/10.1029/2017TC004846

Booth-Rea, G., Jabaloy-Sánchez, A., Azdimousa, A., Asebriy, L., Vílchez, M. V., & Martínez-Martínez, J. M. (2012). Upper-crustal extension during oblique collision: The Temsamane extensional detachment (eastern Rif, Morocco). *Terra Nova*, *24*(6), 505–512.

Booth-Rea, G., Martínez-Martínez, J. M., & Giaconia, F. (2015). Continental subduction, intracrustal shortening, and coeval upper-crustal extension: PT evolution of subducted south Iberian paleomargin metapelites (Betics, SE Spain). *Tectonophysics*, *663*, 122–139. https://doi.org/10.1016/j.tecto.2015.08.036

Booth-Rea, G., Ranero, C., Martínez-Martínez, J. M., & Grevemeyer, I. (2007). Crustal types and Tertiary tectonic evolution of the Alborán Sea, western Mediterranean. *Geochemistry, Geophysics, Geosystems*, *8*, Q10004. https://doi.org/10.1029/2007gc001639

Booth-Rea, G., Ranero, C. R., & Grevemeyer, I. (2018). The Alboran volcanic-arc modulated the Messinian faunal exchange and salinity crisis. *Scientific Reports*, *8*. https://doi.org/10.1038/s41598-018-31307-7

Bott, M. H. P. (1959). The mechanics of oblique slip faulting. *Geological Magazine*, *96*, 109–117. https://doi.org/10.1017/S0016756800059987

Bouillin, J. P., Duran-Delga, M., & Olivier, P. (1986). Betic Rifian and Tyrrhenian arc: Distinctive features, genesis and development stages. In F. Wezel (Ed.), *The origin of arcs* (pp. 281–304). Elsevier. https://doi.org/10.1016/B978-0-444-42688-8.50017-5

Bouillin, J. P., & Kornprobst, J. (1974). Associations ultrabasiques de Petite Kabylie; peridotites de type alpin et complexe stratifie; comparaison avec les zones internes betico-rifaines. *Bulletin de la Societe Geologique de France*, *7*(2), 183–194. https://doi.org/10.2113/gssgfbull.s7-xvi.2.183

Boukhalfa, K., Soussi, M., Ozcan, E., Banerjee, S., & Tounekti, A. (2020). The Oligo-Miocene siliciclastic foreland basin deposits of northern Tunisia: Stratigraphy, sedimentology and paleogeography. *Journal of African Earth Sciences*, *170*, 103932. https://doi.org/10.1016/j.jafrearsci.2020.103932

Bourrouilh, R. (1983). *Estratigrafía, sedimentología y tectónica de la isla de Menorca y del noreste de Mallorca (Baleares): La terminación nororiental de las cordilleras béticas en el mediterráneo occidental*. Memoria del Instituto geológico y minero de España (p. 99). IGME.

Bover, P., Quintana, J., & Alcover, J. A. (2008). Three islands, three worlds: Paleogeography and evolution of the vertebrate fauna from the Balearic Islands. *Quaternary International*, *182*(1), 135–144. https://doi.org/10.1016/j.quaint.2007.06.039

Bruguier, O., Bosch, D., Caby, R., Vitale-Brovarone, A., Fernandez, L., Hammor, D., et al. (2017). Age of UHP metamorphism in the Western Mediterranean: Insight from rutile and minute zircon inclusions in a diamond-bearing garnet megacryst (Edough Massif, NE Algeria). *Earth and Planetary Science Letters*, *474*, 215–225. https://doi.org/10.1016/j.epsl.2017.06.043

Burrus, J. (1984). Contribution to a geodynamic synthesis of the Provencal Basin (north-western Mediterranean). *Marine Geology*, *55*(3–4), 247–269. https://doi.org/10.1016/0025-3227(84)90071-9

Capella, W., Spakman, W., van Hinsbergen, D. J., Chertova, M. V., & Krijgsman, W. (2020). Mantle resistance against Gibraltar slab dragging as a key cause of the Messinian Salinity Crisis. *Terra Nova*, *32*(2), 141–150. https://doi.org/10.1111/ter.12442

Carmignani, L., & Kligfield, R. (1990). Crustal Extension in the Northern Apennines—The transition from compression to extension in the Alpi Apuane Core Complex. *Tectonics*, *9*(6), 1275–1303. https://doi.org/10.1029/tc009i006p01275

Casas, A. M., Gil, M. A., & Simón, J. L. (1990). Los métodos de análisis de paleoesfuerzos a partir de poblaciones de fallas: Sistemática y técnicas de aplicación. *Estudios Geológicos*, *46*, 385–398. https://doi.org/10.3989/egeol.90465-6469

Casas, J. M., & Sabat, F. (1987). An example of three-dimensional analysis of thrust-related tectonites. *Journal of Structural Geology*, *9*(5–6), 647–657. https://doi.org/10.1016/0191-8141(87)90149-0

Céspedes, A., Giménez, J., & Sàbat, F. (2001). Caracterización del campo de esfuerzos neógenos en Mallorca mediante el análisis de poblaciones de fallas. *Geogaceta*, *30*, 199–202.

Chazot, G., Abbassene, F., Maury, R. C., Déverchère, J., Bellon, H., Ouabadi, A., & Bosch, D. (2017). An overview on the origin of post-collisional Miocene magmatism in the Kabylies (northern Algeria): Evidence for crustal stacking, delamination and slab detachment. *Journal of African Earth Sciences*, *125*, 27–41. https://doi.org/10.1016/j.jafrearsci.2016.10.005

Cherchi, A., & Montadert, L. (1982). Oligo-Miocene rift of Sardinia and the early history of the western Mediterranean basin. *Nature*, *298*(5876), 736–739. https://doi.org/10.1038/298736a0

Chertova, M. V., Spakman, W., Geenen, T., van den Berg, A. P., & van Hinsbergen, D. J. J. (2014). Underpinning tectonic reconstructions of the western Mediterranean region with dynamic slab evolution from 3-D numerical modeling. *Journal of Geophysical Research-Solid Earth*, *119*, 5876–5902. https://doi.org/10.1002/2014JB011150

Chiarabba, C., & Chiodini, G. (2013). Continental delamination and mantle dynamics drive topography, extension and fluid discharge in the Apennines. *Geology*, *4*(6), 715–718. https://doi.org/10.1130/g33992.1

Cohen, C. R. (1980). Plate tectonic model for the Oligo-Miocene evolution of the western Mediterranean. *Tectonophysics*, *68*(3–4), 283–311. https://doi.org/10.1016/0040-1951(80)90180-8

Colom, G. (1973). Esbozo de las principales lito-facies de los depósitos jurásico-cretáceos de las Baleares y su evolución preorogénica. *Memorias de la Real Academia de Ciencias*, *25*(2), 116.

Colom, G. (1980). Sobre la posible extensión del Aquitaniense marino a lo largo de las sierras de Levante de Mallorca. *Bolleti de la Societat d'Historia Natural de les Balears*, *24*, 7–14.

Colom, G., & Sacares, J. (1968). Hallazgo del Aquitaniense marino en Mallorca. *Acta Geológica Hispánica*, *3*(5), 135–137.

Costamagna, L. G., & Schäfer, A. (2013). The Cixerri Fm (Middle Eocene-Early Oligocene): Analysis of a "Pyrenean" continental molassic system in southern Sardinia. *Journal of Mediterranean Earth Sciences Special Issue*, 41–44.

de Capoa, P., Di Staso, A., Perrone, V., & Zaghloul, M. N. (2007). The age of the foredeep sedimentation in the Betic–Rifian Mauretanian units: A major constraint for the reconstruction of the tectonic evolution of the Gibraltar Arc. *Comptes Rendus Geoscience*, *339*(2), 161–170. https://doi.org/10.1016/j.crte.2007.01.003

de Galdeano, C. S., & Vera, J. A. (1992). Stratigraphic record and palaeogeographical context of the Neogene basins in the Betic Cordillera, Spain. *Basin Research*, *4*(1), 21–36. https://doi.org/10.1111/j.1365-2117.1992.tb00040.x

de Jong, K. (2003). Very fast exhumation of high-pressure metamorphic rocks with excess 40Ar and inherited 87Sr, Betic Cordilleras, southern Spain. *Lithos*, *70*(3–4), 91–110. https://doi.org/10.1016/s0024-4937(03)00094-x

de Jong, K., Féraud, G., Ruffet, G., Amouric, M., & Wijbrans, J. R. (2001). Excess argon incorporation in phengite of the Mulhacén Complex: Submicroscopic illitization and fluid ingress during late Miocene extension int hte Betic Zone, south-eastern Spain. *Chemical Geology*, *178*, 159–195. https://doi.org/10.1016/s0009-2541(00)00411-3

de la Peña, L. G., Grevemeyer, I., Kopp, H., Díaz, J., Gallart, J., Booth-Rea, G., et al. (2020). The lithospheric structure of the Gibraltar Arc System from Wide Angle Seismic data. *Journal of Geophysical Research: Solid Earth*, *125*, e2020JB019854. https://doi.org/10.1029/2020JB019854

de la Peña, L. G., Ranero, C. R., Gràcia, E., & Booth-Rea, G. (2020). The evolution of the westernmost Mediterranean basins. *Earth-Science Reviews*, *214*, 103445. https://doi.org/10.1016/j.earscirev.2020.103445

de Ruig, M. J. (1995). Extensional diapirism in the eastern Prebetic foldbelt, southeastern Spain. In M. P. A. Jackson, D. G. Roberts, & S. Snelson (Eds.), *Salt tectonics: A global perspective* (Vol. 65, pp. 353–367). AAPG Memoir.

Díaz, J., & Gallart, J. (2009). Crustal structure beneath the Iberian Peninsula and surrounding waters: A new compilation of deep seismic sounding results. *Physics of the Earth and Planetary Interiors*, *173*, 181–190. https://doi.org/10.1016/j.pepi.2008.11.008

Díaz, J., Gil, A., & Gallart, J. (2013). Uppermost mantle seismic velocity and anisotropy in the Euro-Mediterranean region from Pn and Sn tomography. *Geophysical Journal International*, *192*(1), 310–325. https://doi.org/10.1093/gji/ggs016

Di Vincenzo, G., Grande, A., Prosser, G., Cavazza, W., & DeCelles, P. G. (2016). 40Ar–39Ar laser dating of ductile shear zones from central Corsica (France): Evidence of Alpine (middle to late Eocene) syn-burial shearing in Variscan granitoids. *Lithos*, *262*, 369–383. https://doi.org/10.1016/j.lithos.2016.07.022

Donoso, J. G., Linares, D., Pascual, I., & Serrano, F. (1982). Datos sobre la edad de las secciones del Mioceno Inferior de Port d'es Canonge y Randa (Mallorca). *Bolleti de la Societat d'Historia Natural de les Balears*, *26*, 229–232.

Driussi, O., Briais, A., & Maillard, A. (2015). Evidence for transform motion along the South Balearic margin and implications for the kinematics of opening of the Algerian basin. *Bulletin de la Societe Geologique de France*, *186*(4–5), 353–370. https://doi.org/10.2113/gssgfbull.186.4-5.353

Driussi, O., Maillard, A., Ochoa, D., Lofi, J., Chanier, F., Gaullier, V., et al. (2015). Messinian Salinity Crisis deposits widespread over the Balearic Promontory: Insights from new high-resolution seismic data. *Marine and Petroleum Geology*, *66*, 41–54. https://doi.org/10.1016/j.marpetgeo.2014.09.008

Duggen, S., Hoernle, K., Klügel, A., Geldmacher, J., Thirlwall, M., Hauff, F., & Oates, N. (2008). Geochemical zonation of the Miocene Alborán Basin volcanism (westernmost Mediterranean): Geodynamic implications. *Contributions to Mineralogy and Petrology*, *156*(5), 577–593. https://doi.org/10.1007/s00410-008-0302-4

Duggen, S., Hoernle, K., van den Bogaard, P., & Harris, C. (2004). Magmatic evolution of the Alboran region: The role of subduction in forming the western Mediterranean and causing the Messinian salinity crisis. *Earth and Planetary Science Letters*, *218*, 91–108. https://doi.org/10.1016/S0012-821X(03)00632-0

Duggen, S., Hoernle, K., van den Bogaard, P., Rupke, L., & Morgan, J. P. (2003). Deep roots of the Messinian salinity crisis. *Nature*, *422*, 602–606. https://doi.org/10.1038/nature01553

El-Sharkawy, A., Meier, T., Lebedev, S., Behrmann, J. H., Hamada, M., Cristiano, L., et al. (2020). The slab puzzle of the Alpine-Mediterranean region: Insights from a new, high-resolution, shear wave velocity model of the upper mantle. *Geochemistry, Geophysics, Geosystems*, *21*(8). https://doi.org/10.1029/2020GC008993

Etchecopar, A. (1984). *Etude des états de contrainte en tectonique cassante et simulations de déformations plastiques (approch mathématique). M.S. thesis*. U.S.T.L. Montpellier.

Etchecopar, A., Vasseur, G., & Daignieres, M. (1981). An inverse problem in microtectonics for the determination of stress tensors from fault population analysis. *Journal of Structural Geology*, *3*, 51–65. https://doi.org/10.1016/0191-8141(81)90056-0

Etheve, N., de Lamotte, D. F., Mohn, G., Martos, R., Roca, E., & Blanpied, C. (2016). Extensional vs contractional Cenozoic deformation in Ibiza (Balearic Promontory, Spain): Integration in the West Mediterranean back-arc setting. *Tectonophysics*, *682*, 35–55. https://doi.org/10.1016/j.tecto.2016.05.037

Etheve, N., Mohn, G., Frizon de Lamotte, D., Roca, E., Tugend, J., & Gómez-Romeu, J. (2018). Extreme Mesozoic crustal thinning in the eastern Iberia margin: The example of the Columbrets Basin (Valencia Trough). *Tectonics*, *37*(2), 636–662. https://doi.org/10.1002/2017TC004613

Faccenna, C., & Becker, T. W. (2020). Topographic expressions of mantle dynamics in the Mediterranean. *Earth-Science Reviews*, *209*, 103327. https://doi.org/10.1016/j.earscirev.2020.103327

Faccenna, C., Becker, T. W., Auer, L., Billi, A., Boschi, L., Brun, J. P., et al. (2014). Mantle dynamics in the Mediterranean. *Reviews of Geophysics*, *52*(3), 283–332. https://doi.org/10.1002/2013RG000444

Faccenna, C., Becker, T. W., Lucente, F. P., Jolivet, L., & Rossetti, F. (2001). History of subduction and back arc extension in the Central Mediterranean. *Geophysical Journal International*, *145*(3), 809–820. https://doi.org/10.1046/j.0956-540x.2001.01435.x

Faccenna, C., Piromallo, C., Crespo-Blanc, A., Jolivet, L., & Rossetti, F. (2004). Lateral slab deformation and the origin of the western Mediterranean arcs. *Tectonics*, *23*. https://doi.org/10.1029/2002TC001488

Fernandez, L., Bosch, D., Bruguier, O., Hammor, D., Caby, R., Arnaud, N., et al. (2020). Vestiges of a fore-arc oceanic crust in the Western Mediterranean: Geochemical constraints from North-East Algeria. *Lithos*, *370–371*, 105649. https://doi.org/10.1016/j.lithos.2020.105649

Ferrandini, J., Gattacceca, J., Ferrandini, M., Deino, A., & Janin, M. C. (2003). Chronostratigraphy and paleomagnetism of Oligo-Miocene deposits of Corsica (France): Geodynamic implications for the liguro-provencal basin spreading. *Bulletin de la Societe Geologique de France*, *174*(4), 357–371. https://doi.org/10.2113/174.4.357

Fichtner, A., & Villaseñor, A. (2015). Crust and upper mantle of the western Mediterranean—Constraints from full-waveform inversion. *Earth and Planetary Science Letters*, *428*, 52–62. https://doi.org/10.1016/j.epsl.2015.07.038

Fontboté, J. M., Guimerà, J., Roca, E., Sàbat, F., Santanach, P., & Fernández-Ortigosa, F. (1990). The Cenozoic geodynamic evolution of the Valencia trough (western Mediterranean). *Revista de la Sociedad Geologica de Espana*, *3*(3–4), 249–259.

Fornos, J. J., Marzo, M., Pomar, L., Ramos-Guerrero, E., & Rodríguez-Perea, A. (1991). Evolución tectosedimentaria y anàlisis estratigráfico del Terciario de la isla de Mallorca. In F. Colombo (Ed.), *I Congreso del Grupo Español del Terciario, Vic. Libro Guia Excursión no. 2. Dept. G.D.G.P.* (p. 145). Universitat de Barcelona.

Frasca, G., Gueydan, F., & Brun, J. P. (2015). Structural record of Lower Miocene westward motion of the Alboran Domain in the Western Betics, Spain. *Tectonophysics*, *657*, 1–20. https://doi.org/10.1016/j.tecto.2015.05.017

Freeman, R., Sabat, F., Lowrie, W., & Fontboté, J. M. (1989). Paleomagnetic results from Mallorca (Balearic Islands, Spain). *Tectonics*, *8*(3), 591–608. https://doi.org/10.1029/TC008i003p00591

Galindo-Zaldívar, J., & González-Lodeiro, F. (1988). Faulting phase differentiation by means of computer search on a grid pattern. *Annales Tectonicae*, *2*(2), 90–97.

Gallais, F., Graindorge, D., Gutscher, M. A., & Klaeschen, D. (2013). Propagation of a lithospheric tear fault (STEP) through the western boundary of the Calabrian accretionary wedge offshore eastern Sicily (Southern Italy). *Tectonophysics*, *602*, 141–152. https://doi.org/10.1016/j.tecto.2012.12.026

García-Castellanos, D., & Villaseñor, A. (2011). Messinian salinity crisis regulated by competing tectonics and erosion at the Gibraltar arc. *Nature*, *480*(7377), 359–363. https://doi.org/10.1038/nature10651

García-Dueñas, V., Balanyá, J. C., & Martínez-Martínez, J. M. (1992). Miocene extensional detachments in the outcropping basement of the Northern Alboran Basin (Betics) and their tectonic implications. *Geo-Marine Letters*, *12*, 88–95. https://doi.org/10.1007/BF02084917

Garrido, C. J., Gueydan, F., Booth-Rea, G., Precigout, J., Hidas, K., Padron-Navarta, J. A., & Marchesi, C. (2011). Garnet lherzolite and garnet-spinel mylonite in the Ronda peridotite: Vestiges of Oligocene backarc mantle lithospheric extension in the western Mediterranean. *Geology*, *39*, 927–930. https://doi.org/10.1130/G31760.1

Geel, T., & Roep, T. B. (1998). Oligocene to middle Miocene basin development in the Eastern Betic Cordilleras, SE Spain (Velez Rubio Corridor-Espuna): Reflections of West Mediterranean plate-tectonic reorganizations. *Basin Research*, *10*, 325–343. https://doi.org/10.1046/j.1365-2117.1998.00068.x

Geel, T., Roep, T. B., Ten Kate, W., & Smit, J. (1992). Early-Middle Miocene stratigraphic turning points in the Alicante region (SE Spain): Reflections of Western Mediterranean plate-tectonic reorganizations. *Sedimentary Geology*, *75*(3–4), 223–239. https://doi.org/10.1016/0037-0738(92)90094-8

Gelabert, B. (1998). *La estructura geológica de la mitad occidental de la Isla de Mallorca. Colección Memorias* (Vol. 104, p. 129). Instituto Geológico y Minero de España.

Gelabert, B., Sabat, F., & Rodríguez-Perea, A. (1992). A structural outline of the Serra de Tramuntana of Mallorca (Balearic Islands). *Tectonophysics*, *203*(1–4), 167–183. https://doi.org/10.1016/0040-1951(92)90222-R

Gelabert, B., Sàbat, F., & Rodríguez-Perea, A. (2002). A new proposal for the late Cenozoic geodynamic evolution of the western Mediterranean. *Terra Nova*, *14*(2), 93–100. https://doi.org/10.1046/j.1365-3121.2002.00392.x

Giaconia, F., Booth-Rea, G., Martínez-Martínez, J. M., Azañón, J. M., Storti, F., & Artoni, A. (2014). Heterogeneous extension and the role of transfer faults in the development of the southeastern Betic basins (SE Spain). *Tectonics*, *33*, 2467–2489. https://doi.org/10.1002/2014TC003681

Goffé, B., Michard, A., García-Dueñas, V., González-Lodeiro, F., Monie, P., Campos, J., et al. (1989). 1st evidence of high-pressure, low-temperature metamorphism in the Alpujarride Nappes, Betic Cordilleras (SE Spain). *European Journal of Mineralogy*, *1*, 139–142. https://doi.org/10.1127/ejm/01/1/0139

González-Jiménez, J. M., Marchesi, C., Griffin, W. L., Gervilla, F., Belousova, E. A., Garrido, C. J., et al. (2017). Zircon recycling and crystallization during formation of chromite-and Ni-arsenide ores in the subcontinental lithospheric mantle (Serranía de Ronda, Spain). *Ore Geology Reviews*, *90*, 193–209.

Govers, R., & Wortel, M. J. R. (2005). Lithosphere tearing at STEP faults: Response to edges of subduction zones. *Earth and Planetary Science Letters*, *236*(1–2), 505–523. https://doi.org/10.1016/j.epsl.2005.03.022

Grevemeyer, I., Ranero, C. R., Leuchters, W., Booth-Rea, G., & Gallart, J. (2011). *Seismic constraints on the nature of crust in the Algerian-Balearic Basin-implications for lithospheric construction at back-arc spreading centres* (p. T53D–04). American Geophysical Union, Fall Meeting.

Guerrera, F., Martín-Martín, M., Perrone, V., & Tramontana, M. (2005). Tectono-sedimentary evolution of the southern branch of the Western Tethys (Maghrebian Flysch Basin and Lucanian Ocean): Consequences for Western Mediterranean geodynamics. *Terra Nova*, *17*(4), 358–367. https://doi.org/10.1111/j.1365-3121.2005.00621.x

Guimerà, J., Mas, R., & Alonso, Á. (2004). Intraplate deformation in the NW Iberian Chain: Mesozoic extension and Tertiary contractional inversion. *Journal of the Geological Society*, *161*(2), 291–303. https://doi.org/10.1144/0016-764903-055

Haidar, S., Déverchère, J., Graindorge, D., Arab, M., Medaouri, M., & Klingelhoefer, F. (2021). Back-arc dynamics controlled by slab rollback and tearing: A reappraisal of seafloor spreading and kinematic evolution of the Eastern Algerian basin (western Mediterranean) in Middle-Late Miocene. *ESSOAr Preprint*. https://doi.org/10.1002/essoar.10506942.1

Hall, C. E., Gurnis, M., Sdrolias, M., Lavier, L. L., & Müller, R. D. (2003). Catastrophic initiation of subduction following forced convergence across fracture zones. *Earth and Planetary Science Letters*, *212*, 15–30. https://doi.org/10.1016/S0012-821X(03)00242-5

Handy, M. R., Schmid, S. M., Bousquet, R., Kissling, E., & Bernoulli, D. (2010). Reconciling plate-tectonic reconstructions of Alpine Tethys with the geological–geophysical record of spreading and subduction in the Alps. *Earth-Science Reviews*, *102*(3–4), 121–158. https://doi.org/10.1016/j.earscirev.2010.06.002

Hewitt, G. M. (2011). Mediterranean peninsulas: The evolution of hotspots. In *Biodiversity hotspots* (pp. 123–147). Springer. https://doi.org/10.1007/978-3-642-20992-5_7

Heymes, T., Monié, P., Arnaud, N., Pêcher, A., Bouillin, J. P., & Compagnoni, R. (2010). Alpine tectonics in the Calabrian–Peloritan belt (southern Italy): New 40Ar/39Ar data in the Aspromonte Massif area. *Lithos*, *114*, 451–472. https://doi.org/10.1016/j.lithos.2009.10.011

Hidas, K., Booth-Rea, G., Garrido, C. J., Martínez-Martínez, J. M., Padrón-Navarta, J. A., Konc, Z., et al. (2013). Backarc basin inversion and subcontinental mantle emplacement in the crust: Kilometre-scale folding and shearing at the base of the proto-alborán lithospheric mantle (Betic Cordillera, southern Spain). *Journal of the Geological Society*, *170*, 47–55. https://doi.org/10.1144/jgs2011-151

Hidas, K., Garrido, C. J., Booth-Rea, G., Marchesi, C., Bodinier, J. L., Dautria, J. M., et al. (2019). Lithosphere tearing along STEP faults and synkinematic formation of lherzolite and wehrlite in the shallow subcontinental mantle. *Solid Earth*, *10*, 1099–1121. https://doi.org/10.5194/se-10-1099-2019

Hidas, K., Konc, Z., Garrido, C. J., Tommasi, A., Vauchez, A., Padrón-Navarta, J. A., et al. (2016). Flow in the western Mediterranean shallow mantle: Insights from xenoliths in Pliocene alkali basalts from SE Iberia (eastern Betics, Spain). *Tectonics*, *35*(11), 2657–2676. https://doi.org/10.1002/2016TC004165

Hidas, K., Varas-Reus, M. I., Garrido, C. J., Marchesi, C., Acosta-Vigil, A., Padron-Navarta, J. A., et al. (2015). Hyperextension of continental to oceanic-like lithosphere: The record of late gabbros in the shallow subcontinental lithospheric mantle of the westernmost Mediterranean. *Tectonophysics*, *650*, 65–79. https://doi.org/10.1016/j.tecto.2015.03.011

Hippolyte, J. C., Bergerat, F., Gordon, M. B., Bellier, O., & Espurt, N. (2012). Keys and pitfalls in mesoscale fault analysis and paleostress reconstructions, the use of Angelier's methods. *Tectonophysics*, *581*, 144–162. https://doi.org/10.1016/j.tecto.2012.01.012

Hollister, J. (1942). La posición de las Baleares en las orogenias varisca y alpina. *Publicación Extraordinaria*, *I*, 71–102. Geología de España.

IGME. (2003). *Investigación Geotérmica en La Isla De Mallorca* (p. 167). Unpublished report.

Iribarren, L., Vergés, J., Camurri, F., Fullea, J., & Fernàndez, M. (2007). The structure of the Atlantic-Mediterranean transition zone from the Alboran Sea to the Horseshoe Abyssal Plain (Iberia-Africa plate boundary). *Marine Geology*, *243*, 97–119. https://doi.org/10.1016/j.margeo.2007.05.011

Jabaloy-Sánchez, A., Talavera, C., Rodríguez-Peces, M. J., Vázquez-Vílchez, M., & Evans, N. J. (2021). U-Pb geochronology of detrital and igneous zircon grains from the Águilas Arc in the Internal Betics (SE Spain): Implications for Carboniferous-Permian paleogeography of Pangea. *Gondwana Research*, *90*, 135–158.

Jiménez-Bonilla, A., Crespo-Blanc, A., Balanyá, J. C., Expósito, I., & Díaz-Azpiroz, M. (2020). Analogue models of fold-and-thrust wedges in progressive arcs. Comparison with the Gibraltar Arc external wedge. *Frontiers in Earth Science*, *8*. https://doi.org/10.3389/feart.2020.00072

Jiménez-Bonilla, A., Torvela, T., Balanyá, J. C., Expósito, I., & Díaz-Azpiroz, M. (2016). Changes in dip and frictional properties of the basal detachment controlling orogenic wedge propagation and frontal collapse: The external central Betics case. *Tectonics*, *35*(12), 3028–3049. https://doi.org/10.1002/2016TC00419

Jiménez-Munt, I., Sabadini, R., Gardi, A., & Bianco, G. (2003). Active deformation in the Mediterranean from Gibraltar to Anatolia inferred from numerical modeling and geodetic and seismological data. *Journal of Geophysical Research: Solid Earth*, *108*(B1), ETG 2-1–ETG 2-24. https://doi.org/10.1029/2001JB001544

Jolivet, L., Augier, R., Faccenna, C., Negro, F., Rimmele, G., Agard, P., et al. (2008). Subduction, convergence and the mode of backarc extension in the Mediterranean region. *Bulletin de la Societe Geologique de France*, *179*, 525–550. https://doi.org/10.2113/gssgfbull.179.6.525

Jolivet, L., Augier, R., Robin, C., Suc, J. P., & Rouchy, J. M. (2006). Lithospheric-scale geodynamic context of the Messinian salinity crisis. *Sedimentary Geology*, *188*, 9–33. https://doi.org/10.1016/j.sedgeo.2006.02.004

Jolivet, L., Daniel, J., Truffert, C., & Goffé, B. (1994). Exhumation of deep-crustal metamorphic rocks and crustal extension in arc and back-arc regions. *Lithos*, *33*, 3–30. https://doi.org/10.1016/0024-4937(94)90051-5

Jolivet, L., & Faccenna, C. (2000). Mediterranean extension and the Africa-Eurasia collision. *Tectonics*, *19*(6), 1095–1106. https://doi.org/10.1029/2000tc900018

Jolivet, L., Menant, A., Roche, V., Le Pourhiet, L., Maillard, A., Augier, R., et al. (2021). Transfer zones in Mediterranean back-arc regions and tear faults. *Bulletin de la Société Géologique de France*, *192*(1), 11. https://doi.org/10.1051/bsgf/2021006

Keller, J. V. A., Minelli, G., & Pialli, G. (1994). Anatomy of late orogenic extension: The Northern Apennines case. *Tectonophysics*, *238*(1–4), 275–294. https://doi.org/10.1016/0040-1951(94)90060-4

Kettle, S. (2016). Sedimentology of a Middle Jurassic base-of-slope environment, Cutri Formation, Mallorca. *Journal of Iberian Geology*, *42*(1), 95–112. https://doi.org/10.5209/rev_jige.2016.v42.n1.50710

Kirchner, K. L., Behr, W. M., Loewy, S., & Stockli, D. F. (2016). Early Miocene subduction in the western Mediterranean: Constraints from Rb-Sr multimineral isochron geochronology. *Geochemistry, Geophysics, Geosystems*, *17*(5), 1842–1860. https://doi.org/10.1002/2015gc006208

Kumar, A., Fernàndez, M., Vergés, J., Torne, M., & Jiménez-Munt, I. (2020). Opposite symmetry in the lithospheric structure of the Alboran and Algerian basins and their margins (Western Mediterranean): Geodynamic implications. *Journal of Geophysical Research: Solid Earth*, *126*(7), e2020JB021388.

Lacombe, O. (2012). Do fault slip data inversions actually yield "paleostresses" that can be compared with contemporary stresses? A critical discussion. *Comptes Rendus Geoscience*, *344*(3–4), 159–173. https://doi.org/10.1016/j.crte.2012.01.006

Laouar, R., Satouh, A., Salmi-Laouar, S., Abdallah, N., Cottin, J. Y., Bruguier, O., et al. (2017). Petrological, geochemical and isotopic characteristics of the Collo ultramafic rocks (NE Algeria). *Journal of African Earth Sciences*, *125*, 59–72. https://doi.org/10.1016/j.jafrearsci.2016.10.012

Leblanc, M., & Temagoult, A. (1989). Chromite pods in a lherzolite massif (Collo, Algeria): Evidence of oceanic-type mantle rocks along the West Mediterranean Alpine Belt. *Lithos*, *23*(3), 153–162. https://doi.org/10.1016/0024-4937(89)90002-9

Leprêtre, A., Klingelhoefer, F., Graindorge, D., Schnurle, P., Beslier, M. O., Yelles, K., et al. (2013). Multiphased tectonic evolution of the Central Algerian margin from combined wide-angle and reflection seismic data off Tipaza, Algeria. *Journal of Geophysical Research Atmospheres*, *118*, 3899–3916. https://doi.org/10.1002/jgrb.50318

Leprêtre, R., de Lamotte, D. F., Combier, V., Gimeno-Vives, O., Mohn, G., & Eschard, R. (2018). The Tell-Rif orogenic system (Morocco, Algeria, Tunisia) and the structural heritage of the southern Tethys margin. *Bulletin de la Societe Geologique de France*, *189*(2), 10. https://doi.org/10.1051/bsgf/2018009

Levander, A., Bezada, M. J., Niu, F., Humphreys, E. D., Palomeras, I., Thurner, S. M., et al. (2014). Subduction-driven recycling of continental margin lithosphere. *Nature*, *515*(7526), 253–256. https://doi.org/10.1038/nature13878

Li, B., & Massonne, H. J. (2018). Two Tertiary metamorphic events recognized in high-pressure metapelites of the Nevado-Filábride Complex (Betic Cordillera, S Spain). *Journal of Metamorphic Geology*, *36*(5), 603–630. https://doi.org/10.1111/jmg.12312

Liesa, C. L., & Simón, J. L. (2009). Evolution of intraplate stress fields under multiple remote compressions: The case of the Iberian Chain (NE Spain). *Tectonophysics*, *474*(1–2), 144–159. https://doi.org/10.1016/j.tecto.2009.02.002

Liesa, C. L., Simón, J. L., Ezquerro, L., Arlegui, L. E., & Luzón, A. (2019). Stress evolution and structural inheritance controlling an intracontinental extensional basin: The central-northern sector of the Neogene Teruel Basin. *Journal of Structural Geology*, *118*, 362–376. https://doi.org/10.1016/j.jsg.2018.11.011

Lonergan, L. (1993). Timing and kinematics of deformation in the Malaguide complex, internal zone of the Betic Cordillera, Southeast Spain. *Tectonics*, *12*, 460–476. https://doi.org/10.1029/92TC02507

Lonergan, L., & Johnson, C. (1998). Reconstructing orogenic exhumation histories using synorogenic detrital zircons and apatites: An example from the Betic Cordillera, SE Spain. *Basin Research*, *10*, 353–364. https://doi.org/10.1046/j.1365-2117.1998.00071.x

Lonergan, L., & Platt, J. (1995). The Malaguide-Alpujarride boundary: A major extensional contact in the Internal Zone of the eastern Betic Cordillera, SE Spain. *Journal of Structural Geology*, *17*, 1665–1671. https://doi.org/10.1016/0191-8141(95)00070-T

Lonergan, L., & White, N. (1997). Origin of the Betic-Rif mountain belt. *Tectonics*, *16*, 504–522. https://doi.org/10.1029/96TC03937

López Sánchez-Vizcaíno, V., Rubatto, D., Gómez-Pugnaire, M. T., Trommsdorff, V., & Müntener, O. (2001). Middle Miocene high-pressure metamorphism and fast exhumation of the Nevado-Filábride complex, SE Spain. *Terra Nova*, *13*, 327–332. https://doi.org/10.1046/j.1365-3121.2001.00354.x

Luján, M., Crespo-Blanc, A., & Balanyá, J. C. (2006). The Flysch Trough thrust imbricate (Betic Cordillera): A key element of the Gibraltar Arc orogenic wedge. *Tectonics*, *25*(6). https://doi.org/10.1029/2005TC001910

Lustrino, M., Duggen, S., & Rosenberg, C. L. (2011). The Central-Western Mediterranean: Anomalous igneous activity in an anomalous collisional tectonic setting. *Earth-Science Reviews*, *104*(1–3), 1–40. https://doi.org/10.1016/j.earscirev.2010.08.002

Maillard, A., Jolivet, L., Lofi, J., Thinon, I., Couëffé, R., Canva, A., & Dofal, A. (2020). Transfer zones and associated volcanic province in the eastern Valencia Basin: Evidence for a hot rifted margin? *Marine and Petroleum Geology*, *119*, 104419. https://doi.org/10.1016/j.marpetgeo.2020.104419

Maillard, A., & Mauffret, A. (1999). Crustal structure and riftogenesis of the Valencia Trough (north-western Mediterranean Sea). *Basin Research*, *11*(4), 357–379. https://doi.org/10.1046/j.1365-2117.1999.00105.x

Mancilla, F. L., Booth-Rea, G., Stich, D., Pérez-Peña, J. V., Morales, J., Azañón, J. M., et al. (2015). Slab rupture and delamination under the Betics and Rif constrained from receiver functions. *Tectonophysics*, *663*, 225–237. https://doi.org/10.1016/j.tecto.2015.06.028

Marchesi, C., Garrido, C. J., Bosch, D., Bodinier, J. L., Hidas, K., Padron-Navarta, J. A., & Gervilla, F. (2012). A Late Oligocene suprasubduction setting in the westernmost Mediterranean revealed by intrusive pyroxenite dikes in the Ronda peridotite (southern Spain). *The Journal of Geology*, *120*, 237–247. https://doi.org/10.1086/663875

Marín, M., Roca, E., Marcuello, A., Cabrera, L., & Ferrer, O. (2021). Mesozoic structural inheritance in the Cenozoic evolution of the central Catalan coastal ranges (western Mediterranean): Structural and magnetotelluric analysis in the Gaià-Montmell high. *Tectonophysics*, *814*, 228970.

Marrone, S., Monié, P., Rossetti, F., Aldega, L., Bouybaouene, M., Charpentier, D., et al. (2021). Timing of Alpine orogeny and postorogenic extension in the Alboran domain, Inner Rif Chain, Morocco. *Tectonics*, *40*(7), e2021TC006707. https://doi.org/10.1029/2021tc006707

Marrone, S., Monié, P., Rossetti, F., Lucci, F., Theye, T., Bouybaouene, M. L., & Zaghloul, M. N. (2020). The pressure–temperature–time–deformation history of the Beni Mzala unit (Upper Sebtides, Rif belt, Morocco): Refining the Alpine tectono-metamorphic evolution of the Alboran Domain of the western Mediterranean. *Journal of Metamorphic Geology*, *39*(2). https://doi.org/10.1111/jmg.12587

Marti, J., Mitjavila, J., Roca, E., & Aparicio, A. (1992). Cenozoic magmatism of the Valencia Trough (Western Mediterranean)—Relationship between structural evolution and volcanism. *Tectonophysics*, *203*, 145–165. https://doi.org/10.1016/0040-1951(92)90221-Q

Martin, L. A., Rubatto, D., Brovarone, A. V., & Hermann, J. (2011). Late Eocene lawsonite-eclogite facies metasomatism of a granulite sliver associated to ophiolites in Alpine Corsica. *Lithos*, *125*(1–2), 620–640. https://doi.org/10.1016/j.lithos.2011.03.015

Martín-Chivelet, J., López-Gómez, J., Aguado, R., Arias, C., Arribas, J., Arribas, M. E., et al. (2019). The Late Jurassic–Early Cretaceous rifting. In C. Quesada & J. T. Oliveira (Eds.), *The geology of Iberia: A geodynamic approach: Volume 3: The Alpine Cycle* (pp. 169–249). Springer.

Martín-Closas, C., & Ramos-Guerrero, E. (2005). Paleogene charophytes of the Balearic Islands (Spain). *Geológica Acta*, *3*(1), 39–58. https://doi.org/10.1344/105.000001413

Martín-Martín, M., Estévez, A., Martín-Rojas, I., Guerrera, F., Alcalá, F. J., Serrano, F., & Tramontana, M. (2018). The Agost Basin (Betic Cordillera, Alicante province, Spain): A pull-apart basin involving salt tectonics. *International Journal of Earth Sciences*, *107*(2), 655–671. http://doi.org/10.1007/s00531-017-1521-6

Martín-Martín, M., Guerrera, F., Rodríguez-Estrella, T., Serrano, F., Alcalá, F. J., Raffaelli, G., & Tramontana, M. (2018). Miocene tectono-sedimentary evolution of the eastern external Betic Cordillera (Spain). *Geodinamica Acta*, *30*(1), 265–286. http://doi.org/10.1080/09853111.2018.1493879

Martín-Suárez, E., García-Alix, A., Minwer-Barakat, R., Agustí, J., & Freudenthal, M. (2012). Filling the gap: First evidence of early Tortonian continental deposits in southern Iberia. *Journal of Vertebrate Paleontology*, *32*(6), 1421–1428.

Martínez, F. J., Dietsch, C., Aleinikoff, J., Cirés, J., Arboleya, M. L., Reche, J., & Gómez-Gras, D. (2016). Provenance, age, and tectonic evolution of Variscan flysch, southeastern France and northeastern Spain, based on zircon geochronology. *GSA Bulletin*, *128*(5–6), 842–859.

Martínez-Martínez, J. M. (2006). Lateral interaction between metamorphic core complexes and less-extended, tilt-block domains: The Alpujarras strike-slip transfer fault zone (Betics, SE Spain). *Journal of Structural Geology*, *28*(4), 602–620.

Martínez-Martínez, J. M., & Azañón, J. M. (1997). Mode of extensional tectonics in the southeastern Betics (SE Spain): Implications for the tectonic evolution of the peri-Alborán orogenic system. *Tectonics*, *16*(2), 205–225. https://doi.org/10.1029/97TC00157

Martínez-Martínez, J. M., Soto, J. I., & Balanyá, J. C. (2002). Orthogonal folding of extensional detachments: Structure and origin of the Sierra Nevada elongated dome (Betics, SE Spain). *Tectonics*, *21*. https://doi.org/10.1029/2001TC001283

Mas, G., Gelabert, B., & Fornós, J. J. (2014). *Evidencias de desplazamiento direccional de la falla de Sencelles (Mallorca, Islas Baleares)* (Vol. 47). Segunda reunión Ibérica sobre fallas activas y paleosismología.

Mattei, M., Cifelli, F., Rojas, I. M., Blanc, A. C., Comas, M., Faccenna, C., & Porreca, M. (2006). Neogene tectonic evolution of the Gibraltar Arc: New paleomagnetic constrains from the Betic chain. *Earth and Planetary Science Letters*, *250*(3–4), 522–540. https://doi.org/10.1016/j.epsl.2006.08.012

Mauffret, A., de Lamotte, D., Lallemant, S., Gorini, C., & Maillard, A. (2004). E-W opening of the Algerian Basin (Western Mediterranean). *Terra Nova*, *16*(5), 257–264. https://doi.org/10.1111/j.1365-3121.2004.00559.x

Maury, R. C., Fourcade, S., Coulon, C., Bellon, H., Coutelle, A., Ouabadi, A., et al. (2000). Post-collisional Neogene magmatism of the Mediterranean Maghreb margin: A consequence of slab breakoff. *Comptes Rendus de l'Academie des Sciences – Series IIA: Earth and Planetary Science*, *331*(3), 159–173. https://doi.org/10.1016/s1251-8050(00)01406-3

Medaouri, M., Déverchère, J., Graindorge, D., Bracene, R., Badji, R., Ouabadi, A., et al. (2014). The transition from Alboran to Algerian basins (Western Mediterranean Sea): Chronostratigraphy, deep crustal structure and tectonic evolution at the rear of a narrow slab rollback system. *Journal of Geodynamics*, *77*, 186–205. https://doi.org/10.1016/j.jog.2014.01.003

Mennecart, B., Zoboli, D., Costeur, L., & Pillola, G. L. (2017). Reassessment of the latest Oligocene ruminant from Sardara, the last non-insular mammal from Sardinia (Italy). *Neues Jahrbuch für Geologie und Paläontologie - Abhandlungen*, *286*, 97–104. https://doi.org/10.1127/njgpa/2017/0688

Mitjavila, J., Ramos-Guerrero, E., & Martí, J. (1990). Les roches pyroclastiques du Puig de l'Ofre (Serra de Tramuntana, Majorque): Position géologique et datation K-Ar. *Comptes rendus de l'Académie des Sciences. Série 2, Mécanique, Physique, Chimie, Sciences de l'univers, Sciences de la Terre*, *311*(6), 687–692.

Moragues, L., Booth-Rea, G., Ruano, P., Azañón, J. M., Gaidi, S., & Pérez-Peña, J. V. (2018). Middle Miocene extensional tectonics in Southeast Mallorca Island (Western Mediterranean). *Revista de la Sociedad Geologica de Espana*, *31*, 2.

Negredo Moreno, A. M., Mancilla, F. D. L., Clemente, C., Morales, J., & Fullea, J. (2020). Geodynamic modeling of edge-delamination driven by subduction-transform edge propagator faults: The Westernmost Mediterranean Margin (Central Betic Orogen) Case Study. *Frontiers of Earth Science*, *8*. https://doi.org/10.3389/feart.2020.533392

Olmo-Zamora, P., Alvaro-López, M., Battle-Gargallo, A., & Ramírez del Pozo, J. (1981). *MAGNA 670, Soller. Mapa Geológico de España 1:50.000*. IGME.

Olmo-Zamora, P., Alvaro-López, M., Battle-Gargallo, A., & Ramírez del Pozo, J. (1982). *MAGNA 671, Inca. Mapa Geológico de España 1:50.000*. IGME.

Orife, T., & Lisle, R. J. (2006). Assessing the statistical significance of palaeostress estimates: Simulations using random fault-slips. *Journal of Structural Geology*, *28*, 952–956. https://doi.org/10.1016/j.jsg.2006.03.005

Parcerisa Duocastella, D., Gómez Gras, D. M., Roca Abella, E., Madurell Malapeira, J., & Agustí Segarra, J. (2007). The Upper Oligocene of Montgat (Catalan coastal ranges, Spain): New age constraints to the western Mediterranean basin opening. *Geológica Acta*, *5*(1), 3–17.

Parés, J. M., & Roca, E. (1996). The significance of tectonic-related tertiary remagnetization along the margins of the Valencia trough. *Journal of Geodynamics*, *22*(3–4), 207–227.

Parés, J. M., Sàbat, F., & Santanach, P. (1986). La structure des Serres de Llevant de Majorque (Baléares, Espagne): Données de la région au Sud de Felanitx. *Comptes rendus de l'Académie des sciences. Série 2, Mécanique, Physique, Chimie, Sciences de l'univers, Sciences de la Terre*, *303*(6), 475–480.

Pedrera, A., Ruiz-Constán, A., García-Senz, J., Azor, A., Marín-Lechado, C., Ayala, C., et al. (2020). Evolution of the South-Iberian paleomargin: From hyperextension to continental subduction. *Journal of Structural Geology*, *138*, 104122. https://doi.org/10.1016/j.jsg.2020.104122

Pellen, R., Aslanian, D., Rabineau, M., Leroux, E., Gorini, C., Silenziario, C., et al. (2016). The Minorca Basin: A buffer zone between the Valencia and Liguro-Provençal Basins (NW Mediterranean Sea). *Terra Nova*, *28*(4), 245–256. https://doi.org/10.1111/ter.12215

Peréz-Valera, L. A., Rosenbaum, G., Sánchez-Gómez, M., Azor, A., Fernández-Soler, J. M., Peréz-Valera, F., & Vasconcelos, P. M. (2013). Age distribution of lamproites along the Socovos Fault (southern Spain) and lithospheric scale tearing. *Lithos*, *180*, 252–263. https://doi.org/10.1016/j.lithos.2013.08.016

Piromallo, C., & Morelli, A. (2003). P wave tomography of the mantle under the Alpine-Mediterranean area. *Journal of Geophysical Research*, *108*, 2056. https://doi.org/10.1029/2002JB001757

Platt, J. P., Anczkiewicz, R., Soto, J. I., Kelley, S. P., & Thirlwall, M. (2006). Early Miocene continental subduction and rapid exhumation in the western Mediterranean. *Geology*, *34*, 981–984. https://doi.org/10.1130/G22801A.1

Platt, J. P., Kelley, S. P., Carter, A., & Orozco, M. (2005). Timing of tectonic events in the Alpujárride Complex, Betic Cordillera, southern Spain. *Journal of the Geological Society*, *162*, 1–462. https://doi.org/10.1144/0016-764903-039

Platt, J. P., & Vissers, R. L. M. (1989). Extensional collapse of thickened continental lithosphere: A working hypothesis for the Alboran Sea and Gibraltar arc. *Geology*, *17*(6), 540–543. https://doi.org/10.1130/0091-7613(1989)017<0540:ecotcl>2.3.co;2

Platt, J. P., Whitehouse, M. J., Kelley, S. P., Carter, A., & Hollick, L. (2003). Simultaneous extensional exhumation across the Alboran Basin: Implications for the causes of late orogenic extension. *Geology*, *31*(3), 251. http://doi.org/10.1130/0091-7613(2003)031<0251:seeata>2.0.co;2

Pomar, L., Esteban, M., Calvet, F., & Barón, A. (1983). La Unidad Arrecifal del Mioceno superior de Mallorca. In L. Pomar, A. Obrador, J. Fornos, & A. Rodríguez-Perea (Eds.), *El Terciario de las Baleares (Mallorca-Menorca. Guía de las excursiones del X Congreso Nacional de Sedimentología). Menorca 1983* (pp. 21–44). Institut d'Estudis Baleàrics, Universitat de Palma de Mallorca.

Pomar, L., & Rodríguez-Perea, A. (1983). In L. Pomar, A. Obrador, J. J. Fornos & A. Rodríguez-Perea (Eds.), *El Neógeno inferior de Mallorca: Randa. El Terciario de las Baleares (Mallorca-Menorca). Guía de las excursiones del X Congreso Nacionial de Sedimentología. Menorca 1983* (pp. 115–137). Institut d'Estudis Baleàrics, Universitat de Palma de Mallorca.

Poort, J., Lucazeau, F., Le Gal, V., Dal Cin, M., Leroux, E., Bouzid, A., et al. (2020). Heat flow in the Western Mediterranean: Thermal anomalies on the margins, the seafloor and the transfer zones. *Marine Geology*, *419*, 106064. https://doi.org/10.1016/j.margeo.2019.106064

Précigout, J., Gueydan, F., Garrido, C. J., Cogné, N., & Booth-Rea, G. (2013). Deformation and exhumation of the Ronda peridotite (Spain). *Tectonics*, *32*, 1011–1025.

Ramon, X., & Simo, A. (1986). Análisis sedimentológico y descripción de las secuencias deposicionales del Neógeno postorogénico de Mallorca. *Boletin Geologico y Minero*, *97*(4), 445–472.

Ramos-Guerrero, E., Berrio, I., Fornós, J. J., & Moragues, L. (2000). Chapter 40: The Middle Miocene Son Verdera Lacustrine-Palustrine System (Santa Margalida Basin, Mallorca). In E. H. Gierlowski-Kordesch & K. R. Kelts (Eds.), *Lake basins trough space and time. AAPG studies in geology* (Vol. 46, pp. 441–448). The American Association of Petroleum Geologists. https://doi.org/10.1306/St46706C40

Ramos-Guerrero, E., Rodriguez-Perea, A., Sabat, F., & Serra-Kiel, J. (1989). Cenozoic tectosedimentary evolution of Mallorca Island. *Geodinamica Acta*, *3*(1), 53–72. https://doi.org/10.1080/09853111.1989.11105174

Rehault, J. P., Boillot, G., & Mauffret, A. (1984). The western Mediterranean basin geological evolution. *Marine Geology*, *55*, 447–477. https://doi.org/10.1016/0025-3227(84)90081-1

Roca, E. (2001). The Northwest Mediterranean Basin (Valencia Trough, Gulf of Lions and Liguro-Provencal basins): Structure and geodynamic evolution. *Mémoires du Muséum National d'Historie Naturelle*, *186*, 671–706.

Roca, E., Beamud, E., Rubinat, M., Soto, R., & Ferrer, O. (2013). Paleomagnetic and inner diapiric structural constraints on the kinematic evolution of a salt-wall: The Bicorb-Quesa and northern Navarrés salt-wall segments case (Prebetic Zone, SE Iberia). *Journal of Structural Geology*, *52*, 80–95. https://doi.org/10.1016/j.jsg.2013.04.003

Roca, E., & Guimerà, J. (1992). The Neogene structure of the Eastern Iberian Margin—Structural constraints on the crustal evolution of the Valencia trough (Western Mediterranean). *Tectonophysics*, *203*(1–4), 203–218. https://doi.org/10.1016/0040-1951(92)90224-T

Roca, E., Guimerà, J., & Salas, R. (1994). Mesozoic extensional tectonics in the southeast Iberian Chain. *Geological Magazine*, *131*(2), 155–168. https://doi.org/10.1017/s0016756800010694

Roca, E., Sans, M., Cabrera, L., & Marzo, M. (1999). Oligocene to Middle Miocene evolution of the central Catalan margin (northwestern Mediterranean). *Tectonophysics*, *315*(1–4), 209–229. https://doi.org/10.1016/s0040-1951(99)00289-9

Roca, E., Sans, M., & Koyi, H. A. (2006). Polyphase deformation of diapiric areas in models and in the eastern Prebetics (Spain). *AAPG Bulletin*, *90*(1), 115–136. https://doi.org/10.1306/07260504096

Rodríguez-Fernández, J., Azor, A., & Azañón, J. M. (2011). The Betic Intramontane Basins (SE Spain): Stratigraphy, Subsidence, and Tectonic History. In C. Busby & A. Azor (Eds.), *Tectonics of sedimentary basins: Recent advances* (pp. 461–479). John Wiley & Sons. https://doi.org/10.1002/9781444347166.ch23

Rodríguez-Perea, A. (1984). *El Mioceno de la Serra Nord de Mallorca. Estratigrafia, sedimentología e implicaciones estructurales* (Doctoral Thesis). Universitat de les Illes Balears.

Romagny, A., Jolivet, L., Menant, A., Bessière, E., Maillard, A., Canva, A., et al. (2020). Detailed tectonic reconstructions of the Western Mediterranean region for the last 35 Ma, insights on driving mechanismsReconstructions détaillées de la Méditerranée occidentale depuis 35 Ma, implications en terme de mécanismes moteur. *Bulletin de la Societe Geologique de France*, *191*(1). https://doi.org/10.1051/bsgf/2020040

Rosenbaum, G., & Lister, G. S. (2004). *Formation of arcuate orogenic belts in the western Mediterranean region* (Vol. 383, pp. 41–56). Geological Society of America Special Publication. https://doi.org/10.1130/0-8137-2383-3(2004)383[41:FOAOBI]2.0.CO;2

Rosenbaum, G., Lister, G. S., & Duboz, C. (2002). Reconstruction of the tectonic evolution of the western Mediterranean since the Oligocene. *Journal of the Virtual Explorer*, *8*, 107–130. https://doi.org/10.3809/jvirtex.2002.00053

Rossetti, F., Faccenna, C., Goffé, B., Monié, P., Argentieri, A., Funiciello, R., & Mattei, M. (2001). Alpine structural and metamorphic signature of the Sila Piccola Massif nappe stack (Calabria, Italy): Insights for the tectonic evolution of the Calabrian Arc. *Tectonics*, *20*(1), 112–133. https://doi.org/10.1029/2000tc900027

Rossetti, F., Faccenna, C., Jolivet, L., Funiciello, R., Tecce, F., & Brunet, C. (1999). Syn- versus post-orogenic extension: The case study of Giglio Island (Northern Tyrrhenian Sea, Italy). *Tectonophysics*, *304*, 71–93. https://doi.org/10.1016/s0040-1951(98)00304-7

Rossetti, F., Glodny, J., Theye, T., & Maggi, M. (2015). Pressure–temperature–deformation–time of the ductile Alpine shearing in Corsica: From orogenic construction to collapse. *Lithos*, *218*, 99–116. https://doi.org/10.1016/j.lithos.2015.01.011

Rossetti, F., Goffé, B., Monié, P., Faccenna, C., & Vignaroli, G. (2004). Alpine orogenic P-T-t-deformation history of the Catena Costiera area and surrounding regions (Calabrian Arc, southern Italy): The nappe edifice of north Calabria revised with insights on the Tyrrhenian-Apennine system formation. *Tectonics*, *23*(6). https://doi.org/10.1029/2003TC001560

Roure, F., Casero, P., & Addoum, B. (2012). Alpine inversion of the North African margin and delamination of its continental lithosphere. *Tectonics*, *31*(3). https://doi.org/10.1029/2011tc002989

Saadallah, A., & Caby, R. (1996). Alpine extensional detachment tectonics in the Grande Kabylie metamorphic core complex of the Maghrebides (northern Algeria). *Tectonophysics*, *267*(1–4), 257–273. https://doi.org/10.1016/S0040-1951(96)00101-1

Sàbat, F., Gelabert, B., & Rodríguez-Perea, A. (2018). Minorca, an exotic Balearic island (western Mediterranean). *Geológica Acta*, *16*(4), 411–426. https://doi.org/10.1344/GeologicaActa2018.16.4.5

Sàbat, F., Gelabert, B., Rodríguez-Perea, A., & Giménez, J. (2011). Geological structure and evolution of Majorca: Implications for the origin of the Western Mediterranean. *Tectonophysics*, *510*(1–2), 217–238. https://doi.org/10.1016/j.tecto.2011.07.00

Sàbat, F., Muñoz, J. A., & Santanach, P. (1988). Transversal and oblique structures at the Serres-de-Llevant Thrust Belt (Mallorca Island). *Geologische Rundschau*, *77*(2), 529–538.

Sallarès, V., Gailler, A., Gutscher, M. A., Graindorge, D., Bartolomé, R., Gracia, E., et al. (2011). Seismic evidence for the presence of Jurassic oceanic crust in the central Gulf of Cadiz (SW Iberian margin). *Earth and Planetary Science Letters*, *311*(1–2), 112–123.

Santamaría-López, Á., Lanari, P., & de Galdeano, C. S. (2019). Deciphering the tectono-metamorphic evolution of the Nevado-Filábride complex (Betic Cordillera, Spain) – A petrochronological study. *Tectonophysics*, *767*, 128158.

Schettino, A., & Turco, E. (2006). Plate kinematics of the Western Mediterranean region during the Oligocene and Early Miocene. *Geophysical Journal International*, *166*, 1398–1423. https://doi.org/10.1111/j.1365-246X.2006.02997.x

Serck, C. S., Braathen, A., Olaussen, S., Osmundsen, P. T., Midtkandal, I., Yperen, A. E. V., & Indrevær, K. (2020). Supradetachment to rift basin transition recorded in continental to marine deposition; Paleogene Bandar Jissah Basin, NE Oman. *Basin Research*, *33*, 544–569. https://doi.org/10.1111/bre.12484

Sevillano, A., Rosales, I., Bádenas, B., Barnolas, A., & López-García, J. M. (2018). Spatial and temporal facies evolution of a Lower Jurassic carbonate platform, NW Tethyan margin (Mallorca, Spain). *Facies*, *65*, 3. https://doi.org/10.1007/s10347-018-0545-0

Simancas, J. F. (2018). A reappraisal of the Alpine structure of the Alpujárride Complex in the Betic Cordillera: Interplay of shortening and extension in the westernmost Mediterranean. *Journal of Structural Geology*, *115*, 231–242. https://doi.org/10.1016/j.jsg.2018.08.001

Simón, J. L. (1986). Analysis of a gradual change in stress regime (example from the eastern Iberian Chain, Spain). *Tectonophysics*, *124*(1–2), 37–53.

Simón, J. L. (2019). Forty years of paleostress analysis: Has it attained maturity? *Journal of Structural Geology*, *125*, 124–133. https://doi.org/10.1016/j.jsg.2018.02.011

Simón, J. L., Arlegui, L. E., Lafuente, P., & Liesa, C. L. (2012). Active extensional faults in the central-eastern Iberian Chain, Spain. *Journal of Iberian Geology*, *38*(1), 127–144.

Simón, J. L., Casas-Sainz, A. M., & Gil-Imaz, A. (2021). Controversial epiglyptic thrust sheets: The case of the Daroca Thrust (Iberian Chain, Spain). *Journal of Structural Geology*, *145*, 104298.

Simón-Gómez, J. (1989). Late Cenozoic stress field and fracturing in the Iberian Chain and Ebro Basin (Spain). *Journal of Structural Geology*, *11*(3), 285–294.

Speranza, F., Villa, I. M., Sagnotti, L., Florindo, F., Cosentino, D., Cipollari, P., & Mattei, M. (2002). Age of the Corsica–Sardinia rotation and Liguro–Provençal Basin spreading: New paleomagnetic and Ar/Ar evidence. *Tectonophysics*, *347*(4), 231–251. https://doi.org/10.1016/s0040-1951(02)00031-8

Sperner, B., & Zweigel, P. (2010). A plea for more caution in fault–slip analysis. *Tectonophysics*, *482*(1–4), 29–41. https://doi.org/10.1016/j.tecto.2009.07.019

Suarez, E. M., Freudenthal, M., & Agusti, J. (1993). Micromammals from the Middle Miocene of the Granada basin (Spain). *Geobios*, *26*(3), 377–387. https://doi.org/10.1016/S0016-6995(93)80028-P

Sun, M., & Bezada, M. (2020). Seismogenic Necking During Slab Detachment: Evidence From Relocation of Intermediate-Depth Seismicity in the Alboran Slab. *Journal of Geophysical Research: Solid Earth*, *125*(2), e2019JB017896. https://doi.org/10.1029/2019JB017896

Torné, M., Pascal, G., Buhl, P., Watts, A. B., & Mauffret, A. (1992). Crustal and velocity structure of the Valencia trough (western Mediterranean), Part I. A combined refraction/wide-angle reflection and near-vertical reflection study. *Tectonophysics*, *203*(1–4), 1–20. https://doi.org/10.1016/0040-1951(92)90212-O

Torres-Roldán, R. L., Poli, G., & Peccerillo, A. (1986). An Early Miocene arc-tholeiitic magmatic dike event from the Alboran Sea-Evidence for precollisional subduction and back-arc crustal extension in the westernmost Mediterranean. *Geologische Rundschau*, *75*, 219–234.

van Hinsbergen, D. J. J., Torsvik, T. H., Schmid, S. M., Maţenco, L. C., Maffione, M., Vissers, R. L., et al. (2020). Orogenic architecture of the Mediterranean region and kinematic reconstruction of its tectonic evolution since the Triassic. *Gondwana Research*, *81*, 79–229. https://doi.org/10.1016/j.gr.2019.07.009

van Hinsbergen, D. J. J., Vissers, R. L. M., & Spakman, W. (2014). Origin and consequences of western Mediterranean subduction, rollback, and slab segmentation. *Tectonics*, *33*(4), 393–419. https://doi.org/10.1002/2013TC003349

Varas-Reus, M. I., Garrido, C. J., Marchesi, C., Bosch, D., Acosta-Vigil, A., Hidas, K., et al. (2017). Sr-Nd-Pb isotopic systematics of crustal rocks from the western Betics (S. Spain): Implications for crustal recycling in the lithospheric mantle beneath the westernmost Mediterranean. *Lithos*, *276*, 45–61. https://doi.org/10.1016/j.lithos.2016.10.003

Vergés, J., & Fernàndez, M. (2012). Tethys–Atlantic interaction along the Iberia–Africa plate boundary: The Betic–Rif orogenic system. *Tectonophysics*, *579*, 144–172. https://doi.org/10.1016/j.tecto.2012.08.032

Vergés, J., Fernàndez, M., & Martínez, A. (2002). The Pyrenean orogen: Pre-, syn-, and post-collisional evolution. *Journal of the Virtual Explorer*, *8*, 55–74. https://doi.org/10.3809/jvirtex.2002.00058

Vergés, J., & Sàbat, F. (1999). Constraints on the Neogene Mediterranean kinematic evolution along a 1000 km transect from Iberia to Africa. *Geological Society, London, Special Publications*, *156*(1), 63–80.

Vitale Brovarone, A., & Herwartz, D. (2013). Timing of HP metamorphism in the Schistes Lustrés of Alpine Corsica: New Lu–Hf garnet and lawsonite ages. *Lithos*, *172–173*, 175–191. https://doi.org/10.1016/j.lithos.2013.03.009

Watts, A. B., & Torné, M. (1992). Subsidence history, crustal structure, and thermal evolution of the Valencia Trough: A young extensional basin in the western Mediterranean. *Journal of Geophysical Research*, *97*(B13), 20021–20041. https://doi.org/10.1029/92JB00583

Wortel, M. J. R., & Spakman, W. (2000). Subduction and slab detachment in the Mediterranean-Carpathian Region. *Science*, *290*, 1910–1917. https://doi.org/10.1126/science.290.5498.1910

Žalohar, J., & Vrabec, M. (2007). Paleostress analysis of heterogeneous fault-slip data: The Gauss method. *Journal of Structural Geology*, *29*(11), 1798–1810. https://doi.org/10.1016/j.jsg.2007.06.009

Zhou, X., Li, Z. H., Gerya, T. V., Stern, R. J., Xu, Z., & Zhang, J. (2018). Subduction initiation dynamics along a transform fault control trench curvature and ophiolite ages. *Geology*, *46*(7), 607–610. https://doi.org/10.1130/G40154.1